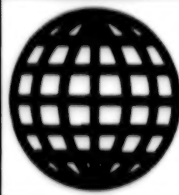


JPRS-UMS-92-001  
4 FEBRUARY 1992



FOREIGN  
BROADCAST  
INFORMATION  
SERVICE

# ***JPRS Report***

## **Science & Technology**

---

***Central Eurasia:  
Materials Science***

# Science & Technology

## Central Eurasia: Materials Science

JPRS-UMS-92-001

### CONTENTS

4 February 1992

**NOTICE TO READERS:** Given the course of events in the former Soviet Union, FBIS changed the titles of its Soviet publications to "Central Eurasia" on 6 January 1992. The "USSR: Materials Science" report has been renamed "Central Eurasia: Materials Science."

#### ANALYSIS, TESTING

Capillary Method of Flaw Detection: Present Status and Forecast of Further Developments (Review)	
[A.S. Borovikov; <i>TEKHNICHESKAYA DIAGNOSTIKA I NERAZRUSHAYUSHCHIY KONTROL</i> , No 4, Oct-Dec 91]	1
Ultrasonic Inspection of Welds in Drilling Bits	
[V.A. Troitsky, Yu.K. Bondarenko, et al.; <i>TEKHNICHESKAYA DIAGNOSTIKA I NERAZRUSHAYUSHCHIY KONTROL</i> , No 4, Oct-Dec 91]	1
Problems in Standardization of Nondestructive Inspection	
Construction	
[D.A. Korshunov; <i>TEKHNICHESKAYA DIAGNOSTIKA I NERAZRUSHAYUSHCHIY KONTROL</i> , No 4, Oct-Dec 91]	2
Long-Range Stress Fields Close To Disperse Particles Arising During the Explosion Alloying of Metal Materials	
[S.M. Usherenko, S.I. Gubenko, et al.; <i>METALLOFIZIKA</i> , Jul 91]	2
Growth and Structure Formation of Complex Crystals With a Single-Faceted Niobium Surface	
[O.M. Burabash, B.A. Zaderiy, et al.; <i>METALLOFIZIKA</i> , Jul 91]	3
Thermochemical Treatment of Invar Alloys of the System Fe-Ni	
[A.O. Mekhratov, T.A. Shukyurov, et al.; <i>METALLOFIZIKA</i> , Jul 91]	3
The Laue Diffraction of a Spherical X-Ray Wave on a Crystal With Statistically Distributed Defects	
[K.T. Gabrielyan; <i>METALLOFIZIKA</i> , Jul 91]	4
The Electrical Structure and Location of Hydrogen Atoms in Ti <sub>x</sub> CoH <sub>x</sub> Alloys	
[V.V. Nemoshakko, Ye.V. Sedyakina, et al.; <i>METALLOFIZIKA</i> , Jul 91]	4
Change in the Local Structure of Fe <sub>85-x</sub> Co <sub>x</sub> B <sub>15</sub> Amorphous Alloys as a Function of Their Co Content and Irradiation With $\gamma$ -Quanta	
[V.V. Polotnyuk, A.M. Shalayev, et al.; <i>METALLOFIZIKA</i> , Jul 91]	4
Erosion Wear Model of Brittle Material Under Impact of Solid Particles Accelerated in Gas Nozzles	
[L.I. Urbanovich, Ye.M. Kramchenkov, et al.; <i>TRENIYE I IZNOS</i> , No 4, Jul-Aug 91]	5
On Correlation of Wear in Gas- and Hydroabrasive Jets	
[P.K. Kallas; <i>TRENIYE I IZNOS</i> , No 4, Jul-Aug 91]	5
Plastic Deformation Development and Cu-Fe-O Amorphous-Crystalline Alloy Formation in Contact Interaction Zone of Cu-Steel 45 Friction Pair	
[A.V. Vereshchak, V.V. Gorskiy, et al.; <i>TRENIYE I IZNOS</i> , No 4, Jul-Aug 91]	6
Measuring Powder Material's Load Carrying Capacity Under Boundary Friction	
[V.N. Antsiferov, N.N. Maslennikov, et al.; <i>TRENIYE I IZNOS</i> , No 4, Jul-Aug 91]	6
Control of Telescopic Expansion Joint Seal Unit Operation in Floating Derrick	
[N.B. Ananichev, V.I. Atopov; <i>TRENIYE I IZNOS</i> , No 4, Jul-Aug 91]	6
Investigation of Friction Surface Submicrorelief by Scanning Tunnel Microscopy Method	
[S.A. Chishik, I.M. Troyanovskiy, et al.; <i>TRENIYE I IZNOS</i> , No 4, Jul-Aug 91]	7
Chemical Analysis Monitoring of Magnetic Alloy Composition in Sm-Co-Fe-Cu-Zr System	
[Ye.V. Yukhimano (deceased), V.A. Dubok; <i>POROSHKOVAYA METALLURGIYA</i> , No 11, Nov 91]	7
Niobium Analysis in Rock After Precipitation of Complex With Pyrogallol on Silica by Ethylene Oxide Polymers	
[O.A. Kostyuk, R.F. Mustafayev, et al.; <i>ZAVODSKAYA LABORATORIYA</i> , Jun 91]	7
Photometric Analysis of Petroleum in Waste Water	
[V.I. Yegorov, S.V. Vasilyeva, et al.; <i>ZAVODSKAYA LABORATORIYA</i> , Jun 91]	8
Extractive X-Ray Fluorescent Aluminum Analysis in Nonferrous Metal Alloys	
[F.I. Lobanov, N.N. Andreyeva, et al.; <i>ZAVODSKAYA LABORATORIYA</i> , Jun 91]	8
Extractive X-Ray Fluorescent Scandium Analysis in Process Solutions	
[A.I. Zebreva, N.N. Andreyeva, et al.; <i>ZAVODSKAYA LABORATORIYA</i> , Jun 91]	8
Elevated-Sensitivity Energy-Dispersion X-Ray Fluorescence Analyzer	
[P.A. Galtsev, B.S. Iokhin; <i>ZAVODSKAYA LABORATORIYA</i> , Jun 91]	9

Use of Various Types of Flames for Photometric Analysis of Sodium, Potassium, and Lithium Impurities in Glass	9
[T.V. Drozhzhina, L.V. Ganyushkina, et al.; ZAVODSKAYA LABORATORIYA, Jun 91]	9
Measurement of Semiconductor Samples' Magnetoresistance	9
[N.N. Polyakov; ZAVODSKAYA LABORATORIYA, Jun 91]	9
Magnetothermal Carbide Phase Analysis in Steel by Changes in Remanent Magnetization	9
[V.A. Dubrov; ZAVODSKAYA LABORATORIYA, Jun 91]	9
On Interrelation Between Principal Characteristics of Steel's Mechanical Properties	10
[L.A. Sosnovskiy; ZAVODSKAYA LABORATORIYA, Jun 91]	10
Measurement of Long-Term Strength of High-Temperature Materials by Parametric Method	10
[M.N. Stepnov, I.A. Inozemtseva, et al.; ZAVODSKAYA LABORATORIYA, Jun 91]	10
MR-5-8V Corrosion-Mechanical Testing Machine	10
[V.M. Kushnarenko, A.P. Fot, et al.; ZAVODSKAYA LABORATORIYA, Jun 91]	10
Effect of Niobium Microadditions to Cu-Ga Alloy on Mechanical Strength of Diamond/Metal Contact	11
[Yu.V. Naydich, V.P. Umanskiy, et al.; SVERKHTVERDYYE MATERIALY, No 5(74), Sep-Oct 91]	11
Thermographic Analysis of Ti-C-Ni System Powder Alloys	11
[I.P. Kushtalova, L.F. Stasyuk, et al.; SVERKHTVERDYYE MATERIALY, No 5(74), Sep-Oct 91]	11
Survival Probability Estimate of Semiconductor Chips During Machining	11
[O.A. Privarnikov, V.N. Shevchenko; SVERKHTVERDYYE MATERIALY, No 5(74), Sep-Oct 91]	11
Structure and Composition of Titanium Nitride Plasma-Diffusion Coats	12
[A.V. Byakova, V.G. Gorbach, et al.; IZVESTIYA VYSSHIKH UCHEBNYKH ZAVEDENIY: CHERNAYA METALLURGIYA, Jun 91]	12
Austenite Inclusions and Grain Size in Structural Steels	12
[V.K. Florov, G.N. Basova, et al.; IZVESTIYA VYSSHIKH UCHEBNYKH ZAVEDENIY: CHERNAYA METALLURGIYA, Jun 91]	12
Retained Austenite and Wear Resistance of Alloyed Casehardened Steels	12
[A.L. Geller, V.N. Yurko; IZVESTIYA VYSSHIKH UCHEBNYKH ZAVEDENIY: CHERNAYA METALLURGIYA, Jun 91]	12

## COATINGS

Increasing Die and Mold Durability by Ion Plasma Coating. II. Coat Transition Zone Structure	14
[J.L. Illichev, Yu.S. Gushchin, et al.; PODROSHKOVAYA METALLURGIYA, Nov 91]	14
Structural and Property Behavior of Titanium Nitride-Coated Hard-Alloy Tool as Function of Heating by Ion Jet During Spraying	14
[F.I. Shchedrina, A.A. Sklyarov, et al.; METALLURGICHESKAYA I GORNORUDNAYA PROMYSHLENNOST, No 4(162), Oct-Dec 91]	14

## COMPOSITE MATERIALS

Predicting Characteristics of Mechanical and Physical Properties of Hollow-Sphere-Reinforced Plastics	15
[Yu.A. Dzenis, R.D. Maksimov; MEKHANIKA KOMPOZITNYKH MATERIALOV, No 3, May-Jun 91]	15
Friction Properties of Hard-Faced Alloy-Steel 45 Pair in Heavy-Duty Loading Conditions in Argillaceous Mud	15
[V.I. Dvoruk, A.I. Belyy; TRENIE I IZNOS, Vol 12 No 4, Jul-Aug 91]	15
Wettability and Contact Interaction in Graphite-Nickel-Titanium Melt System	16
[V.M. Perevertaylo, V.G. Delevi, et al.; SVERKHTVERDYYE MATERIALY, No 5(74), Sep-Oct 91]	16
Effect of Graphite-Like Boron Nitride Structure and Properties on Elbor Synthesis	16
[A.N. Porada, S.N. Pikalov, et al.; SVERKHTVERDYYE MATERIALY, No 5(74), Sep-Oct 91]	16

## CORROSION

Purity and Quality Requirements for Rare-Earth Metals and Alloys With Magnetic and Magnetostrictive Properties	17
[A.V. Yelyutin, O.Yu. Pasechnik, et al.; VYSOKOCHISTYYE VESHCHESTVA, No 3, May-Jun 91]	17
Production of High-Purity Silver and Copper Monohalides	17
[N.V. Lichkova, V.N. Zagorodiyev; VYSOKOCHISTYYE VESHCHESTVA, No 3, May-Jun 91]	17
High-Purity Refractory Metals	18
[G.S. Burkhanov; VYSOKOCHISTYYE VESHCHESTVA, No 3, May-Jun 91]	18

FERROUS METALS

Resistance of Steels With Higher than 600 MPa 0.2% Yield Strength and Their Welds to Fracture Under Static Load [L.I. Mikhoduy, S.B. Kasatkin, et al.; <i>PROBLEMY PROCHNOSTI</i> , Jul 91]	19
Resistance of Ferritic-Pearlitic Steels and Their Welds to Cyclic Cracking [M.N. Georgiyev; <i>PROBLEMY PROCHNOSTI</i> , Jul 91]	19
Strain and Heat Treatment Hardening of Rolled Structural Steel: Problems of Production and Consumption [N.P. Lyakishev, S.P. Yefimenko, et al.; <i>IZVESTIYA AKADEMII NAUK SSSR, No 3, 91</i> ]	20
Dependence of Surface Tension of Iron-Arsenic Melts on Temperature [P.S. Kharlashin; <i>IZVESTIYA VYSSHIKH UCHEBNYKH ZAVEDENIY: CHERNAYA METALLURGIYA</i> , Jul 91]	20
On Possibility of Refining Ferrous Red Mud by Liquid Phase Reduction Process [V.S. Valavin, S.K. Vildanov, et al.; <i>IZVESTIYA VYSSHIKH UCHEBNYKH ZAVEDENIY: CHERNAYA METALLURGIYA</i> , Jul 91]	21
Metallization of Iron-Containing Nickel-Making Byproduct Pellets in Cuba [Yu.S. Yusin, Yu.B. Voytovskiy, et al.; <i>IZVESTIYA VYSSHIKH UCHEBNYKH ZAVEDENIY: CHERNAYA METALLURGIYA</i> , Jul 91]	21
On Calcium's Effect on Steels With Various Carbon Contents [Ye.L. Zats, V.N. Radchenko, et al.; <i>IZVESTIYA VYSSHIKH UCHEBNYKH ZAVEDENIY: CHERNAYA METALLURGIYA</i> , Jul 91]	21
Physical Simulation of Continuously Cast Steel Ingot Solidification on Planar Pattern [V.V. Stulov, Yu.G. Gontarev, et al.; <i>IZVESTIYA VYSSHIKH UCHEBNYKH ZAVEDENIY: CHERNAYA METALLURGIYA</i> , Jul 91]	22
High-Temperature Unit for Measuring Molten Metal Viscosity [V.Yu. Korolev, A.F. Vishkarev, et al.; <i>IZVESTIYA VYSSHIKH UCHEBNYKH ZAVEDENIY: CHERNAYA METALLURGIYA</i> , Jul 91]	22
Analyzing Gaseous Phase Composition During Melt Processing by Methane and Propane in Vacuum [B.V. Linchevskiy, V.A. Mashin, et al.; <i>IZVESTIYA VYSSHIKH UCHEBNYKH ZAVEDENIY: CHERNAYA METALLURGIYA</i> , Jul 91]	22
Investigation of Viscosity and Melting Point of Boron-Containing Protective Lubricating Mixtures for Steel Casting [V.L. Zhuk, S.V. Timofeyeva, et al.; <i>IZVESTIYA VYSSHIKH UCHEBNYKH ZAVEDENIY: CHERNAYA METALLURGIYA</i> , Jun 91]	23
Viscosity and Desulfurizing Ability of Natural and Synthetic Blast Furnace CaO-MgO-Al <sub>2</sub> O <sub>3</sub> -SiO <sub>2</sub> Slags [S.Yu. Gruzdeva, N.L. Zhilo, et al.; <i>IZVESTIYA VYSSHIKH UCHEBNYKH ZAVEDENIY: CHERNAYA METALLURGIYA</i> , Jul 91]	23
New Type of Steel-Making Unit [N.M. Skorokhod, N.A. Antonov, et al.; <i>METALLURGICHESKAYA I GORNORUDNAYA PROMYSHLENNOST</i> , No 4(162), Oct-Dec 91]	23
Molten Steel Treatment by Powder Wire in Ingot Mold [V.A. Vikhlevshchuk, V.M. Chernogritskiy, et al.; <i>METALLURGICHESKAYA I GORNORUDNAYA PROMYSHLENNOST</i> , No 4(162), Oct-Dec 91]	24
On Saturating Iron With Carbon During Blast Furnace Smelting [G.A. Volovik, V.I. Kotov, et al.; <i>IZVESTIYA VYSSHIKH UCHEBNYKH ZAVEDENIY: CHERNAYA METALLURGIYA</i> , Jun 91]	24
Development of Ferrous Metallurgy Viewed [Yu. Dolgorukov; <i>EKONOMIKA SOVETSKOY UKRAINY</i> , Aug 91]	24

NONMETALLIC MATERIALS

Assessment of Wear Resistance of Diamond-Hard Alloy Cutting Tips [V.M. Epshteyn, G.S. Nikiforov, et al.; <i>SVERKHTVERDYYE MATERIALY</i> , No 5(74), Sep-Oct 91]	31
Investigation of Microimpurity Content of Ultradisperse Diamond [T.M. Gubarevich, N.M. Kostyukova, et al.; <i>SVERKHTVERDYYE MATERIALY</i> , No 5(74), Sep-Oct 91]	31
Properties of Compacts From Natural Diamond Crystals From Metamorphic Rocks [O.A. Voronov, A.A. Kaurov, et al.; <i>SVERKHTVERDYYE MATERIALY</i> , No 5(74), Sep-Oct 91]	31
Use of Differential Diamond Crushers for Cocoa Bean Grinding [E.D. Kizikov, I.P. Kushtalova, et al.; <i>SVERKHTVERDYYE MATERIALY</i> , No 6(75), Nov-Dec 91]	32

Turning of Car Parts Rebuilt by Spraying With Subsequent Coat Fusing [V.N. Potseluyko, S.V. Ignatyev, et al.; <i>SVERKHTVERDYYE MATERIALY</i> , No 6(75), Nov-Dec 91]	32
Optimization of Diamond Microturning Conditions of Metal Mirrors [G.G. Dobrovolskiy, Yu.A. Dyatlov, et al.; <i>SVERKHTVERDYYE MATERIALY</i> , No 6(75), Nov-Dec 91]	32
Diamond Powder Deironing in Linear Traveling Magnetic Field [V.P. Terekhov, A.P. Shiryayev; <i>SVERKHTVERDYYE MATERIALY</i> , No 6(75), Nov-Dec 91]	32
Metallographic Investigation of Sintered Diamond Compacts: Discussion [G.M. Kimstach, A.A. Urtayev, et al.; <i>SVERKHTVERDYYE MATERIALY</i> , No 6(75), Nov-Dec 91]	33
New Brands of Graphite-Like Boron Nitride: High-Quality Precursor for Synthesizing Superhard Materials [A.N. Porada, S.N. Pikalov, et al.; <i>SVERKHTVERDYYE MATERIALY</i> , No 6(75), Nov-Dec 91]	33
Physicomechanical Properties of Nickel-Molybdenum-Bonded Titanium Nitride Cermets [M.A. Kuzenkova, O.N. Kaydash, et al.; <i>SVERKHTVERDYYE MATERIALY</i> , No 6(75), Nov-Dec 91]	33
Simple Phonon Frequency Distribution Functions for Diamond and BN <sub>sph</sub> [L.A. Shulman; <i>SVERKHTVERDYYE MATERIALY</i> , No 6(75), Nov-Dec 91]	34
Carbon Phase Transformations in Diamond Under Laser Irradiation [A.P. Rudenko, A.I. Gorshkov, et al.; <i>SVERKHTVERDYYE MATERIALY</i> , No 6(75), Nov-Dec 91]	34
Effect of Nongraphitized Starting Carbon Material Phase on Synthesis Behavior and Diamond Crystal Quality [B.K. Dymov, Ya.A. Kalashnikov, et al.; <i>SVERKHTVERDYYE MATERIALY</i> , No 6(75), Nov-Dec 91]	34
Refractories Made of Molten Materials With a Mullite Composition [V.A. Ustichenko, N.V. Pitak; <i>OGNEUPORY</i> , Jul 91]	35
Electron Microscopy Studies of the Structure and Phase Composition of the System BaO-B <sub>2</sub> O <sub>3</sub> in Metallization Coatings [E.L. Karyakina, L.G. Rabinkov; <i>OGNEUPORY</i> , Jul 91]	35
Natural Aluminosilicate Raw Material for Producing Mullite-Silica Fibrous Materials [I.G. Subochev, N.V. Pitak; <i>OGNEUPORY</i> , Jul 91]	36
Research on the Technology of Castable Refractory Thermal Insulation Products [Ya.Z. Shapiro, L.G. Litvin; <i>OGNEUPORY</i> , Jul 91]	36
Lime Binder-Based Dinas Products for Lining Coke Furnaces [V.L. Bulakh, R.F. Rud; <i>OGNEUPORY</i> , Jul 91]	36
A Study of the Effectiveness of Refining Melts by Filtration [V.N. Kozhurkov, E.B. Yarikhin, et al.; <i>OGNEUPORY</i> , Jul 91]	37
New Types of Calcium-Containing Mineralizers To Produce Dinas Products [I.V. Khonchik, V.I. Drozd, et al.; <i>OGNEUPORY</i> , Jul 91]	37

## PREPARATIONS

New Powder Friction Materials in Braking Devices [A.D. Ignatovskiy, I.Z. Tomsinskiy; <i>TRENIYE I IZNOS</i> , Vol 12 No 4, Jul-Aug 91]	38
Mechanism of Additional Iron Powder Reduction in Falling Layer [V.A. Maslov, Yu.A. Aleksandrov; <i>POROSHKOVAYA METALLURGIYA</i> , Sep 91]	38
Effect of Powder Dispersion on Brass' Hot Compaction Temperature [V.S. Krushanov, T.G. Garbovitskaya; <i>POROSHKOVAYA METALLURGIYA</i> , Sep 91]	38
Methods of Estimating Ductility During Plastic Working of Powder Metals. II. Fracture Criteria Allowing for Stressed State [A.A. Notych, Ye.V. Zvonarev; <i>POROSHKOVAYA METALLURGIYA</i> , Sep 91]	38
Shock Waves During Dynamic Compaction of Powders and Porous Bodies. II. Shock Wave Propagation in Porous Materials With Reinforcing Frame [L.A. Maksimenko, A.L. Maksimenko, et al.; <i>POROSHKOVAYA METALLURGIYA</i> , Sep 91]	39
Joint Effect of Various Flow Mechanisms in Porous Polycrystalline Body During Hot Compaction. III. Series Connection Model [M.S. Kovalchenko; <i>POROSHKOVAYA METALLURGIYA</i> , Sep 91]	39
Extrusion Patterns of Bimetal Powder Materials. I. Taut Strained State During Extrusion of Dissimilar Materials [N.V. Manukyan, S.G. Agbalyan, et al.; <i>POROSHKOVAYA METALLURGIYA</i> , Sep 91]	39
Metal Coating of Diamond Powders With Adhesion-Active Metals. I. Refractory Metal Deposition From Gaseous Phase [A.P. Oganyan; <i>POROSHKOVAYA METALLURGIYA</i> , Sep 91]	40
Resistivity of Iron Disilicide-Molybdenum Trioxide-Glass Composites [S.I. Vecherskiy, F.A. Sidorenko; <i>POROSHKOVAYA METALLURGIYA</i> , Sep 91]	40
Powder Magnetic Abrasive Tool Forming. III. Annular Turning Magnetic Abrasive Tool Forming [M.D. Krymskiy; <i>POROSHKOVAYA METALLURGIYA</i> , Sep 91]	40
Hafnium Interaction With Ruthenium and Iridium [V.N. Yeremenko, L.S. Kriklya, et al.; <i>POROSHKOVAYA METALLURGIYA</i> , Sep 91]	41

Conductivity and Thermoelectric Coefficient of Hot-Compaction Aluminum Boride and Carbaboride Samples [A.I. Kharlamov, L.M. Murzin, et al.; <i>POROSHKOVAYA METALLURGIYA</i> , Sep 91]	41
Structural Modification of Sintered Composite Tube Cathodes in High-Current Gaseous Discharge [V.I. Baranova, S.N. Novikov; <i>POROSHKOVAYA METALLURGIYA</i> , Sep 91]	41
Comparison of Requirements for Vehicle Cardan Shaft Tubes and Ways to Improve Their Quality [G.I. Gulyayev, K.I. Shkabatur, et al.; <i>METALLURGICHESKAYA I GORNORUDNAYA PROMYSHLENNOST</i> , No 4(162), Oct-Dec 91]	42
Electrically Welded Thin-Walled Tubes for Automotive Industry [V.I. Mizera, K.I. Shkabatur, et al.; <i>METALLURGICHESKAYA I GORNORUDNAYA PROMYSHLENNOST</i> , No 4(162), Oct-Dec 91]	42
Temperature and Mechanical Conditions of Hot Die Forging of Titanium Powder Blanks [V.A. Pavlov, M.I. Nosenko, et al.; <i>POROSHKOVAYA METALLURGIYA</i> , Nov 91]	42
Role of Elastic Stresses During Sintering of Nonisomeric Crystal Particles [Yu.I. Boyko, Yu.L. Galchinskaya, et al.; <i>POROSHKOVAYA METALLURGIYA</i> , Nov 91]	43
Structure Formation Processes in Powder Copper-Chromium-Graphite Materials [V.A. Dymchenko, Ye.A. Kurirova; <i>POROSHKOVAYA METALLURGIYA</i> , Nov 91]	43
Diamond Powder Metallizing by Adhesion-Active Metals. II. Structural Analysis of Metallized Diamond Powders [A.P. Oganyan; <i>POROSHKOVAYA METALLURGIYA</i> , Nov 91]	43
Mold Design for Electric Discharge Sintering of Diamond Tool From Cu-Sn-Based Powder Composites [A.V. Svechkov, A.A. Baydenko, et al.; <i>POROSHKOVAYA METALLURGIYA</i> , Nov 91]	44

## TREATMENTS

Controlling Continuous Rolling Mill Rate Condition [A.S. Fedosiyenko; <i>IZVESTIYA VYSSHIKH UCHEBNYKH ZAVEDENIY: CHERNAYA METALLURGIYA</i> , Jun 91]	45
Strip Thickness Measuring System of Narrow-Strip Hot Rolling Mill [B.I. Kuznetsov, V.I. Kovalev; <i>IZVESTIYA VYSSHIKH UCHEBNYKH ZAVEDENIY: CHERNAYA METALLURGIYA</i> , Jun 91]	45
Crack Resistance of Steel 20Kh13 Following Electron-Beam Machining and Plasma Jet Spraying [V.I. Petrov, V.A. Kuznetsov, et al.; <i>IZVESTIYA VYSSHIKH UCHEBNYKH ZAVEDENIY: CHERNAYA METALLURGIYA</i> , Jun 91]	45
Investigation of Cooling Rate's Effect on Structural Parameters of Steel 38KhN3MFA [Yu.F. Ivanov, E.V. Kozlov; <i>IZVESTIYA VYSSHIKH UCHEBNYKH ZAVEDENIY: CHERNAYA METALLURGIYA</i> , Jun 91]	46
Investigation of Brand D Steel Ingot Piercing Process [V.Ya. Osadchiy, I.N. Leontyeva, et al.; <i>IZVESTIYA VYSSHIKH UCHEBNYKH ZAVEDENIY: CHERNAYA METALLURGIYA</i> , Jul 91]	46
Diamond Drawing Die Strength Analysis [V.N. Kissyuk, V.N. Lvov, et al.; <i>IZVESTIYA VYSSHIKH UCHEBNYKH ZAVEDENIY: CHERNAYA METALLURGIYA</i> , Jul 91]	46
Dislocation Density Behavior in Steel Under Electrically Stimulated Drawing [T.V. Yerilova, V.Ye. Gromov, et al.; <i>IZVESTIYA VYSSHIKH UCHEBNYKH ZAVEDENIY: CHERNAYA METALLURGIYA</i> , Jul 91]	47

## EXTRACTIVE METALLURGY, MINING

Ecology of Massive Explosions in Quarries [E.I. Yefremov, V.D. Petrenko; <i>METALLURGICHESKAYA I GORNORUDNAYA PROMYSHLENNOST</i> , No 4(162), Oct-Dec 91]	48
Ways of Increasing Exploitation Efficiency of Deep Levels at Ingulets Mining and Ore Dressing Combine [A.V. Krivosheyev; <i>METALLURGICHESKAYA I GORNORUDNAYA PROMYSHLENNOST</i> , No 4(162), Oct-Dec 91]	48
Electric Fuze Network Switching System to Expand Short-Delay Blasting Capabilities [V.R. Dyadyushko, V.A. Zayarnyuk, et al.; <i>METALLURGICHESKAYA I GORNORUDNAYA PROMYSHLENNOST</i> , No 4(162), Oct-Dec 91]	48
Fertile Mixture Application: New Soil Reclamation Method [V.M. Rakhamanin, Yu.M. Gukaylo, et al.; <i>METALLURGICHESKAYA I GORNORUDNAYA PROMYSHLENNOST</i> , No 4(162), Oct-Dec 91]	48

MISCELLANEOUS

Effect of Powder Material Structure Factor on Strength and Ductility of WC-Co Detonation Gun Coatings /V.K. Fedorenko, R.K. Ivashchenko, et al.; <i>POROSHKOVAYA METALLURGIYA</i> , Nov 91/	50
Permanent Isotropic Magnets From Ferromagnetic Powders With Organic Composite Coating /V.V. Nepomnyashchiy; <i>POROSHKOVAYA METALLURGIYA</i> , Nov 91/	50
Probabilistic Method of Monitoring Performance Margin of Aircraft Gas-Turbine Engine Parts on Basis of Maximum-Temperature Criterion /A.N. Vetrov, A.G. Kucher, et al.; <i>PROBLEMY PROCHNOSTI</i> , Oct 91/	50
Automatic Stand for Testing Structural Materials in Compound State of Stress /F.F. Giginyak, O.K. Shkodzinskiy, et al.; <i>PROBLEMY PROCHNOSTI</i> , Oct 91/	51

**Capillary Method of Flaw Detection: Present Status and Forecast of Further Developments (Review)**

927D0012A Kiev TEKHNICHESKAYA DIAGNOSTIKA I NERAZRUSHAYUSHCHIY KONTROL in Russian No 4, Oct-Dec 91 pp 8-23

[Article by A.S. Borovikov, candidate of technical sciences, Institute of Electric Welding imeni Ye.O. Paton, UkrSSR Academy of Sciences, Kiev]

UDC 620.179.111

[Abstract] The present status and developments of the capillary method of flaw detection are reviewed, this new method of nondestructive testing and inspection having been conceived in 1983 and much progressed since. It is based essentially on the theory of the ultrasonic capillary effect. Its two principal parameters of the inspection process are the time taken by the penetrant fluid to fill a blind crack in an acoustic vibration field and the time necessary for impregnating the layer of sorbent photochromic developer varnish with the penetrant fluid till its sensitivity threshold as flaw indicator has been reached. The time to fill a crack depends on properties of the fluid (dynamic viscosity, wetting angle and surface tension in air), on the crack dimensions (width of opening, depth), on the ambient pressure, and on the penetrant microstructure. The time to sensitize the developer depends not only on those properties of the penetrant, on the ratio of penetration depth to crack depth, and on the ambient pressure, but also on characteristics of the developer, namely its permeability and porosity, and on the thickness of its layer. Comprehensive theoretical and experimental studies covering both applied materials science with emphasis on chemistry and inspection technology with emphasis on reliability including measurement techniques are underway, as a result of which new penetrant and developer materials become available while the inspection process is being constantly improved. At the same time there is research being done on radically new methods of capillary defectoscopy, methods based on electrogasdynamics of aqueous penetrant aerosols and altogether different methods involving desorption of a radioisotopic indicator gas such as  $^{85}\text{Kr}$ . Progress made in the past 4 years and new proposals indicating likely future trends were reported at the Twelfth All-Union Conference on Non-destructive Inspection held on 11-13 September 1990 in Sverdlovsk. Noteworthy results of theoretical research are: 1) construction of an original new model describing diffusion-migration of a penetrant into a sorbent developer as a two-stage process (P.P. Prokhorenko); 2) discovery of heretofore unknown bilateral filling of conical blind capillaries by fluid penetrants (G.I. Dovgalyo, N.P. Migun, P.P. Prokhorenko), also discovery that completely filling a cavity (flaw) with the penetrant is detrimental for developing by the dry process and beneficial for developing by the wet process; 3) removal of one penetrant from a capillary by means of another penetrant with liberation of heat as they are mixed and

subsequent heating of the trapped gas (N.V. Dezhkunov, A.P. Kornev, I.P. Stoycheva); 4) discovery of a strong dependence of the developing rate on the thickness of the developer layer when the developer is a low-permeability material (G.I. Dovgalyo, N.P. Migun). Noteworthy results of engineering research are: 1) new principle of surface preparation for inspection by chemical modification (G.P. Semenov, M.K. Fedorova); 2) use of a microphotometer (IFO-45) measuring the contrast ratio of the image of the indicator trace, for most effective inspection by ultrasonic capillary impregnation (N.V. Delenkovskiy, I.V. Stoycheva, R.A. Vylinskiy); 3) feasibility of surface finish estimation on the basis of the surface potential during stabilization of air characteristics within the inspection zone under widely varying conditions (I.V. Terentyev, A.A. Sannikov). Noteworthy unconventional new inspection materials and method are: 1) use of a volatile penetrant and diffuse recording of the color of its vapor with the aid of a developer-indicator shell (N.G. Berezkina, M.N. Larichev, I.O. Leypunskiy, G.L. Yeremin), for capillary nondestructive inspection of composite materials and of polished metal surfaces; 2) industrial flaw detectors with the new "Shirvanol" luminophor, developed at the Baku Institute of Petrochemical Processes, replacing the old "Noriol A" (L.A. Sokolova, Z.Ya. Merkulova, S.G. Bart). Figures 7; references 30.

**Ultrasonic Inspection of Welds in Drilling Bits**

927D0012B Kiev TEKHNICHESKAYA DIAGNOSTIKA I NERAZRUSHAYUSHCHIY KONTROL in Russian No 4, Oct-Dec 91 pp 24-31

[Article by V.A. Troitskiy, doctor of technical sciences, Yu.K. Bondarenko, candidate of technical sciences, Yu.B. Yeskov, A.S. Melnikov, A.L. Shekero, and A.V. Davidovich, Institute of Electric Welding imeni Ye.O. Paton, UkrSSR Academy of Sciences, Kiev]

UDC 620.179.16

[Abstract] On the basis of experimental laboratory studies, an ultrasonic system has been developed at the Institute of Electric Welding specifically for inspection of welding seams on drill bits produced at the Drogobych manufacturing plant. The method was tested on model specimens of welding seams with defects of the under-weld type, joints with such seams placed in an immersion bath on a conveyor together with sets of ultrasonic transducers. Tests were performed with split-compound and ultrasound-compound transducer pairs operating at 2.5 MHz or 5 MHz frequency, an ultrasound-compound transducer operating at 10 MHz and a focusing lens, a UD-11UA or UD2-12 flaw detector, and with an S1-83 oscilloscope. The performance characteristics of each transducer set was first evaluated in terms of detection of an echo signal returning from a reference reflector, namely: dependence of the detectability factor on the clearance between transducer and inspection piece, dependence of both echo-signal and interference-signal

amplitudes on the width of that clearance, and dependence of the detectability factor on the distance between transducer and reference reflector along the inspection piece surface at various widths of the clearance between transducer and inspection piece. Tests were then performed on class III 269.97/9S3 GNU and 1AN GNU drill bits. An analysis of the data has revealed that cavities and plane defects parallel to the seam surface are best detected in inspection by either the echo-pulse method or the shadow method using a combination of various volume waves and three ultrasonic transducers placed in the seam region: on one side a radiator emitting shear waves, on the opposite side a receiver of shear waves, and a compound transducer emitting longitudinal waves for detection of cavities and receiving them along with longitudinal waves coming from the edge of a vertical plane defect which reflects shear waves while transforming them. Optimum for inspection of those drill bits were found to be 5 MHz and 10 MHz operating frequencies with a 13 mm wide clearance between transducer and drill bit surface. Figures 6; references 4.

### Problems in Standardization of Nondestructive Inspection in Construction

927D0012C Kiev TEKHNICHESKAYA  
DIAGNOSTIKA I NERAZRUSHAYUSHCHIY  
KONTROL in Russian No 4, Oct-Dec 91 pp 62-64

[Article by D.A. Korshunov, candidate of technical sciences, Scientific Research Institute of Building Structures, Kiev]

UDC 620.179.006.05

[Abstract] Revision of standards pertaining to nondestructive inspection of concrete and reinforced concrete is proposed, for the purpose of making them more compatible with international practices. A comprehensive revision will affect current All-Union State Standards which apply to various methods of inspection for cure and strength, ultrasonic testing included. It will also involve adaptation of foreign methods such as the in-situ Koma-meter+Lok-test (German Instruments Ltd., Copenhagen/DENMARK). It will require scientific and engineering solutions to problems in statistical methods of product quality control, in establishment of a single acceptable strength standard and determination of the volume of concrete it refers to, in error estimation based on the appropriate regression formula taking into account variability of the strength of concrete, for purposes of calibration of measurements and correction of

readings as well as subsequent product grading and classification, also in search of both technically and economically feasible alternative testing methods and equipment, especially in connection with changeover from manual to computer-aided automatic inspection. Major obstacles to implementation of a restandardization program, which must be overcome if trade with other countries is to expand, are insufficient information about and limited dissemination of relevant existing standards. References 6.

### Long-Range Stress Fields Close To Disperse Particles Arising During the Explosion Alloying of Metal Materials

927D0021A Kiev METALLOFIZIKA in Russian Vol 17 No 7, Jul 91 (manuscript received 14 Sep 90; after revision 14 Jun 91) pp 57-64

[Article by S.M. Usherenko, S.I. Gubenko, and V.F. Nozdrin, Metallurgy Institute, Dnepropetrovsk]

UDC 534.2:621.385.833

[Abstract] The authors of the study reported herein examined the role of long-range stress fields in the formation of the dislocation structure of metals subjected to explosion alloying. Specimens of Armco iron and molybdenum were subjected to annealing and forging, and specimens of EZ and 08Cr18Ni10Ti steels were subjected to annealing in order to prepare the starting structure. Particles of  $\text{Si}_3\text{N}_4$  or  $\text{Ti} + \text{TiB}_2$  were used with the Armco iron and Mo, and particles of  $\text{TiCn} + \text{Ni}$  were used with the steels. The particles in the fraction ranged from 40 to 125  $\mu\text{m}$  in size. The specimens were then subjected to treatment in a high-speed stream of working medium produced by using the energy of an explosive. The particles were accelerated to a speed of 2 km/s, and the pressure of their collision with the target reached 15 GPa. The microstructure of the specimens before and after treatment was studied by using a Neophot-21 optical microscope and an EVM-100B transmission electron microscope to examine polished microsections of the alloyed materials. The residual long-range stress fields were measured by electron microscopy based on the parameters of the flexural extinction contours. The studies performed confirms that during the process of explosion alloying, long-range stress fields arise at sites of the braking of the disperse particles accelerated by the energy of the explosion. These fields generate wave relaxation processes in the metal matrix that in turn affect the fine structure of the metal and contribute to the hardening of the treated material. Figures 4; references 8 (Russian).

**Growth and Structure Formation of Complex Crystals With a Single-Faceted Niobium Surface**

927D0021D Kiev METALLOFIZIKA in Russian Vol 17 No 7, Jul 91 (manuscript received 2 Oct 90; after revision 18 Jan 91) pp 103-106

[Article by O.M. Barabash, B.A. Zaderiy, M.Yu. Masmov, S.P. Oshkderov, O.P. Karasevskaya, and S.S. Kotenko, Metal Physics Institute, UkrSSR Academy of Sciences, Kiev]

UDC 548.5.55.734.2:539.382

[Abstract] The authors of the study reported herein examined the growth and formation of the structures of crystals of complex shape with a single-faceted niobium surface. Specifically, they examined the structure of crystals grown by electron beam remelting of polycrystalline blanks with increased speeds of shifting the fused zone from 10 to 20 m/h. Using the said speed enabled the authors to increase heat application and the temperature gradient in the melt at the crystallization front (which amounted to about 1,000°C/cm under the given conditions). The complex crystals were grown in one to four passes of the fused zone along a polycrystalline blank with a diameter of 18 mm, a wall thickness of 1.5 mm, and a length of 40 mm. The structure of the study crystals was studied by x-ray structural analysis and optical microscopy. Creep tests lasting 100 hours were conducted at a temperature of 1,673 K and at stresses of 5 and 6 MPa. During the process of directed crystallization, shifting the melted zone along the specimen was found to result in the formation of a single-faceted surface characterized by a bandlike macrostructure formed of helical curved bands. These bands were found to have an identical monocrystalline orientation. The number of bands varied from 15 to 60 depending on the directed crystallization regimen. Increasing the number of passes resulted in a reduction in the number of bands. The slope of the bands to the generatrix of the cylindrical surface of the monocrystals was also found to vary from 0 to 60° depending on the directed crystallization regimen. The method used in the study reported here resulted in monocrystals with directions of predominant growth close to (100), (110), and (111). The internal substructure of the monocrystalline bands was found to be characterized by a cellular substructure formed directly during the process of directed hardening under conditions of a cellular crystallization front. The cells varied in size from 5 to 15 μm; however, cells as large as 30 μm were also encountered. Two types of cellular substructures were formed, i.e., substructures with isotropic and anisotropic dislocation distributions. The substructure crystals produced by the method described was found to possess a good heat stability that substantially improves mechanical properties at temperatures all the way up to 1,673 K. Figures 5, table 1; references 4 (Russian).

**Thermochemical Treatment of Invar Alloys of the System Fe-Ni**

927D0021F Kiev METALLOFIZIKA in Russian Vol 17 No 7, Jul 91 (manuscript received 17 Apr 90; after revision 1 Apr 91) pp 111-114

[Article by A.O. Mekhrabov, T.A. Shukyurov, K.G. Binnatov, V.A. Aliyev, Yu.L. Radionov, and I.I. Alizade, Construction Engineering Institute, Baku]

UDC 669.018.298; 539.374

[Abstract] Preliminary research conducted by the authors of this article indicated that nitriding alloys of the system Fe-Ni by means of thermochemical treatment techniques can improve their Invar properties. In the study reported herein, they worked to discover the laws governing the change in the properties of Invar metal alloys of the system Fe-Ni after nitriding. Fe-Ni alloys containing 29, 30.4, 33, and 35 atomic percent Ni were used for the studies. The alloys were produced at the Central Scientific Research Institute of Ferrous Metallurgy imeni I.P. Bardin. The specimens were subjected to preliminary annealing at 1,270 K and were quenched in water. The nitriding process used consisted of thermochemical treatment of the test alloys in an atmosphere heated to the temperature of the thermal dissociation of ammonia. The Invar Fe-Ni alloys were nitrided at 920 K in a specially constructed chamber. To keep oxygen from entering the medium surrounding the specimens, the chamber was flushed with pure argon until the nitriding process began. The duration of the thermochemical treatment process was varied from 5 to 180 minutes. The techniques of Mossbauer effect spectroscopy, roentgenography, dilatometry, and microhardness measurement were used to perform a series of comparative tests on specimens of pure and nitrided Invar Fe-Ni alloys. When diffractograms of the pure and nitrided specimens were compared, it was discovered that the basic reflexes are maintained in the nitrided specimens but are shifted to the side of smaller Bragg reflection angles. A nitride phase of the type  $(Fe, Ni)_{4-x}N_x$  ( $\gamma$ -phase) was discovered to have formed in the nitrided specimens. Nitriding was found to increase the microhardness of a test alloy's matrix. As the duration of the nitriding process was extended from 5 to 60 minutes, microhardness increased to about 2,000 kgf/mm<sup>2</sup>. After 60 minutes, the nitrogen was found to have penetrated the test specimens to a depth of 150 to 200 μm. The  $\gamma$ -resonance spectra of specimens nitrided for 30 minutes indicated the formation of nitride phases. An analysis of the densities of the distribution of the effective magnetic field of  $^{57}Fe$  nuclei in the study Fe-Ni alloys after hardening and nitriding for 30 and 60 minutes indicated that the hardened alloy is in a paramagnetic state and that, after nitriding, the function  $P(H)$  has three distinctive points corresponding to  $H_{eff}$  values of 0, 150, and about 210 kOe. Figures 4; references 7 (Russian).

**The Laue Diffraction of a Spherical X-Ray Wave on a Crystal With Statistically Distributed Defects**

927D0021B Kiev METALLOFIZIKA in Russian Vol 17 No 7, Jul 91 (manuscript received 26 Jun 90) pp 85-92

[Article by K.T. Gabrielyan, Yerevan State University]

UDC 539.26/27

[Abstract] The kinematic theory of diffraction is the theoretical foundation of various x-ray-based methods of investigating polycrystals and highly distorted crystals with individually indistinguishable defects. Crystals with rather perfect structures are investigated based on the results of the dynamic theory of the scattering of x-rays. Despite the many works that have been written on these topics, no exhaustive theory of the scattering of x-rays in crystals with macroscopic uniformly distributed defects has yet been developed. Working within the framework of the theory that has already been developed, the author of this article derives a system of differential equations describing the diffraction of x-rays in a crystal with chaotically arranged, individually indistinguishable defects. He then finds an analytic solution of this system for a spherical wave falling onto a crystal from a small source close to the surface. The calculated intensities of the diffracted wave are compared with existing results based on the Kato statistical theory of diffraction. Significant differences between the author's results and those based on Kato's diffraction theory are found. They are explained by the closed nature of the equation system used by the author and by the fact that he gives consistent consideration to boundary conditions. References 12: 4 Russian, 8 Western.

**The Electron Structure and Location of Hydrogen Atoms in  $TiCoH_x$  Alloys**

927D0021E Kiev METALLOFIZIKA in Russian Vol 17 No 7, Jul 91 (manuscript received 6 Feb 91) pp 107-111

[Article by V.V. Nemoshkalenko, Ye.V. Sedyakina, L.M. Sheludchenko, and V.A. Yatsenko, Metal Physics Institute, UkrSSR Academy of Sciences, Kiev]

UDC 541.44:530.145

[Abstract] The authors of the study reported herein calculated the electron structure of clusters simulating the hydride  $TiCoH_x$  with different populations of interstitial hydrogen atoms. The calculations were performed within the framework of the self-consistent method of scattered waves. The authors then proceeded to compare the results of these calculations with experimentally obtained x-ray emission spectra of  $K\beta_3$ - and  $La_{1,2}$ -series of the metal components of hydrides of the system  $TiCoH_x$  ( $x = 0.88$  and  $1.42$ ). Overall, the energy position of the main characteristic features observed in the x-ray emission K- and L-spectra of Ti were found to be in agreement with the characteristic features of the calculated curves for a cluster with a tetrahedral hydrogen

position. No such agreement was observed in the case of a cluster with an octahedral hydrogen position. An examination of the  $K\beta_3$ - and  $La_{1,2}$ -bands of Co in the  $\beta_1$  and  $\beta_2$  phases of  $TiCoH$  indicated that the valence electrons of the p-symmetry of Co participate in the formation of what has been termed a hybrid zone. The fact that the  $La_{1,2}$  bands of Co in the hydrides are in no way different from the  $La_{1,2}$  bands in the starting  $TiCo$  was taken as confirmation of the fact that the d-electrons of Co do not participate in the formation of a chemical bond with hydrogen. Instead, the d-states of Co remain localized at the Fermi level where they participate in the formation of a metal-metal bond with the d-electrons of the titanium. After comparing the partial state densities of the valence electrons of both types of clusters with emission K- and L-spectra, the authors concluded that hydrogen atoms mainly populate the tetrahedral positions in the crystal lattice of  $TiCoH_x$  hydrides. Figures 3; references 9: 6 Russian, 3 Western.

**Change in the Local Structure of  $Fe_{85-x}Co_xB_{15}$  Amorphous Alloys as a Function of Their Co Content and Irradiation With  $\gamma$ -Quanta**

927D0021C Kiev METALLOFIZIKA in Russian Vol 17 No 7, Jul 91 (manuscript received 12 Nov 90; after revision 20 Mar 91) pp 96-102

[Article by V.V. Polotnyuk, A.M. Shalayev, V.V. Kotov, T.V. Yefimova, G. Vlasak (Physics Institute, Electrophysics Research Center, Slovak Academy of Sciences, Bratislava), and V.M. Shkapa, Metal Physics Institute, UkrSSR Academy of Sciences, Kiev]

UDC 539.213:620.18

[Abstract] The authors of the study reported herein examined the local structure of  $Fe_{85-x}Co_xB_{15}$  amorphous alloys (where  $x = 12, 15, 17, 21$ , and  $25$ ) as a function of their Co content and irradiation with  $\gamma$ -quanta. Specimens of the study alloys were produced in the form of strips about  $30 \mu m$  thick and  $10 mm$  wide by the method of hardening a plane stream. At a temperature below  $60^\circ C$  they were irradiated with  $\gamma$ -quanta with an energy of about  $1.2 MeV$  in a dose of  $2.58 \times 10^5$  coulombs [ $C/kg$ ] ( $10^9 R$ ) at an intensity of  $0.517 C/kg \cdot s$ . NSR spectra of the specimens in the frequency range from  $170$  to  $310 \pm 0.5 MHz$  were obtained by the spin echo method at  $4.2 K$  before and after  $\gamma$ -quanta irradiation. The spectra of the irradiated specimens were found to be the sum (superimposition) of an entire series of peaks, with each corresponding to a specified atomic circle. In the frequency interval from  $170$  to  $310 MHz$  a number of basic peaks were identified at  $192, 208, 218, 245, 253$ , and  $278 MHz$  with a precision of  $\pm 1 MHz$ . Also present in the spectrum were dozens of satellite peaks in the form of bumps or weak variations in intensity. The half-width of the homogeneous lines generally did not exceed  $6 MHz$ . The ratio of the intensity of the individual peaks was found to change as a function of the alloy's zirconium and after irradiation, although their position (frequency)

was not found to depend on these factors. Working under the assumptions that (1) the frequency of the NSR spectra is directly proportional to the content of Co (Fe) in the first coordination sphere and (2) the boron atoms are located in substitution positions and number 1, 2, or 3 in the first coordination sphere for the given concentration of boron atoms ( $C_B = 0.15$ ), the authors proceed to develop a model method of interpreting (decoding) the NSR spectra and determining the configurations of the Co, Fe, and B atoms in the nearest circle corresponding to the resonance peaks of the NSR spectra. The workings of the proposed method are illustrated by way of the example of the alloy  $Fe_{64}Co_{21}B_{15}$ . Two types of short-range order are used to interpret the spectra. The authors state that their decision to use two types of short-range order in this manner is indirectly substantiated by the fact that two stages of crystallization (the initial formation of an  $\alpha$ -solid FeCo solution followed by the formation of  $Fe_3B$  and  $(FeCo)_3B$  and  $Co_3B$  borides) are observed in  $Fe_{85-x}Co_xB_{15}$  amorphous alloys. After analyzing the effects of irradiation on the said alloys, the authors concluded that irradiation results in additional expansion of the frequency boundaries of the spectrum (i.e., in the appearance of new types of order, including FeCo). They conclude by demonstrating that the changes in the NSR spectra of the study alloys detected after irradiation are not stimulated by cooling. Figures 1, table 1; references 10: 9 Russian, 1 Western.

#### Erosion Wear Model of Brittle Material Under Impact of Solid Particles Accelerated in Gas Nozzles

927D0048B Minsk TRENIE I IZNOS in Russian  
Vol 12 No 4, Jul-Aug 91 pp 617-623

[Article by L.I. Urbanovich, Ye.M. Kramchenkov, Yu.N. Chunakov, Lipetsk Polytechnic Institute]

UDC 629.193.1

[Abstract] Simulation of erosion in power plants and transport devices where solid particles are accelerated by a gas flow using experimental units operating by the particle acceleration principle and the use of such units for examining gas-abrasive erosion are discussed and a problem of developing a model which would describe the acceleration of particles of various diameters inside a cylindrical gas nozzle, their acceleration in a jet after escaping from the nozzle, and erosive deformation and breakdown of the material surface layer during the impact of the entire erodent mass is formulated. To this end, the target material is assumed to be brittle. The assumptions made in developing the model are summarized. Bernoulli's, Clapeyron's, and continuity equations

are used to describe the gas motion in the nozzle. The erodent particles of a known grain size whose diameters are distributed by Rosin's and Rammel's or lognormal law are accelerated both in the nozzle and the jet; since the erodent concentration in the two-phase system is low, the particles do not interact with each other. The model makes it possible to predict the degree of erosion wear for given target strength and mechanical properties as well as gas flow parameters, incidence angle, and nozzle configuration as well as identify the effect of elevated and lowered temperatures on erosive wear if the temperature dependence of the notch sensitivity index, hardness, and Young modulus is known. It is recommended that light gases, e.g., hydrogen and helium, be used for creating high collision velocities in future experiments. Figures 5; references 13: 8 Russian; 5 Western.

#### On Correlation of Wear in Gas- and Hydroabrasive Jets

927D0048C Minsk TRENIE I IZNOS in Russian  
Vol 12 No 4, Jul-Aug 91 pp 633-639

[Article by P.K. Kallas, Tallinn Engineering University]

UDC 620.178.167

[Abstract] Gas-abrasive and hydroabrasive wear is defined pursuant to GOST 27674—88 as resulting from the effect of solids or solid particles which are entrained by a gas or liquid flow, i.e., differ in the character of the medium. Titanium carbide powder alloys are tested under identical conditions in a TsUK-3M centrifugal accelerator and a hydroabrasive wear tester at an 80 m/s jet velocity and 30, 60, and 90° angles of attack using quartz sand with a 10,000-12,000 GPa hardness and a 0.1-0.3 mm grain size as the abrasive and water+1 mass % of sand as the hydroabrasive medium. The correlation between the wear rates (in  $mm^3$  per 1 kg of abrasive material reaching the sample) in various experimental units is estimated by a linear regression coefficient. Given a 95% confidence of 18 measurement, the linear regression coefficient is  $|A| \geq 0.47$  yet the wear rate in the hydroabrasive jet is 4.25 times lower than that in an abrasive jet without water because the particle velocity is lower than that of the liquid while water forms a stable film on the material surface which consumes a certain proportion of the abrasive particle energy. Wear types correlate in gas- and hydroabrasive jets under the same testing conditions if the mechanical action of abrasive particles is dominant; the wear rate is virtually identical if the abrasive particle velocities are equal in both jets and the effects of the media may be ignored; and tests of hydroabrasive wear of materials which are stable in a liquid medium may be replaced with tests with abrasive particles in an air jet using the TsUK-3M accelerator. Figures 3; tables 3; references 15.

**Plastic Deformation Development and Cu-Fe-O Amorphous-Crystalline Alloy Formation in Contact Interaction Zone of Cu-Steel 45 Friction Pair**

927D0048D Minsk TRENIE I IZNOS in Russian  
Vol 12 No 4, Jul-Aug 91 pp 660-666

[Article by A.V. Vereshchak, V.V. Gorskiy, A.N. Grapachevskiy, Institute of Physics of Metals at the Ukrainian Academy of Sciences, Kiev]

UDC 669.017:531.43

[Abstract] The formation of metastable amorphous-crystalline alloys of metals with oxygen on working surfaces as a result of irreversible structure, composition, and property changes under friction conditions is discussed and the sequence of modifications in the structure, composition, and properties of copper's contact zone in a Cu-steel 45 friction pair during the running in and a transition to a steady state is investigated. The friction interaction is studied in a steel 45 disc-copper block pair in a standard 2070SMT-1 friction machine at a normal load of 100 N and sliding speed of 3 m/s in the air with water-cooled surfaces. The degree of hardening throughout the contact zone is determined by measuring the microhardness. The quantitative electron probe microanalysis is carried out in angle laps making it possible to stretch the analyzed zone twenty- to thirty-fold. The microstructure through the contact zone is examined under a transmission electron microscope. An analysis shows that high-strength protective coats from the amorphous-crystalline Cu-Fe-O alloy (AKS) form on the surface after the development of plastic straining, strain hardening, and the resulting plastic strain localization throughout the contact depth and width as a result of rapid hardening of metal areas which are supersaturated with oxygen; upon reaching a critical localization value, the plastic strain mechanism changes and hydrodynamic flow occurs. Also, a transition to a steady state accompanied by a decrease in the friction coefficient and wear is observed due to qualitative and quantitative changes in the surface friction layers during the run in and correlates with the thickness of the developing Cu-Fe-O amorphous-crystalline alloy layers fully screening the lower layers of original materials from direct contact. Figures 4; tables 1; references 12: 7 Russian; 5 Western.

**Measuring Powder Material's Load Carrying Capacity Under Boundary Friction**

927D0048F Minsk TRENIE I IZNOS in Russian  
Vol 12 No 4, Jul-Aug 91 pp 683-686

[Article by V.N. Antsiferov, N.N. Maslennikov, A.A. Shatsov, I.A. Polovnikov, Republican Powder Metallurgy Engineering Scientific Center, Perm]

UDC 621.785:669.14

[Abstract] Constraints on the applicability of powder materials under contact loading conditions are discussed and the tribotechnical and mechanical properties of a number of powder materials are examined; in particular, the maximum contact pressure sustainable without catastrophic wear is determined. The characteristics of antifriction properties of powder steel and brass with various Fe, Cu, C, Sn, Al, Ni, Mo, and Cu<sub>2</sub>O compositions, i.e., the porosity, crack resistance, pressure, wear rate, friction coefficient, and critical pressure, are summarized. Iron-based test materials are prepared by annealing iron powder in a nonflowing atmosphere, preparing a charge of iron and colloidal graphite in a mixer, compacting it by molding in steel molds, and sintering. Copper-based materials are made by the same technology. The mechanical properties of materials are measured pursuant to GOST 18227-85 and impact strength—pursuant to GOST 25506-85. The structure is examined under a Neophot-21 optical microscope while the friction surfaces—under a REM-200 scanning electron microscope. Friction tests are carried out pursuant to GOST 26614-85 in an SMTs-2 tester. The tests demonstrate that the properties of these materials are at least equal to those produced using other sintering atmospheres. An expression which links the critical pressure limiting the powder material's applications to porosity characteristic, parameters of the bearing surface curve, and the notch sensitivity index threshold is derived. Figures 2; tables 1; references 12: 11 Russian; 1 Western.

**Control of Telescopic Expansion Joint Seal Unit Operation in Floating Derrick**

927D0048H Minsk TRENIE I IZNOS in Russian  
Vol 12 No 4, Jul-Aug 91 pp 727-733

[Article by N.B. Ananichev, V.I. Atopov, Volgograd Civil Engineering Institute]

UDC 622.242.4:620.162.4

[Abstract] The operation of the telescopic expansion joint seal assembly whose principal element is a joint of two tubes moving one inside the other is described and it is shown that friction and wear of the seal's rubber part in the steel tube are the diagnostic variables in the operation of the telescopic compensating joint seal

assembly while the seal contact with the tube, i.e., hermetic sealing, is ensured by the control pressure which is one of the main factors affecting the seal wear. The taut strained state (NDS) of the seal is considered at a random control pressure which ensures hermetic sealing. An analysis of the stress distribution and contact pressures in the seal at low control pressures shows that the stressed state is highly nonuniform in the seal and that both low and high control pressures lead to a highly nonuniform wear distribution in the seal contact surface. High control pressures lead to an elevated seal wear along the contact area contour. An analysis made by the finite elements method (MKE) makes it possible to develop recommendations for determining the optimum control pressure (0.35 MPa) ensuring a hermetic joint seal and the maximum seal longevity. It is noted that the seal wear at the optimum control pressure is examined in the presence of abrasives of various grain sizes in the contact zone and at various ambient temperatures. Figures 7; references 4.

#### Investigation of Friction Surface Submicrorrelief by Scanning Tunnel Microscopy Method

927D0048A Minsk TRENIE I IZNOS in Russian  
Vol 12 No 4, Jul-Aug 91 pp 596-603

[Article by S.A. Chizhik, A.M. Troyanovskiy, A.I. Sviridenok, Metal-Polymer System Mechanics Institute, Gomel and Resource Saving Problems Institute at the Belarus Academy of Sciences, Grodno, and Microelectronics and Especially Pure Materials Technology Problems Institute at the USSR Academy of Sciences, Chernogolovka]

UDC 621.9.015:621.385.833

[Abstract] The experience of microrrelief studies of solid surfaces is reviewed and the task and method of examining the submicrorrelief of friction surfaces by the scanning tunnel microscopy (STM) method are formulated. The surfaces of an aluminum alloy which serves as the basis of data media on hard discs are investigated; to this end, the surfaces are subjected to three types of machining: finishing by a diamond tool, grinding by an abrasive jet, and polishing by a free abrasive material. The machined surfaces are then studied under a scanning tunnel microscope in a vacuum. An analysis of the standard deviation of the surface profile shows that the type of machining affects primarily the long-wave surface microrrelief component and becomes dominant with an increase in the scanning path length. In small scanning areas, the long-wave topography components do not fall within the instrument field of view and the standard deviation drops to a certain value which depends little on the machining type but is probably specific to each material. In the case under study this value is 2.0-2.5 nm. Direct measurements also reveal a two-level topography profile, i.e., roughness and subroughness. It is noted that the above study does not exhaust scanning tunnel microscopy applications to tribology. The authors are grateful to M.S. Khaykin and V.S. Edelman for support, the staff of the Data Media Department at the

Computer Science Research Institute at the Lithuanian Production Association "Sigma" for discussing the results, and Ye.V. Kovalev for help with programming. Figures 5; references 20: 17 Russian; 3 Western.

#### Chemical Analysis Monitoring of Magnetic Alloy Composition in Sm-Co-Fe-Cu-Zr System

927D00521 Kiev POROSHOVAYA METALLURGIYA in Russian No 11(347), Nov 91 pp 94-96

[Article by Ye.V. Yukhimeno (deceased), V.A. Dubok, Material Science Problems Institute at the Ukrainian Academy of Sciences]

UDC 543.43:621.543

[Abstract] The development of reliable procedures for precise analytical monitoring of the chemical composition of both end and intermediate products in the technological cycle of making five-component Sm-, Co-, Cu-, Fe-, and Zr-containing magnetic alloys which are accessible to any chemical lab and make it possible to attain reproducible properties of the alloys is discussed. Several method of determining the concentration of individual alloy components with a 95% confidence are summarized and it is shown that the method of hydrolytic cobalt and copper separation from the easily hydrolized zirconium, iron, and samarium ions using borax as the precipitating agent makes it possible to fully separate the mutually interfering elements in Sm-Co-Fe-Cu-Zr alloys without repeat precipitation as well as use the chelatometry titration method. The proposed chemical analysis monitoring method is distinguished by its simplicity and is sufficiently accurate and proximate. Tables 2; references 4.

#### Niobium Analysis in Rock After Precipitation of Complex With Pyrogallol on Silica by Ethylene Oxide Polymers

927D00534 Moscow ZAVODSKAYA LABORATORIYA in Russian Vol 57 No 6, Jun 91 pp 7-8

[Article by O.A. Kozmenko, R.F. Mustafayev, A.M. Lazutkin, Geology and Geophysics Institute at the Siberian Branch of the USSR Academy of Sciences, Novosibirsk, and Novosibirsk Branch of Kemerovo Scientific Production Association Karbotit]

UDC 546 882.543.42.062

[Abstract] The possibility of using ethylene oxide polymers (PEO) as a coagulating agent for extracting niobium from chloride solutions on freshly precipitated silica complex of pyrogallol-Nb is investigated and the spectral photometry method with sulfochlorophenol S is used for the post-concentration analysis. Chemically pure grade agents, distilled water, and polyethylene oxide TU-6-05-231-340-86 are used in the study. Ethylene oxide polymers with a molecular mass (m.m.) of  $2.6 \times 10^6$  is used for niobium analysis. The experimental procedure is outlined. Five eclogite batches with a  $(7.3 \pm 0.2) \times 10^{-4}$  g/t niobium content are tested with a 0.95

confidence using both ethylene oxide polymers and gelatin. The results demonstrate that the use of ethylene oxide polymers is preferable to the more traditional gelatin and makes it possible to decrease the batch weight of the sample to be analyzed, increase the analysis accuracy, reduce the outlay of agents, and shorten the analysis duration. Tables 1; references 3: 2 Russian, 1 Western.

#### Photometric Analysis of Petroleum in Waste Water

927D0053B Moscow ZAVODSKAYA LABORATORIYA  
in Russian Vol 57 No 6, Jun 91 pp 17

[Article by V.I. Yegorova, S.V. Vasilyeva, V.A. Vasilyev, V.S. Stolyarova, Novomoskovsk Branch of the Chemical Engineering Institute imeni D.I. Mendeleyev]

[Abstract] A photometric method developed for determining the petroleum concentration in synthetic liquid fuel plant's waste water is described; crude oil is used as a reference in the analysis. The sampling, sample preparation, and analysis procedure are described and a formula for computing the petroleum concentration is cited. Light filter No. 3 with a transmission wavelength of  $\lambda = 400 \pm 5$  nm is used in the photometry analysis. The procedure is refined by different methods using artificial mixtures. Petroleum concentration data for five mixtures obtained by the proposed method are compared to the results found from the calibration curve, comparison method, and graphic method. The results are quite consistent. Thus, the proposed method makes it possible to determine the petroleum concentration in liquid fuel waste water. Tables 1.

#### Extractive X-Ray Fluorescent Aluminum Analysis in Nonferrous Metal Alloys

927D0053C Moscow ZAVODSKAYA LABORATORIYA  
in Russian Vol 57 No 6, Jun 91 pp 18-19

[Article by F.I. Lobanov, N.N. Andreyeva, N.V. Ivanova, A.I. Zebreva, L.M. Filippova, Yu.A. Ilyukevich, Kazakh State University imeni S.M. Kirov Alma-Ata]

UDC 546.621:542.61+543.422.8

[Abstract] Aluminum analysis in nonferrous metal alloys and products of metallurgical processing with the help of X-ray spectral, titrimetric, and spectrophotometry methods and their shortcomings are discussed and a combined method of determining the aluminum concentration in copper, nickel, and zinc alloys is summarized. The method involves extracting the metal beforehand and separating it from the alloys' base constituent with

the help of low-melting organic substances and determining the extracted metal content by the X-ray fluorescent analysis. Higher carboxylic acids (VKK) of C<sub>17</sub> to C<sub>20</sub> fractions and their mixtures with di-2ethylhexylphosphoric acid (D2EGFK) are used as the agents while metal extraction is conducted in temperature-controlled glass vessels or heat-resistant conical flasks. The effect of the aqueous phase acidity, temperature, phase contact duration, phase volume ratio, and aluminum and reagent concentration on the extraction degree and distribution coefficients is examined. The results obtained by the extractive X-ray fluorescent analysis are compared to those produced by the X-ray fluorescent analysis using samples of nonferrous metals made by the Mtsensk branch of the Giprosvetmetobrabotka Institute. The proposed combined method's reproducibility is characterized by its standard deviation and it makes it suitable for analyzing aluminum in copper, nickel, and zinc alloys with a low aluminum content. Tables 2; references 7: 6 Russian; 1 Western.

#### Extractive X-Ray Fluorescent Scandium Analysis in Process Solutions

927D0053D Moscow ZAVODSKAYA LABORATORIYA  
in Russian Vol 57 No 6, Jun 91 pp 19-21

[Article by A.I. Zebreva, N.N. Andreyeva, F.I. Lobanov, O.A. Manuilova, Yu.A. Ilyukevich, Kazakh State University imeni S.M. Kirov, Alma-Ata]

UDC 546.621:542.61+543.422.8

[Abstract] The importance of proximate sufficiently reliable methods of scandium analysis in solutions with a complex chemical content for monitoring scandium feedstock processing indicators is emphasized and traditional methods are summarized. The possibility of analyzing scandium in process solutions of metal production by a combined extractive X-ray fluorescent (ERF) method is examined. Higher carboxylic acids (VKK) of C<sub>17</sub>-C<sub>20</sub> and C<sub>21</sub>-C<sub>25</sub> fractions and their mixtures with, e.g., tributylphosphate and di-2ethylhexylphosphoric acid (D2EGFK) are used as the agents. The analytical procedure is described in detail. The results of scandium analysis in metallurgical process solutions by the extractive X-ray fluorescent method are cited and compared to those obtained by the extractive spectrophotometric method (ESF). The method's reproducibility characterized by the standard deviation of a single measurement from data of 16 parallel analyses is 0.11 and 0.19 given a 0.07 and 0.004 g/l scandium concentration, respectively. A comparison demonstrates that in scandium analysis by the ERF method, the relative standard deviation decreases and the analysis becomes more efficient. The method may be used for monitoring the scandium content in process solutions with a complex chemical composition. Figures 2; tables 1; references 8: 7 Russian; 1 Western.

**Elevated-Sensitivity Energy-Dispersion X-Ray Fluorescence Analyzer**

927D0053E Moscow ZAVODSKAYA LABORATORIYA  
in Russian Vol 57 No 6, Jun 91 pp 21-24

[Article by P.A. Galtsev, B.S. Iokhin]

UDC 543.426

[Abstract] The need for nondestructive proximate laboratory methods of elementary analysis with a  $<10^{-5}\%$  detection threshold (PO) for monitoring waste water of metallurgical processes for the presence of various metals, analyzing geological samples for silver and biological entities for toxic elements, and analyzing environmental samples is identified. It is shown that energy-dispersion X-ray fluorescent analysis (EDRFA) using Si(Li) detectors for recording, high-power X-ray tube for excitation, and sample radiant energy preselection (PSE) based on cylindrical Bragg's pyrolytic graphite reflectors are suitable for monitoring the content of nuclear power plants' (AES) spent fuel solutions. The advantages of the energy preselection principle over the traditional X-ray fluorescent analysis (RFA) in increasing the signal/noise ratio and lowering the detection threshold is demonstrated and the operating principles of energy-dispersion X-ray fluorescent analysis are explained. Energy band characteristics of the reflectors and excitation sources are summarized and detection thresholds of various elements are cited. The principal components of the energy-dispersion X-ray fluorescent analysis instrument are quite affordable and have suitable dimensions for plant lab conditions. It may become possible soon to replace cryogenic Si(Li) detectors with thermoelectric-cooled Si(Li) detectors, making it possible to decrease its overall dimensions and streamline its maintenance. Figures 4; tables 2; references 13: 9 Russian, 4 Western

**Use of Various Types of Flames for Photometric Analysis of Sodium, Potassium, and Lithium Impurities in Glass**

927D0053F Moscow ZAVODSKAYA LABORATORIYA  
in Russian Vol 57 No 6, Jun 91 pp 28-29

[Article by T.V. Drozhzhina, L.V. Ganyushkina, L.A. Chistyakova, L.V. Potekhina, Materials Science Research Institute imeni A.Yu. Malinin, Moscow]

UDC 535.24:666.266.6

[Abstract] The need for constant monitoring of the sodium, potassium, and lithium microimpurity concentrations in glass on the basis of silicon, boron, antimony, zinc, aluminum and rare earth metal (RZE) oxides as well as silicon, lead, boron, aluminum, and tantalum oxides due to the negative effect of alkali metal ions on the quality and service life of insulating materials is identified and an attempt is made to determine the optimum conditions for decomposing and atomizing a

sample, studying the effect of principal component fluctuations on the legitimate signal strength, and using various types of flames for analysis. The experiment is carried out in Perkin-Elmer models 403 and 2280 atomic absorption spectrometers in the emission mode. The following detection thresholds are achieved:  $6 \times 10^{-5}$  for sodium,  $7 \times 10^{-5}$  for potassium,  $5 \times 10^{-5}$  for lithium (in percent by mass). The analysis procedure and conditions are described. The procedure is checked by comparative analysis of glass with pure control solutions and by the additions methods. The relative error in analyzing glass with a complex composition does not exceed 12% (a standard deviation of 0.10). Tables 2; references 1.

**Measurement of Semiconductor Samples' Magnetoresistance**

927D0053G Moscow ZAVODSKAYA LABORATORIYA  
in Russian Vol 57 No 6, Jun 91 pp 33-36

[Article by N.N. Polyakov, Lipetsk State Teachers College]

UDC 537.311.33

[Abstract] The importance of knowing the semiconductor magnetoresistance and Hall coefficient for determining the free charge carrier concentration and mobility in semiconductor samples and practical difficulties of measuring the magnetoresistance of semiconductor materials are identified. A simple and reliable procedure is suggested for measuring physical magnetoresistance of rectangular semiconductor samples, making it possible, in addition, to measure the Hall coefficient and conductivity. The theoretical principles underlying the method are explained and the measurement procedure is described. The procedure is experimentally checked with *n*-type standard germanium wafers with a  $3 \times 10^{14} \text{ cm}^{-3}$  free electron concentration at room temperature. The results of experimental measurement of Hall's electromotive force (EDS) and relative magnetoresistance as a function of magnetic field induction of an *n*-type germanium sample are cited. The proposed procedure is promising for comprehensive studies of semiconductor crystals and films under lab conditions. Figures 3; tables 1; references 6.

**Magnetothermal Carbide Phase Analysis in Steel by Changes in Remanent Magnetization**

927D0053H Moscow ZAVODSKAYA  
LABORATORIYA in Russian Vol 57 No 6,  
Jun 91 pp 40-41

[Article by V.A. Dubrov, Ukrainian Scientific Research Institute of Metals, Kharkov]

UDC 538.24

[Abstract] The principle of magnetothermal analysis of the carbide phase in steel is outlined and a procedure of magnetothermal analysis of the carbide phase based on

measuring the remanent magnetization behavior and automatically plotting magnetothermal curves (thermomagnetograms) while heating or cooling the samples is described. A block diagram of the magnetothermal analysis unit used in the study is presented and the measurement procedure is summarized. Remanent magnetization is determined (in relative units) by measuring the leakage field by a ferroprobe magnetometer connected to a potentiometer. The method's high sensitivity is confirmed by the fact that it is able to identify cementite in iron at a 0.013% carbon content by mass. Magnetothermal curves of remanent magnetization may also be used to monitor the structural state of steel and its heat treatment conditions. Thus, the magnetothermal curves of the dependence of remanent magnetization on temperature plotted automatically make it possible to identify ferromagnetic iron carbides by the values of their Curie points. Figures 3; references 6.

**On Interrelation Between Principal Characteristics of Steel's Mechanical Properties**  
927D0053I Moscow ZAVODSKAYA LABORATORIYA  
in Russian Vol 57 No 6, Jun 91 pp 44-45

[Article by L.A. Sosnovskiy, Belarus Railroad Engineering Institute, Gomel]

UDC 620.171

[Abstract] The need to estimate both qualitatively and quantitatively the effect of changes in the ductility characteristics of steel on mechanical properties and vice versa so as to develop new alloys and improve their heat treatment conditions is stressed and an attempt is made to establish a robust correlation between the principal characteristics of mechanical properties of structural carbon and alloyed steels. An experimental data bank is used as an information source. A nondimensional complex of ultimate stress for standard bending-with-twisting testing conditions of smooth polished samples pursuant to GOST 25.502-79 and a nondimensional complex of ductility characteristics which represents a ratio of the longitudinal (integral) and transverse (local) ultimate plastic strain are used in the analysis. The results of an analysis of experimental data for carbon and alloyed steels are cited and a bell-shaped curve of the relationship between the two nondimensional complexes is plotted. The spread of experimental data is attributed to differences in the alloys' microstructure. It is speculated that the procedure may be further improved by incorporating impact strength. The results were discussed with Prof. A.P. Gulyayev who suggested that the right branch of the  $K_{\text{ultim}}-K_u$  curve corresponds to brittle failure while viscous failure is realized on the left branch. Figures 3; references 4.

**Measurement of Long-Term Strength of High-Temperature Materials by Parametric Method**

927D0053J Moscow ZAVODSKAYA LABORATORIYA  
in Russian Vol 57 No 6, Jun 91 pp 45-47

[Article by M.N. Stepnov, I.A. Inozemtseva, I.I. Trunin, K.L. Skalaban, Moscow Aviation Engineering Institute imeni K.E. Tsiolkovskiy]

UDC 620.171.311

[Abstract] The use of I.I. Trunin's parametric equation for describing the long-term strength of high-temperature alloys by a unified relationship within temperature and normal life ranges under study with sufficient accuracy is considered. To this end, the possibility of using Trunin's equation for the purpose of experiment design in order to describe the long-term properties of alloys whose fracture behavior changes during the tests using unified coefficient in all segments of the long-term static strength curve is analyzed and the maximum likelihood method is used to determine the unknown variables. The analysis shows that the standard deviation of determining the long-term strength (the longevity logarithm) using the unified curve for all segments of the long-term static strength diagram vs. the experimental data does not, on the average, exceed 2%. Consequently, for the purpose of experiment design, the unknown coefficients in Trunin's equation may with a sufficient accuracy degree be assumed constant for all long-term static strength curve segments of high-temperature materials whose fracture behavior changes during straining. Tables 2; references 6: 5 Russian; 1 Western.

**MR-5-8V Corrosion-Mechanical Testing Machine**  
927D0053K Moscow ZAVODSKAYA LABORATORIYA  
in Russian Vol 57 No 6, Jun 91 pp 60-61

[Article by V.M. Kushnarenko, A.P. Fot, O.I. Steklov, V.S. Ukhakov, G.P. Kovalevskaya, R.N. Uzyakov, Orenburg Polytechnic Institute]

UDC 620.194.2.005

[Abstract] The use of proximate method of estimating the resistance of materials to corrosion cracking (KR) under slow tension at a  $10^{-5} \text{ s}^{-1}$  rate and its inadequacy for corrosion-mechanical testing are discussed. The MR-5-8V multiposition testing machine which increases the efficiency of corrosion-mechanical tests, has a smaller footprint, and makes it possible to test eight samples simultaneously under identical or different exposures to corrosive media during slow tension or under a constant load of up to 50 N per sample is described. Its design and operation are outlined. Steel 20 and 45 samples with a 6 mm diameter (type IV, GOST 1497-84) are tested at a constant straining rate of  $3.6 \times 10^{-6} \text{ m/s}$  in corrosion chambers filled with a standard NACE medium. Test

data attest to the fact that corrosion-mechanical properties of steel 20 are considerably higher than those of steel 45; ion-plasma chrome-plating considerably improves the characteristics of steel 45; the use of inhibitors also increases the hydrogen sulfide cracking resistance. The MR-5-8V machine makes it possible to obtain a proximate estimate of the corrosion cracking strength of various materials and determine the efficacy of anticorrosion measures. Figures 1; tables 1; references 3: 2 Russian; 1 Western.

#### Effect of Niobium Microadditions to Cu-Ga Alloy on Mechanical Strength of Diamond/Metal Contact

927D0035D Kiev SVERKHTVERDYYE MATERIALY in Russian No 5(74), Sep-Oct 91 pp 18-22

[Article by Yu.V. Naydich, V.P. Umnanskiy, I.A. Lavrenenko, Material Science Problems Institute at the Ukrainian Academy of Sciences, Kiev]

UDC 546.882:669.3:669.871:539.412.1:621.791.357

[Abstract] An attempt is made to expand an earlier study of the effect of carbide-forming transition metals (Ti, V, Cr) dissolved in Cu-Ga alloys with 17.5% Ga on the diamond wettability and mechanical strength of the contact with the diamond surface by expanding the range of metals under study and investigating the effect of microadditions of niobium which displays a considerable chemical affinity for carbon on the adhesion and strength of the diamond/metal contact. The contact strength of Cu-Ga-Nb alloys with diamond as a function of the carbide-forming niobium microaddition concentration and the length of melt exposure to the diamond surface is examined at room temperature. An analysis shows that the contact strength increases to 140 MPa with niobium concentration and contact duration, then drops. This behavior is attributed to an increase in thermal stress developing on the diamond/alloy interface. A comparison of the work of adhesion on the interface to the mechanical strength of the contact for Cu-Ga alloys with Ti as well as V, Cr and Nb additions reveals a correlation between these quantities only in the low adhesion-active constituent concentration area. An increase in the work of adhesion related to a decrease in the contact wetting angle with an addition of 0.5% or more of a carbide-forming component to the alloy leads to a decrease in contact strength, i.e., upsets this correlation. Figures 4; references 9: 8 Russian; 1 Western.

#### Thermographic Analysis of Ti-C-Ni System Powder Alloys

927D0035E Kiev SVERKHTVERDYYE MATERIALY in Russian No 5(74), Sep-Oct 91 pp 22-25

[Article by I.P. Kushtalova, L.F. Stasyuk, L.M. Yupko, A.G. Mgebrova, Superhard Materials Institute at the Ukrainian Academy of Sciences, Kiev]

UDC 661.665

[Abstract] Alloys of the Ti-C-Ni systems extensively used as composite and structural materials and the processes of carbide formation in them which ensure secure diamond holding and a high matrix hardness of diamond-containing composite materials operating under abrasive wear conditions are discussed and the specific processes occurring in Ti-C-Ni powder mixtures during heating are examined. The mixtures are prepared from chemically pure titanium, nickel, carbon, and titanium carbide and investigated in the region of alloys rich in titanium by the differential thermal (VDTA-7), metallographic (Neophot-21), X-ray phase (DRON-3), and X-ray spectral microanalysis (Microscan-5) methods. The carbide formation process occurs in a 920-1,030°C range and the alloy melting range is 1,060-1,215°C. It is shown that the alloy structure can be controlled by manipulating the heating temperature and rate. The structure diversity recorded by DTA is due to the nonequilibrium of the resulting states. Figures 2; tables 1; references 3: 2 Russian; 1 Western.

#### Survival Probability Estimate of Semiconductor Chips During Machining

927D0035H Kiev SVERKHTVERDYYE MATERIALY in Russian No 5(74), Sep-Oct 91 pp 65-69

[Article by O.A. Privarnikov, V.N. Shevchenko, Zaporozye Industrial Institute and Karat Scientific Production Association, Lvov]

UDC 621.315.592:621.9

[Abstract] The survival or nondestruction probability of semiconductor chips being machined by a certain loading mechanism depends on the maximum tensile stress developing in them and the mechanical strength of the material. A method is suggested for evaluating the survival probability of semiconductor chips during machining as a function of their geometrical configuration, i.e., diameter, thickness, and initial deflection, surface quality, loading method, and load magnitude. Coefficients which determine the maximum stresses and deflections during the straightening of a concave chip are determined. The evaluation procedure makes it possible to optimize the machining process on the basis of an optimization criterion by selecting the machining method, abrasive grain size, machining conditions, and the permissible deflection at each step. It is recommended that evacuation be applied gradually to the suction cups holding the chip in order to decrease the cracking probability. The use of this principle in SASh-420 machines when polishing KSD1 chips may decrease crack rejects by 20-30%. Figures 1; tables 1; references 8

### Structure and Composition of Titanium Nitride Plasma-Diffusion Coats

927D0054G Moscow *IZVESTIYA VYSSHIKH UCHEBNYKH ZAVEDENIY CHERNAYA METALLURGIYA* in Russian No 6, Jun 91 pp 53-56

[Article by A.V. Byakova, V.G. Gorbach, A.A. Vlasov, A.N. Vashchenko, Kiev Polytechnic Institute]

UDC 669.058:(669.295+669.786)

[Abstract] The beneficial effect of titanium nitride coats on the tool and equipment durability and the shortcomings of existing ion-plasma deposition methods which do not produce reliable bonding with the base metal structure are identified and it is shown that coats produced by combining plasma jet spraying and diffusion deposition are preferable from this viewpoint. The structure and phase and chemical composition of titanium nitride-based coats deposited by the combined plasma-diffusion method are investigated. The coat application process involves successive deposition of a 10-20  $\mu\text{m}$  titanium layer and subsequent nitriding. Samples of steel 12Kh18N10T are used as the base. The configuration and microstructure of the nitride coat and the transition zone are examined. The phase composition of the diffusion layer is studied by the layer-by-layer X-ray structural analysis in a DRON-002 unit and its composition is subsequently examined by X-ray microanalysis under a Camscan electron scanning microscope with a Link-860 energy-dispersion X-ray microanalysis attachment. The quantitative element distribution in the area is examined using a standard Digimap routine with a Lineskan analysis subroutine. The local quantitative analysis is carried out using a ZAF-4 routine. The coats are characterized by the development of a three-phase nitride layer alloyed with carbon, iron, chromium, and nickel and the formation of a developed transition zone on the inner nitride layer boundary consisting of alternating alloyed intermetallic phases as well as an internal steel nitriding zone ensuring a good coat/base bonding. Compared to the single-stage method, the combined deposition procedure makes it possible to produce coats distinguished by a diversity of compositions, morphology, and structure which may have a positive effect on the coat properties. Figures 2; tables 1; references 2: 1 Russian; 1 Western

### Austenite Inclusions and Grain Size in Structural Steels

927D0054H Moscow *IZVESTIYA VYSSHIKH UCHEBNYKH ZAVEDENIY CHERNAYA METALLURGIYA* in Russian No 6, Jun 91 pp 64-66

[Article by V.K. Florov, G.N. Basova, S.K. Kalinovskiy Dnepropetrovsk Metallurgical Institute]

UDC 669.15-194.41.004.12

[Abstract] Intensive austenite grain growth resulting in a significant grain size variation at a temperature exceeding

the recrystallization point in regular-quality structural carbon steel and low-alloyed high-strength steel is noted and an attempt is made to ascertain the role of nonmetallic inclusions and hardening phase particles on the rapid grain growth phenomenon in steel 09G2—a typical representative of steel especially susceptible to overheating. Short-term static tests at a 950-1,050°C temperature were carried out pursuant to GOST 9651—84 in samples with a starting diameter of 10 mm and a design length of 50 mm. The quench hardening temperature was varied within 900-1,250°C in 25°C steps with a total 1.5 min/mm exposure. The fine structure parameters of steel 09G2 samples are determined by X-ray structural analysis in DRON-UM and DRON-1.0 diffractometers with subsequent processing of data on a computer (EVM). The dependence of the austenite grain growth in steel 09G2 and thermal resistance of secondary phase particles on temperature is plotted and the parameters of low-alloyed structural steel susceptibility to overheating are summarized. Hot-rolled strips are analyzed pursuant to GOST 1778-70 while grain boundaries and size are estimated pursuant to GOST 5639—82. An analysis reveals that the austenite grain size is stabilized in carbon and low-alloyed structural steels within a certain heating temperature range due to the retarding effect of intermediate phases and nonmetallic inclusions whose origin, morphology, and distribution are determined by the metallurgical inheritance. The discrete austenite grain growth character discovered in the study should be taken into account in optimizing the parameters of machining and heat treatment or combined austempering treatment. Figures 2; tables 2; references 6.

### Retained Austenite and Wear Resistance of Alloyed Casehardened Steels

927D0054I Moscow *IZVESTIYA VYSSHIKH UCHEBNYKH ZAVEDENIY CHERNAYA METALLURGIYA* in Russian No 6, Jun 91 pp 66-69

[Article by A.L. Geller, V.N. Yurko, Donetsk Polytechnic Institute]

UDC 669.018.25 669.112.227

[Abstract] The relationship between the quality of casehardened surfaces and the amount of retained austenite in them is discussed and the possibility of controlling the retained austenite quantity in the casehardened layer and its effect on the wear resistance of casehardenable steels of various alloying types is investigated. The behavior of metastable austenite under mechanical loading is also examined. Cylindrical samples of steels 20Kh, 25KhGT, 30KhGT, and 12KhN3A with a 7 mm diameter and 20 mm length are examined. The samples are casehardened to a 1.2-1.5 mm depth in an SShTs 6 12/9 furnace during 10 h at 920-920°C in a high-carbon natural gas medium and wear-tested in a unit with an M20 abrasive band pursuant to GOST 13344—79. The

amount of retained austenite is measured by the X-ray structural and chemical analysis methods. The wear resistance and structural parameters of casehardened steels are summarized. The study shows that retained austenite differently affects the wear resistance of casehardened steel depending on a number of factors, primarily the type of steel alloy and heat treatment conditions which, in the final analysis, affect austenite

stability to martensite transition under loading. Manganese and nickel at a concentration of 1-3% differently affect the austenite stability to martensite conversion, especially in low-alloyed steels. Retained austenite produced by oil hardening with a stabilizing exposure has a favorable substructure while casehardened steel tempering increases the austenite durability under mechanical loading. tables 2; references 10.

**Increasing Die and Mold Durability by Ion Plasma Coating. II. Coat Transition Zone Structure**

927D0052H Kiev *POROSHKOVAYA METALLURGIYA* in Russian No 11(347), Nov 91 pp 85-89

[Article by L.L. Ilichev, Yu.S. Gushchin, V.I. Rudakov, S.P. Pismenyuk, Orenburg Polytechnic Institute]

UDC 621.9.014.1

[Abstract] Part I of the report dealing with process parameters, and in particular the ion bombardment heating temperature of structural steels prior to wear resistant coat deposition (KIB), is mentioned and the transition layer formed during the condensation of wear resistant coats on steels 40 and 40Kh widely used for making molds for casting plastic products and curing rubber is investigated. The transition zone between the base metal and titanium nitride coat is studied by the methods of X-ray spectral microanalysis and transmitted light and diffraction microscopy; the study demonstrates the presence of four zones with different elementary compositions—titanium nitride, pure titanium, titanium carbide, and decarburized steel—and reveals their origin and formation mechanisms. The factors which determine the physical-mechanical properties of the hard ion plasma deposited coats are considered. Moreover, the study reveals traces of impurity atoms on contact surfaces in the transition zones. The effect of crystallographic orientation of titanium nitride's habitus planes on the layer's adhesion strength is identified. An electron diffraction spectrum analysis shows that high

adhesion strength corresponds to directions with the highest reticular density of (110) titanium nitride. Figures 1; references 5.

**Structural and Property Behavior of Titanium Nitride-Coated Hard-Alloy Tool as Function of Heating by Ion Jet During Spraying**

927D0051H Dnepropetrovsk *METALLURGICHESKAYA I GORNORUDNAYA PROMYSHLENNOST* in Russian No 4(162), Oct-Dec 91 pp 50-51

[Article by F.I. Shchedrina, A.A. Sklyarov, I.V. Shevtsova, V.A. Margolius, Scientific Production Association *Chermetmekhanizatsiya*]

UDC 669.14.018.25:539.4.015.1:[621.78.062.26-97:669.295.5.867]

[Abstract] The effect of tool base heating by the ion jet during the spraying of titanium nitride coats due to the energy transfer by high-energy titanium ions in the process of elastic collision on the properties and structure of the tool is investigated; the study attempted to establish the optimum temperature condition for ion jet surfacing of tools within a 600-800°C temperature range in a Bulat unit. Metallographic, X-ray structural, X-ray microanalysis, and fractographic studies are conducted in order to determine the reason for the increased tool wear. The tests make it possible to identify the following optimum temperature conditions of ion jet heating of tools from the T5K10, T15K6, and VK-6 hard alloys: a 650-670°C for the T5K10 and T15K6 and 670-700°C for the VK-6. Tables 1.

**Predicting Characteristics of Mechanical and Physical Properties of Hollow-Sphere-Reinforced Plastics**

927D0011.4 *Riga MEKHANIKA KOMPOZITNYKH MATERIALOV* in Russian No 3, May-Jun 91  
pp 403-411

[Article by Yu.A. Dzenis and R.D. Maksimov, Institute of Polymer Mechanics, LaSSR Academy of Sciences, Riga]

UDC 539.4:539.2

[Abstract] The behavior of composite materials consisting of a polymer binder matrix and hollow spherical filler inclusions is predicted by calculation of their mechanical properties including creep and their city, thermophysical properties. The calculation of all properties is based on the same model of an isotropic medium which consists of a thermoplastic or thermosetting polymer binder and a two-phase foam filler in the form of spherical glass shells with an air core inside each, these calculations covering the  $v = 0-0.6$  range of filler volume fraction. Known relations are used accordingly for the effective density  $\rho$ , compressive strength  $\sigma_c$ , Young's modulus  $E$  (also specific modulus  $E/\rho$ ) and Poisson's ratio  $\nu$ , bulk modulus  $K$  and shear modulus  $G$ , thermal conductivity  $\lambda$  and specific heat ( $c_a$  at constant stress,  $c_s$  at constant strain), coefficient of linear thermal expansion  $\alpha$ , compliance  $I$ , and relaxation time  $\tau$ . Both stress and strain tensors are involved in the calculation of mechanical properties and their dependence not only on the filler volume fraction but also on the ratio of glass volume to air volume (ratio of inside-to-outside shell radii) as well as on the respective properties of polymer and glass. The extreme two cases here are solid glass spheres and air-filled pores. Viscoelastic behavior of the aftereffect type is described by Fredholm's integral equation of the second kind with creep kernels  $K_E$  or  $K_G$  which involve the respective compliance coefficient and the relaxation time, moduli of elasticity  $E$  and  $G$  having been replaced with their complex dynamic analogs. This equation is solved for compliance creep as a function of time over a period of 100,000 h. There follows calculation of the degree of creep (relative change of compliance) and the loss tangent (energy dissipation during harmonic viscoelastic deformation) in terms of their dependence on the filler volume fraction. In calculation of the thermophysical properties is considered not only their dependence on the filler volume fraction but also their temperature dependence over the 20-150°C range, which includes glass transition of the polymer binder. The expressions covering this entire gamut of properties are, for an illustrative numerical evaluation, applied to

composites of the "EDT-10 epoxy (binder) + MSO-779 glass microspheres (filler)" system. A comparison of the thus predicted properties with experimentally data obtained by their measurement shows a satisfactory agreement and thus validates this method of their prediction. Noteworthy is that replacement of hollow spheres with solid ones does not significantly lower the degree of creep and that their replacement with air-filled spherical pores makes the degree of creep independent of their volume fraction. The minimum degree of creep is found to be attained with thin glass shells having a 0.98 ratio of inside-to-outside radii. Figures 7; references 26.

**Friction Properties of Hard-Faced Alloy-Steel 45 Pair in Heavy-Duty Loading Conditions in Argillaceous Mud**

927D0048E *Minsk TRENIYE I IZNOS* in Russian  
Vol 12 No 4, Jul-Aug 91 pp 678-682

[Article by V.I. Dvoruk, A.I. Belyy, State Scientific Research and Design Institute of Petroleum Engineering and Electric Welding Institute imeni Ye.O. Paton at the Ukrainian Academy of Sciences, Kiev]

UDC 621.891

[Abstract] The coating of working surfaces with wear-resistant layers by the plasma jet hard-facing method as a means of increasing their durability under intensive abrasive wear conditions is discussed and the results of an examination of the tribotechnical properties of a pair formed by a hard-faced alloy (NS) deposited from a powder wire and steel 45 under heavy-duty loading conditions in an argillaceous mud medium containing abrasive particles are presented. The tests are performed in an upgraded SMTs-2 friction machine by grinding a notch on a parallelepiped block base surface by a disc. The frictional torque is constantly measured during the tests and the samples' wear is determined on an analytical balance accurate within 0.001 g. The results of three measurements are statistically processed and hardness is measured in a TK-2 Rockwell tester. It is shown that alloys hard-faced from powder wire by the plasma jet method are an efficient means of improving the friction properties of working surfaces under sliding friction in a clay mud containing abrasive particles while the wear and hard-faced alloy grinding ability do not always correlate with the initial hardness and are largely determined by the properties of secondary structures forming during friction. On the other hand, the wear and grinding ability of the hard-faced alloy-steel 45 friction pair correlates with the properties of secondary structure: the greater the secondary structure hardening, the lower the wear. Figures 2; references 9.

**Wettability and Contact Interaction in Graphite-Nickel-Titanium Melt System**  
**927D0035B Kiev SVERKHTVERDYYE MATERIALY**  
*in Russian No 5(74). Sep-Oct 91 pp 8-11*

[Article by V.M. Perevertaylo, V.G. Delevi, O.B. Loganova, L.V. Trunovich, Ye.S. Cherepenina, A.V. Gorbach, Superhard Materials Institute at the Ukrainian Academy of Sciences, Kiev]

UDC 539.219.3:620.18

[Abstract] The role of contact interaction of carbonic materials with molten metals in the individual phase structure development on interfaces of multicomponent metallic melts and carbonic material is addressed and the patterns of wetting and contact interaction of nickel-titanium melts with the MGP-6 graphite are examined. Particular attention is focused on studying the effect of the enhancement of interatomic interaction among the components in the melt on the character of interaction in the system in the solid/liquid interface area. The wetting degree is determined at a 1,773K temperature by the sessile drop method in a  $2 \cdot 10^{-3}$  Pa vacuum while simultaneously heating the melt/graphite substrate system. The structure of the alloy and interface areas formed by the Ni-Ti melt contact with graphite and subsequent cooling is examined metallographically under a MIM-8-M microscope and by X-ray spectral microanalysis under a Microscan-5 analyzer. The study reveals a certain titanium temperature range (up to 4% at.) where the melt interaction with graphite is almost the same as that of nickel with carbon while a dense, usually carbide, layer forms at a titanium concentration of 15-55% at. and prevents subsequent carbon diffusion. Loose titanium carbide layers form at Ti concentrations above 55% at. The relationship between interface's capillary characteristics and the interaction of components with each other and the solid phase is examined. The dependence of graphite wetting by the Ni-Ti melt on the

titanium concentration is divided into three areas corresponding to certain features of contact interaction of components with each other and the solid phase. Figures 2; references 8: 7 Russian; 1 Western.

**Effect of Graphite-Like Boron Nitride Structure and Properties on Elbor Synthesis**

**927D0035C Kiev SVERKHTVERDYYE MATERIALY**  
*in Russian No 5(74). Sep-Oct 91 pp 12-14*

[Article by A.N. Porada, S.N. Pikalov, L.I. Feldgun, V.M. Davidenko, I.R. Yalushev, Zaporozhye Production Association Abrazivnyy kombinat and All-Union Scientific Research Institute of Abrasives and Grinding, Leningrad]

UDC 621.923

[Abstract] The effect of the chemical composition, dispersion degree, crystalline structure, and specific surface of various types of graphite-like boron nitride (GNB) used in the USSR for synthesizing elbor borazon material on the elbor properties is examined using conventional procedures. Elbor is synthesized in high-pressure anvil chambers from reaction mixtures containing various graphite-like boron nitride samples with the same percent and phase concentration of the remaining components at constant thermodynamic parameters and time ensuring the maximum yield of 125/100 and 100/80 elbor grain effect (used most widely for making abrasive tools). After the synthesis elbor is chemically enriched, sorted, and hardened in order to produce a material which meets the requirements imposed on LKV elbor. An analysis demonstrates that the graphite-like boron nitride's mean particle size is the principal factor affecting the elbor yield. The use of the GNB-5 elbor also makes it possible to increase elbor strength by 25-30% compared to other brands. The need to develop commercial-scale methods of producing a new brand of graphite-like boron nitride similar in properties to the GNB-5 is identified. Figures 2; tables 1.

**Purity and Quality Requirements for Rare-Earth Metals and Alloys With Magnetic and Magnetostrictive Properties**

927D0014A Moscow VYSOKOCHISTYYE VESHCHESTVA in Russian No 3, May-Jun 91 pp 7-13

[Article by A.V. Yelyutin, O.Yu. Pasechnik, and G.V. Tsygankova, State Scientific Research Institute of Rare-Earth Metals Industry, Moscow]

UDC 669.85/86.5:538.22

[Abstract] As alloys (quasi-binary compounds) of rare-earth metals and especially of neodymium are increasingly used worldwide for permanent magnets better and less costly than SmCo<sub>5</sub>, there arises the problem of material purity and quality control aimed at ensuring the highest possible Curie point and coercive force as well as the largest possible maximum energy product. In this class of alloys belongs the Nd<sub>2</sub>(Fe,Co)<sub>17</sub> ("2-17" including Nd<sub>2</sub>Fe<sub>17</sub> and Nd<sub>2</sub>Fe<sub>14</sub>B (substitution of Co for Fe raises the Curie point, Nd<sub>2</sub>Fe<sub>14</sub>B having the highest Curie point of 402°C and the best magnetic properties), also Pr<sub>1-x</sub>Fe<sub>79</sub>B<sub>x</sub>. The leading industrial users of these materials abroad (General Motors in the U.S., Sumitomo in Japan) as well as the USSR rare-earth metals industry have accordingly set limits on the impurity content while various casting and powder sintering technologies are being developed by magnet manufacturers in the USSR and abroad for attainment of the desirable magnetic properties at a minimum cost. The main natural sources of neodymium in the USSR are loparite concentrate (Lovozerorsk deposits) and yttriosynchrosine concentrate (Ak-Tyuz Kutesaysk deposits), its main sources abroad (China, U.S., India, Brazil) being bastnasite and monazite concentrates. According to available data, natural reserves of neodymium should last for 100 years at projected rates of consumption. Neodymium and other useful rare-earth metals are now most economically extracted from their fluorides. It is to be noted that iron, yttrium, and other rare earth metals present in raw neodymium extracts are not necessarily detrimental impurities, while the amounts of H, C, O, Si, P, S, Cl need to be restricted. On the other hand, its alloys can be modified by addition of other elements: adding Ga or substituting Si for up to 14% Fe will raise the Curie point without significantly worsening the magnetic properties; adding Nb and Zr alone will increase the coercive force without improving the temperature characteristics, but adding Nb together with Dy and Ga will significantly improve those characteristics; adding up to 5% Re will raise the Curie point and increase the anisotropy of properties; adding Al and Ni will lower the Curie point, but adding 0.8-1.2% Al and 0.4-0.5% Si together with Dy will increase the coercive force by up to 15% and raise the maximum allowable carbon content to 0.12% C. Lowering the Cl content will increase the corrosion

resistance. Removal of hydrogen will prevent embrittlement and removal of oxygen, most effectively by casting or sintering under vacuum, will prevent formation of refractory oxides. For sintered Nd alloys, moreover, the impurity content should not exceed 1.3% La+Ce+Sm, 0.1% Ca, 0.1% Cu, 0.3% Ta or Nb. Alloys of rare-earth metals are also used for magnetostrictive devices, only ironless alloys of Tb and Dy now being produced for industrially but the USSR State Institute of the Rare-Metals Industry has already developed several R-Fe alloys (R = Gd, Tb, Dy, Er in various combinations) and devised a technology for their production on an industrial scale. Ingots of these alloys grown by the Czochralski method, after distillation of the rare-earth metals for removal of resident oxygen, included refractory oxides with the oxygen content not exceeding than 0.2-0.7 wt.%. Figures 1; tables 3; references 27.

**Production of High-Purity Silver and Copper Monohalides**

927D0014C Moscow VYSOKOCHISTYYE VESHCHESTVA in Russian No 3, May-Jun 91/1

[Article by N.V. Lichkova and V.N. Zagorodiyev, Institute of Problems in Microelectronic and Extra-Pure Materials Technology, USSR Academy of Sciences, Chernogolovka]

UDC 541.135.546.57.661.857

[Abstract] Extensive research done on producing high-purity Ag and Cu halides for infrared optics by various methods is systematically reviewed and evaluated on the basis of reported data, the five principal methods being: recrystallization, sorption, vacuum distillation, crystallization from the melt, and heat treatment in a halogen atmosphere. It has been established by experience that high-purity Ag halides are best produced from AgNO<sub>3</sub>, after the latter has been recrystallized from its aqueous or from aqueous HNO<sub>3</sub> solution with AgO<sub>2</sub> used as impurity adsorber. While pure AgCl is readily obtained by chlorination of metallic silver at temperatures below its melting point but above the melting point of AgCl, high-purity AgCl can be obtained from high-purity AgNO<sub>3</sub> and high-purity AgI can be obtained by precipitation from aqueous solution of AgNO<sub>3</sub>, HI, or an iodide salt. Another effective method of producing high-purity Ag halides is zone melting, this process requiring the lowest temperature when applied to eutectic salt mixtures as the source material. Most methods of producing high-purity CuCl and CuI involves reduction of cupric compounds, either by recrystallization and precipitation from aqueous solution in the presence of a reducing agent or by reaction of metallic Cu with Cl<sub>2</sub>, HCl, NH<sub>4</sub>Cl, CCl<sub>4</sub> or with I<sub>2</sub>, HI respectively. Extra purity is attained by subsequent zone melting (CuCl, CuI) or thermochemical treatment (CuCl) or vacuum distillation (CuI). Figures 7; tables 14; references 111.

**High-Purity Refractory Metals**

927D0014B Moscow VYSOKOCHISTYYE  
VESHCHESTVA in Russian No 3, May-Jun 91]

[Article by G.S. Burkhanov, Institute of Metallurgy  
imeni A.A. Baykov, USSR Academy of Sciences,  
Moscow]

UDC 669.172

[Abstract] The problem of producing high-purity refractory metals is analyzed by considering that the principal requirements are not only removal of impurities but also prevention or removal of crystal defects and control of the isotopic content. It is demonstrated on crystalline silver, scandium, molybdenum, tungsten and its alloys (W-Re, W-V) how increasing the degree of purity say from 99.9 wt.% to 99.99 wt.% in the raw mineral powder or in the melt affects the crystallization process, also how it affects the temperature characteristics of their mechanical and thermophysical properties in the final state. An important factor in production of high-purity single crystals are defects, namely vacancies and dislocations, each kind differently depending on the composition (impurity content) and influencing different properties of the material. A useful guide is here the constitution diagram depicting the dependence of the defect concentration as well as of the properties on the composition (impurity content). Most effective methods

of separation and purification are those which involve physical, chemical, and combination physical-chemical process such as liquid-phase extraction, transport reaction, distillation and sublimation, directional crystallization, zone refining, ion exchange chromatography, and electron transfer, magnetic separation being the most effective method of mineral extraction and subsequent metal powder purification. Largest and purest tungsten single crystals, weighing up to 10 kg with a carbon content of the order of  $10^{-6}$  atom.% C, have been produced by plasma-arc melting after dissolution of tungsten powder in  $H_2O_2$  or its oxidation in a oxygen stream and subsequent reduction of  $WO_3$  by pure hydrogen. Refractory metals can now be refined for production of single crystals as well as polymorphic or monomorphic solid phases. Highest purity of W and Mo is attained by multiple recrystallization of their salts from molten solution with subsequent reduction to pure metal and zone refining. Highest purity of rare-earth metals (lanthanide series) is attained by combining multiple distillation or sublimation with zone melting and electron transfer. Highest purity of platinum-group metals is attained by combining rerefinement with electron-arc melting. Highest purity of Zr, Hf, and also Nd is attained by combining electron-arc zone melting with subsequent annealing under high vacuum or in a controlled atmosphere and with electron transfer in the solid phase. Figures 3; references 12.

**Resistance of Steels With Higher than 600 MPa 0.2% Yield Strength and Their Welds to Fracture Under Static Load**

927D0001B Kiev PROBLEMY PROCHNOSTI  
in Russian No 7, Jul 91 pp 30-34

[Article by L.I. Mikhoduy, S.B. Kasatkin, S.L. Zhdanov, M.B. Movchan, and G.N. Strizhuis, Kiev]

UDC 536.485:649.14.018.295

[Abstract] An experimental study of high-strength alloy steels with a nominal yield strength  $\sigma_{0.2} > 600$  MPa (13CrMnMoBNb, nitrided 14CrMn2SiVCuN<sub>2</sub>, nitrided 14CrMnNi2MoCuVNbN<sub>2</sub> with  $\sigma_{0.2} > 700$  MPa) and their welds was made, these steels being designated as cold-resistant (-40°C). Specimens of the same steel, 20 mm thick with a spread out edge each, were joined by welding: specimens of 13CrMnMoBNb steel with a PP-AN54 2.2 mm powder-metal rod under a CO<sub>2</sub> gas shield, specimens of 14CrMn2SiVCuN<sub>2</sub> steel with a solid Sv-10CrMn2SiMoN<sub>2</sub> rod and specimens of 14CrMnNi2MoCuVNbN<sub>2</sub> steel with solid Sv-08CrNi2MnMoAl rod under a 78% Ar + 22% CO<sub>2</sub> gas shield. Metallographical examination under a Neofot-2 optical microscope did not reveal any significant structural differences between all these welds, their seams having a fine-disperse microstructure. Rectangular bars 140 mm long with a 15x30 mm<sup>2</sup> cross-section were cut out from these welds for bend tests by the "three points" method. Notches terminating into fatigue cracks had been cut in the seam metal, in the heat-affected zone, and in the parent metal so as to cover the entire weld in the evaluation of its resistance to brittle fracture. These tests were performed at temperatures ranging from +20°C to -60°C. The results indicate no proneness of all three steels to brittle fracture, their embrittlement temperature (second critical) being obviously lower than -60°C and the ratio of breaking fatigue stress to 0.2% yield strength being  $\sigma_{bf}/\sigma_{0.2} > 1$ . The quasi-brittlement temperature (first critical), based on the spread of critical crack opening widths, was found to be -20°C for 14CrMnNi2MoCuVNbN<sub>2</sub> steel and -40°C for the other two steels. Owing to its higher strength, however, 14CrMnNi2MoCuVNbN<sub>2</sub> steel was also found to be more sensitive to stress concentration around fatigue cracks. Welding done with optimum heat cycling had evidently not appreciably lowered the resistance to brittle fracture within the heat-affected zone, the first critical temperature having shifted upward by 20°C (from -40°C to -20°C) for the 14CrMn2SiVCuN<sub>2</sub> steel only. Most resistant to brittle fracture and least sensitive to stress concentration around fatigue cracks were found to be weld seams produced with PP-An54 wire under a CO<sub>2</sub> gas shield and those produced with Sv-08CrNi2MnMoAl wire under an Ar + CO<sub>2</sub> gas shield.

Welds of 14CrMn2SiVCuN<sub>2</sub> steel with seams produced with a Sv-10CrMn2SiMoN<sub>2</sub> (economy alloy steel) rod will not withstand temperatures below -40°C. Figures 5; references 5.

**Resistance of Ferritic-Pearlitic Steels and Their Welds to Cyclic Cracking**

927D0001A Kiev PROBLEMY PROCHNOSTI  
in Russian No 7, Jul 91 pp 25-30

[Article by M.N. Georgiyev, Heavy Machinery Manufacturing Plant, Sofia (Bulgaria)]

UDC 539.4

[Abstract] Experimental data on cyclic loading of ferritic-pearlitic steels (09Mn2Cu, quenched 09Mn2Cu, 10Mn2Nb, nitrided 06Mn2V, 18Mn-sk semikilled, plain carbon grade-3k killed) under three different load conditions are analyzed statistically and theoretically for a fatigue strength evaluation. In long-cycling tests with slow crack growth (V  $\leq 0.01$  mm/cycle) smooth specimens of these steels were found to be all about equally resistant to fatigue cracking in terms of the stress concentration factor  $\Delta K^V$  and their endurance limit in flexure to increase with increasing pearlite content. In short-cycling tests with slow crack growth fatigue cracks in smooth specimens were found to develop and remain within the ferrite phase. In tests performed at the All-Union Scientific Research Institute of Railroad Transportation on low-carbon and low-alloy steels, moreover, welds of all these steels with seams in "as received" condition were found to have approximately the same fatigue strength. In the author's tests performed by the "transverse flexure of bar on two supports" method, with a 25% load cycle asymmetry and with  $5 \times 10^6$  cycles as endurance criterion, cracks in butt welds were found to form principally along the seam and parent metal interface at the edges of the strap. His test data confirm that welds of all these steels have approximately the same endurance limit. The data are analyzed by using viability (maximum stress prior to cracking) as the criterion and  $\Delta K_{th}^* = \Delta K_{V=0.01 \text{ mm/cycle}}$  as the reference stress concentration level relative to which cracked structures become classifiable into those not requiring repair ( $\Delta K < \Delta K_{th}^*$ ) and those still safely defective ( $\Delta K_{th}^* < \Delta K < \Delta K_{allowable}$ ). The results of this analysis are shown to be useful not only for predicting the viability of welded steel structures in railroad rolling stock subject to long-cycling loads but also for design of machine parts with maximum metal economy. The author warns that minimizing the weight of welded steel structures and especially mass produced ones by using higher-strength ferritic-pearlitic steels without consideration of their resistance to cracking under cyclic loads and without a technology available for maximizing that resistance could have disastrous consequences. Figures 6; tables 3; references 17.

### Strain and Heat Treatment Hardening of Rolled Structural Steel: Problems of Production and Consumption

927D0007A Moscow *IZVESTIYA AKADEMII NAUK SSSR* in Russian No 3, 1991 pp 5-12

[Article by N.P. Lyakishev, S.P. Yefimenko, and S.I. Tishayev, Moscow]

UDC 669.14.018.29-12:539.389.2

[Abstract] A technology of quench hardening has been developed for hot rolled structural low-carbon and low-alloy steels, two of its variants having already been introduced in plants of the USSR ferrous metals industry. One variant involves hot rolling to an at least 60 % total reduction at 1150-1050°C temperatures—slow cooling to a temperature near the  $Ar_3$  point within the 800-780°C range—rolling to an at least 40 % total reduction in two or three passes at that temperature—fast cooling with a water shower on the unloading conveyor—winding into coils at a temperature not higher than 580°C. The second variant involves hot rolling at 1150-1050°C starting temperatures with the finishing temperature not lower than 900-840°C—fast water cooling to a mean-mass temperature not higher than 500-600°C—self-tempering of outer layers by heat from inner layers. Mechanical tests were performed on 2-10 mm thick specimens of strip and sheet of grade-3k killed carbon steel and 09Mn2Si alloy steel thus produced in a "2000" continuous wide-strip rolling mill (Cherepovets Metallurgical Combine), their respective yield points of 330-380 N/mm<sup>2</sup> with 20-25 vol.% pearlite and 400-450 N/mm<sup>2</sup> with 10-15 vol.% pearlite exceeding those of conventionally hot rolled stock by 30-40 %. Such an "interrupted" quenching with subsequent self-tempering was found to produce a fine-disperse multi-layer structure, self-tempering at 680-650°C in a "450" mill (West Siberian Metallurgical Combine) yielding 30-50 % better mechanical characteristics than conventional hot rolling. Another variant of "interrupted" quenching, namely with accelerated subsequent self-tempering in the transfer furnace of a "3600" mill ("Azovstal" Metallurgical Combine), was also found to very effectively harden 10-25 mm thick strips of both steels. While quench hardened grade-3k carbon steel is at least as strong or even stronger than conventionally hot rolled 09Mn2Si alloy steel, quench hardened 09Mn2Si alloy steel has better mechanical characteristics than some conventionally hot rolled high-alloy steels such as 10Mn2V and 10CrNiSiCu. The impact strength of quenched grade-3k carbon steel and 09Mn2Si alloy steel at -70°C temperature is  $KCU \geq 40 J/cm^2$  and  $KCU \geq 80 J/cm^2$  respectively. Results of studies made at the Institute of Electric Welding indicate that both quench hardened strip (4-30 mm thick) and sections (up to 12 mm thick) of both steels are weldable by manual, semi-automatic, and automatic processes, uniform seam being attainable without appreciable softening of the metal (not more than 15 % reduction of hardness within surface layers extending not deeper than 2.0 mm) and

joints being attainable with an impact strength  $KCU \geq 30 J/cm^2$ . The problem now is to expand the use of this technology during the 1991-95 period so as to meet projected production quotas and consumer demand for hot rolled high-strength economy steel with guaranteed characteristics. This will require redesigning at least 5-6 different hot rolling mills for production of steel sheet and 4-5 different hot rolling mills for production of steel shapes, including the water supply system and automatic controls. It is important to cool the strip uniformly both along and across the rolls. The parameters of hot rolling and quench hardening must, moreover, be adjustable so as to make this technology adaptable to diverse grades of steel as well as to diverse shapes and sizes of rolled stock. Control of the cooling process must take into account the effect of hot plastic deformation on the kinetics of austenite transformation. In the case of 09Mn2Si steel a 15 % hot plastic deformation of the austenite at 900°C widens the range of ferrite precipitation by raising the temperature at which ferrite formation begins 30-40°C upward and appreciably lowering the temperature at which ferrite formation ends so that pearlite formation will also begin at a lower temperature and, with an only slight dropping of the temperature at which it ends, the temperature range of pearlite formation will be much narrower. A lowering of the rolling temperature would increase the resistance to deformation, which must be avoided. One possible way to ensure that strip of structural low-carbon and low-alloy steels have the required strength is to accelerate its cooling from the austenite range. Water cooling 5-6 mm thick sheet of grade-3k steel from an 800-780°C rolling finish temperature and thus from a temperature below the  $Ar_3$  point should ensure an ultimate tensile strength of 650-700 N/mm<sup>2</sup>, a 0.2 % yield strength of 480-500 N/mm<sup>2</sup>, a 16-20 % elongation, and an impact strength of 60-80 J/cm<sup>2</sup> at -20°C. Figures 4; tables 3; references 11.

### Dependence of Surface Tension of Iron-Arsenic Melts on Temperature

927D0055A Moscow *IZVESTIYA VYSSHIXH UCHEBNYKH ZAVEDENIY: CHERNAYA METALLURGIYA* in Russian No 7, Jul 91 pp 1-3

[Article by P.S. Kharlashin, Mariupol Metallurgical Institute]

UDC 669.132.6-154:532.61.001.5

[Abstract] A lack of data on the effect of arsenic on various properties of liquid iron at different temperatures is stressed in light of the fact that GOST 380-71 specifies that steel smelted from arsenous pig iron may contain up to 0.150% of arsenic. The effect of arsenic on the surface tension and density of liquid iron is examined by the "big" and "sessile" drop methods. The design of the experimental unit and testing procedure is outlined. Samples are made by alloying iron containing 0.001% C, 0.002% Si, 0.004% S, 0.003% O, and no As, P, or Mn with a ferroarsenic alloying mixture containing

30.25% As, 0.01% C, 0.005% S, 0.003% Si, 0.002% O, and traces of P and Mn in a vacuum furnace at a  $6.7 \times 10^{-3}$  Pa pressure. The metal temperature is measured by a PR 30/6 thermocouple and by an optical pyrometer. The results show that  $\beta_{Fe}$  and  $\sigma_{Fe}$  of initial iron at 1,600°C is 7,200 kg/m<sup>2</sup> and 1,850 MJ/m<sup>2</sup> which is consistent with published sources. The experimental values of surface tension of iron and molten ferroarsenic alloying mixture as a function of temperature are approximated by equations whose temperature coefficients are calculated by the least squares method. Poly-thermal curves of the iron-arsenic alloys' surface tension and density are plotted, revealing their negative temperature coefficients. The measurements by "big" and "sessile" drop methods in a pure argon atmosphere make it possible to investigate the temperature dependence of the iron-arsenic alloys' surface tension and demonstrate a good consistency of analytical and experimental values of the  $d/dT$  coefficient of the Fe-As system. Figures 2; tables 1; references 11.

### On Possibility of Refining Ferriferous Red Mud by Liquid Phase Reduction Process

927D0055C Moscow IZVESTIYA VYSSHIKH UCHEBNYKH ZAVEDENIY: CHERNAYA METALLURGIYA in Russian No 7, Jul 91 pp 6-7

[Article by V.S. Valavin, S.K. Vildanov, S.V. Vandaryev, Moscow Steel and Alloy Institute]

UDC 669.181.422

[Abstract] The issue of utilizing red mud—a valuable byproduct of aluminum production—accumulated in aluminum smelter waste dumps, occupying a total area of close to 800 ha, in order to recover iron is addressed. To check the possibility of utilizing red mud as an iron-containing feedstock for the liquid phase reduction (PZhV) refining process, experiments are conducted in order to determine the synthetic final slag viscosity. Viscosity is measured by an EVI-K81 rotary electric viscosimeter. Three types of slag containing various amounts of SiO<sub>2</sub>, Al<sub>2</sub>O<sub>3</sub>, CaO, MgO, TiO<sub>2</sub>, Na<sub>2</sub>O, and FeO of varying basicity are tested and their dependence of viscosity on temperature is plotted. An attempt is made to establish whether titanium carbide forms during the red mud refining since its presence in the molten slag significantly increases the slag's effective viscosity and facilitates the slag thickening during its tapping. The degree of iron oxide reduction from liquid slag is estimated experimentally. An analysis shows that at a 1,450-1,550°C temperature the viscosity of synthetic slags obtained from red mud attests to the possibility of red mud refining by the liquid phase reduction method and that at a 1,500-1,550°C temperature titanium carbide does not form in the molten slag-graphite system. Thus, iron oxide reduction by graphite from molten slag makes it possible to recover iron from red mud by the liquid phase reduction process. Figures 3.

### Metalization of Iron-Containing Nickel-Making Byproduct Pellets in Cuba

927D0055D Moscow IZVESTIYA VYSSHIKH UCHEBNYKH ZAVEDENIY: CHERNAYA METALLURGIYA in Russian No 7, Jul 91 pp 10-13

[Article by Yu.S. Yusfin, Yu.B. Voytkovskiy, T.N. Bazilevich, T.G. Kostyukovich, Guillermo Castedo, Moscow Steel and Alloy Institute]

UDC 669.162.12

[Abstract] The importance of utilizing iron-containing byproducts of the nickel industry in the Republic of Cuba is considered from the viewpoint of both saving domestic resources and protecting the environment: more than 30 million tons of nickel tailings have been warehoused in Cuba and more than 1.5 million tons are added annually from the Moa nickel smelter. A version of the method to produce metal outside the blast furnace by metallizing oxidized pellets in a shaft furnace with subsequent smelting in electric furnaces is investigated for the purpose of developing an ecologically clean process. The composition of the naturally alloyed Moa concentrate used in the experiments is described. The pellet structure and composition are studied by the methods of chemical analysis, optical microscopy, X-ray phase analysis, and nuclear gamma resonance microscopy (YaGRS) and the reproducibility of the results is checked by the data on 2-3 independent measurements. The study shows that the pellet hardening during the oxidizing annealing occurs under the liquid phase sintering conditions and positively affects the pellets' strength during their reduction. The amount of bound carbon in the 0.5 mm thick surface layer is calculated on the basis of nuclear gamma resonance microscopy. The study confirms that in principle, it is possible to obtain highly metallized pellets from naturally alloyed Moa concentrate; the experiment also demonstrates that the end product is an alloy containing up to 5% of Ni, Co, Mn, and other impurity metals rather than pure iron. Characteristic features of naturally alloyed Moa concentrate pellet carburization are compared to those of "pure" Lebedin concentrate; the former have a higher coalescence temperature. Thus, a new factor in controlling the metallized pellet coalescence is established. Figures 3; tables 2; references 2.

### On Calcium's Effect on Steels With Various Carbon Contents

927D0055E Moscow IZVESTIYA VYSSHIKH UCHEBNYKH ZAVEDENIY: CHERNAYA METALLURGIYA in Russian No 7, Jul 91 pp 13-17

[Article by Ye.L. Zats, V.N. Radchenko, A.D. Ryabtsev, Ye.L. Ivanov, Donetsk Polytechnic Institute]

UDC 669.187.56:669.891.112.001.5

[Abstract] Contradictory data on the inoculating and microalloying effect of calcium on various brands of

steel are cited and the refining, inoculating, and microalloying effect of calcium is estimated on the basis of the results of its impact on the chemical composition, non-metallic inclusions, and the structure of low-sulfur steel with various carbon contents which serves as the basis for making virtually all brands of steel. The study shows that as the calcium concentration increases, the sulfur and phosphorus content in steel decrease substantially: high-carbon steels have the lowest sulfur content while low-carbon steels have the lowest phosphorus content. A considerable decrease in the carbon content is manifested most vividly in medium-carbon steel with a calcium concentration exceeding 0.006% and less so in high-carbon steel with a lower calcium content (0.002-0.003%). In high-carbon steel, the greatest deoxidation and denitration effect is attained at significantly lower calcium contents than in low-carbon steels. An increase in the calcium content to 0.003% decreases the oxygen concentration and, consequently, the number and size of oxide inclusions. As the carbon content in steel increases, the oxide inclusions become spheroidized at lower  $[Ca]/[O]$  ratios. Calcium has the greatest inoculating effect on the primary dendritic structure and dendritic inhomogeneity as well as the strongest dispersing impact on the secondary microstructure after refining at a 0.002-0.005% concentration. Figures 3; tables 2; references 8.

### Physical Simulation of Continuously Cast Steel Ingot Solidification on Planar Pattern

927D0055F Moscow *IZVESTIYA VYSSHIKH UCHEBNYKH ZAVEDENIY: CHERNAYA METALLURGIYA* in Russian No 7, Jul 91 pp 22-24

[Article by V.V. Stulov, Yu.G. Gontarev, G.A. Nikolayev, A.G. Yakovenko, O.V. Nosochenko, Dnepropetrovsk State University]

UDC 621.746.51

[Abstract] Steel solidification is simulated by paraffin due to the need to develop a steel casting method through two ladle nozzles with one outlet in each. Since the mold pattern has a blind bottom, the effect of convective melt motion on the ingot rim development in the mold is investigated. A block diagram of the experimental unit and its design are shown and its operation is described. Simulation is carried out for the following similarity criteria:  $Fo = 0.08$ ;  $Fr = (0.9-1.53) \times 10^{-2}$ ; and  $Bi = 64-560$  given a 45-90 s duration of the mold filling with liquid paraffin. The simulation results are presented as the dependence of the relative solidified rim thickness on Fourier's criterion. An analysis of the results indicates that intensive melt agitation inside the incipient ingot decreases the relative rim height by an average of 10-30%. When steel is cast with a molten metal contact zone with the wall, heat extraction in the mold increases and, in turn, increases the rim's rate of growth. Thus, the use of steel casting through two ladle nozzles is expedient for making slabs with a greater

cross-sectional dimension if the ingot cooling conditions in the cope are improved at a 300-400 mm height. An increase in heat removal from the mold shortens the ingot formation time and increases the productivity of the continuous casting machine (MNLZ). Figures 3; references 2.

### High-Temperature Unit for Measuring Molten Metal Viscosity

927D0055G Moscow *IZVESTIYA VYSSHIKH UCHEBNYKH ZAVEDENIY: CHERNAYA METALLURGIYA* in Russian No 7, Jul 91 pp 29-32

[Article by V.Yu. Korolev, A.F. Vishkarev, D.V. Kremenskiy, Yu.I. Nebosov, Moscow Steel and Alloy Institute]

UDC 669.017.111:532.13

[Abstract] The effect of viscosity—a characteristic which determines the kinematics of molten metals and is structurally sensitive and may be used for analyzing the processes of diffusion and mass transfer and determining the kinetics of metallurgical reactions and solidification processes and the ingot structure, i.e., may serve as a useful indicator of the efficiency of various physical and chemical measures—is investigated and the requirements which are imposed on experimental units for measuring viscosity are formulated. An efficient viscosity measuring procedure in the framework of the paraboloid of revolution method is developed and an equation is derived for determining the kinematic viscosity of molten metal. The viscosimeter design and operating principle are described and the dependence of copper's kinematic viscosity on temperature is plotted. The viscosimeter calibration procedure is outlined. A residual standard deviation of  $0.01 \times 10^{-6} \text{ m}^2/\text{s}$  is achieved in nickel smelting. The unit makes it possible to measure the viscosity of molten metals in a 400-2,000°C temperature range and is characterized by simplicity, practical feasibility, and the possibility of completely automating the experiment without sacrificing the accuracy of experimental data. Figures 4; references 5

### Analyzing Gaseous Phase Composition During Melt Processing by Methane and Propane in Vacuum

927D0055H Moscow *IZVESTIYA VYSSHIKH UCHEBNYKH ZAVEDENIY: CHERNAYA METALLURGIYA* in Russian No 7, Jul 91 pp 32-34

[Article by B.V. Linchevskiy, V.A. Mashin, N.V. Mitin, Moscow Metallurgical Night School]

UDC 669.046.558.8

[Abstract] The gaseous phase composition in a vacuum induction furnace is investigated during the smelting of a high-temperature alloy when the metal surface is being treated with a hydrocarbon-containing gas. The gaseous

phase is analyzed by an MKh-7301 radio-frequency mass spectrometer whose sensor is inserted directly in the furnace chamber. The mass spectrometer is calibrated beforehand by pure gases and their mixtures. A spectrogram of the gaseous phase composition in the vacuum induction furnace (VIF) is plotted and the gaseous phase composition is determined in the cold furnace and during the smelting. The mean relative error of the CO, C<sub>2</sub>H<sub>2</sub>, and N<sub>2</sub> analysis is 5% and that of CH<sub>4</sub> is 4%. An intensive release of gases during the metal agitation in the vacuum induction furnace during the smelting of high-temperature alloys is noted. The presence of CO in the mixture fits the hypothesis of metal deoxidation by carbon by the reactions [C]+[O] = [CO] and [C]+2[O] = CO<sub>2</sub>. The role of hydrogen is secondary. Thus, melt treatment with methane makes it possible to noticeably decrease the oxygen content in it. Figures 4; tables 2; references 2.

#### Investigation of Viscosity and Melting Point of Boron-Containing Protective Lubricating Mixtures for Steel Casting

927D0054B Moscow *IZVESTIYA VYSSHIKH UCHEBNYKH ZAVEDENIY. CHERNAYA METALLURGIYA* in Russian No 6, Jun 91 pp 14-16

[Article by V.L. Zhuk, S.V. Timofeyeva, V.N. Moshenskiy, Donetsk Polytechnic Institute]

UDC 669.046:621.746.047

[Abstract] The effect of physical-chemical properties of the protective lubricating mixture and the slag forming from it in the mold on the quality of continuously cast ingots, especially the initial and final melting temperature of the mixture and slag viscosity, is examined and an attempt is made to find an efficient combination of amorphous graphite—the basic constituent of the mixtures—and the boron-containing material, i.e., the datolite concentrate, which improve the physical-chemical properties of the charge or mixture. The rational component ratio is found by measuring the melting range and viscosity of the molten slags formed from mixtures consisting of amorphous graphite with a 20-70% addition of calcinated datolite concentrate as well as the ash made by burning out the amorphous graphite in an air current at a 800-900°C temperature. The melting point is measured in a resistance microfurnace with a platinum electrode. Component ratios, chemical compositions, and melting points of the mixtures are summarized and the dependence of slag viscosity on temperature is plotted. An analysis demonstrates that protective lubricating mixtures for continuous casting containing 45-70% datolite concentrate have the best performance, making it possible to recommend them for use under commercial conditions. Figures 2; tables 1; references 3.

#### Viscosity and Desulfurizing Ability of Natural and Synthetic Blast Furnace CaO-MgO-Al<sub>2</sub>O<sub>3</sub>SiO<sub>2</sub> Slags

927D0055B Moscow *IZVESTIYA VYSSHIKH UCHEBNYKH ZAVEDENIY. CHERNAYA METALLURGIYA* in Russian No 7, Jul 91 pp 3-5

[Article by S.Yu. Gruzdeva, N.L. Zhilo, A.V. Denisov, Scientific Research Institute of Metallurgy and Integrated Iron and Steel Works, Chelyabinsk]

UDC 669.046.582.5

[Abstract] The importance of optimal slag conditions and efficient final slag composition selection for improving the blast furnace performance and pig iron quality, reducing the sulfur content, and increasing the furnace output is emphasized and the temperature dependence of the viscosity of final blast furnace slag from the Chelyabinsk Integrated Iron and Steel Works (ChMK) is investigated. In addition, the effect of CaO substitution with magnesia on the viscosity parameters and desulfurization properties of slags with varying basicity relative to (CaO+MgO):SiO<sub>2</sub> is ascertained in order to select the optimal MgO content and CaO:SiO<sub>2</sub> ratio in slags which ensure normal blast furnace performance and help reduce the sulfur content in pig iron. A rotary electric viscosimeter is used to measure viscosity and a PR 30/6 Pt-Rh thermocouple is used to measure temperature. Polythermal curves of viscosity are plotted on the basis of experimental data. The desulfurizing ability of slags with 8 and 12.5% MgO is examined as a function of the total (CaO+MgO):SiO<sub>2</sub> basicity in graphite crucibles at a 1,500°C temperature using a starting metal with a 0.78% S content and 1:0.5 metal to slag ratio. An analysis of the physical properties of natural and synthetic blast furnace slag makes it possible to recommend that their total basicity be increased from 1.17 to 1.23 in order to decrease the sulfur content in cast iron from 0.028 to 0.022%. Figures 2; tables 1; references 8.

#### New Type of Steel-Making Unit

927D0051E Dnepropetrovsk *METALLURGICHESKAYA I GORNORUDNAYA PROMYSHLENNOST* in Russian No 4/162, Oct-Dec 91 pp 10-11

[Article by N.M. Skorokhod, N.A. Antonov, V.A. Rybinov, Kommunarsk Integrated Iron and Steel Works]

UDC 669.183.21.041.43:658.859:[502.55:628.51]

[Abstract] The environmental impact of open hearth furnaces—the largest source of air pollution at and around the integrated iron and steel works—is discussed and operation of a remodeled double-pool open hearth furnace at the Orsk-Khalilovo Integrated Iron and Steel Works in a transfer mode with a 100% exhaust gas

scrubbing capability is described. An experiment to replace two open hearth furnaces with a single steel-making unit equipped with two gas scrubbers operating parallel to each other is described. The new unit's dust and gas exhaust levels at the workplace are 2-3 times lower than the maximum permissible concentrations (PDK). The unit is practically feasible and easy to control. The unit is being tested and evaluated by the State Environment Protection Committee. Figures 2.

#### Molten Steel Treatment by Powder Wire in Ingot Mold

927D0051F Dnepropetrovsk  
METALLURGICHESKAYA I GORNORUDNAYA  
PROMYSHLENNOST in Russian No 4/162). Oct-Dec  
91 pp 31-32

[Article by V.A. Vikhlevshchuk, V.M. Chernognitskiy, V.A. Polyakov, V.I. Drachev, Yu.G. Badogn, N.M. Omes, Ferrous Metallurgy Institute and Krivorozhstal Integrated Iron and Steel Works]

UDC 669.141.245.046 516:621.746.393]:621.762-426.001.5

[Abstract] The efficacy of using powder wire with silicocalcium and rare earth metal (RZM) alloying compositions for refining converter steels St3sp, 08YuT, 35, 45, and Sv-08G2S in the ingot mold developed by the Ferrous Metallurgy Institute together with the Krivoy Rog Integrated Iron and Steel Works is investigated in order to develop the optimum process. Several wire addition methods are examined and an analysis shows that the best method is to feed the powder wire directly to the ingot mold immediately after casting when the aluminum content in the metal is at least 0.03%. The use of powder wire containing silicocalcium and a rare earth metal alloying mixture makes it possible to decrease the outlay of ferroalloys by 2.5-3 times due to improved absorption of the constituent elements and results in an economic gain of 1-3 rubles per ton. A.G. Mayevskiy, I.P. Khritin, and I.Zh. Dubrov participated in the research. Figures 1; tables 1; references 1.

#### G - Saturating Iron With Carbon During Blast Furnace Smelting

927D0054A Moscow IZVESTIYA VYSSHIKH  
UCHEBNYKH ZAVEDENIY CHERNAYA  
METALLURGIYA in Russian No 6. Jun 91 pp 10-12

[Article by G.A. Volovik, V.I. Kotov, P.G. Kalashnyuk, Dnepropetrovsk Metallurgical Institute]

UDC 669.162.12:622.785

[Abstract] The iron carburization reaction described in today's pig iron metallurgy textbooks is reviewed and its inconsistency with the basic premises of metallurgy is pointed out. The process of iron saturation with carbon in blast furnaces is studied in six smelting series

from different steel mills and the Si, Mn, S, P, and C content in pig iron and CO and H<sub>2</sub> concentration and partial CO pressure and temperature of the blast furnace top gas is summarized. Actual values are graphically compared to calculated data. An analysis shows that iron carburization through intermediate carbide phase formation at all pig iron development stages in the blast furnace as presented in today's textbooks is highly unlikely. In the solid state, reduced iron is carburized according to the Fe-C constitution diagram while in the liquid state, various impurities, melt temperature, carbon monoxide's partial pressure in the blast furnace gas, and other factors affect the final [C] content in pig iron. For modern smelting conditions, the results obtained from the formulas suggested by N.G. Girshovich, Yu.S. Yusin, et al., are the most consistent with actual analytical data. Figures 1; tables 1; references 13.

#### Development of Ferrous Metallurgy Viewed

92UN0145A Kiev EKONOMIKA SOVETSKOY  
UKRAINY in Russian No 8. Aug 91 pp 57-62

[Article by Yu. Dolgorukov, candidate in Economic Sciences: "Scientific-Technical Progress and the Economy's Reserves of Material Resources in the Ferrous Metallurgy of the Ukraine"]

[Text] The course of economic reform has shown the need to seek new approaches to formulating a scientific-technical policy. The scale of expenditures necessary to solve the priority problems of technical updating of metallurgical production is tremendous. It is impossible to find a way out of this situation on the basis of the traditional development of the economy. The material-technical basis of metallurgy that has been created must be qualitatively replaced by a new one, based on the advanced achievements of domestic and world science and practical work. In this case, one of the main elements of the new strategy under the conditions of the transition to a market economy should be choosing the priorities in solving the problem of accelerating scientific-technical progress and a fundamental rise, on this basis, of production efficiency, primarily through a substantial reduction in the materials-intensiveness of production. The level of production costs is, as foreign experience shows, one of the most important factors of the enterprises' competitiveness.

Acceleration of scientific-technical progress requires a new approach to solving the problems of increasing the efficiency of using material resources. In the first place, a considerable improvement will be achieved in their qualitative parameters for improving the consumption structure, and the formation of the scientifically based need for the production of goods which would meet market requirements will be ensured. In the second place, under the conditions of economic reform, the natural internal relation between production progress and resources will be strengthened. This relation will, on the one hand, provide a broader opportunity to draw resources into economic circulation on an intensive

basis, and on the other hand—will give rise to the need for their utmost conservation.

Ferrous metallurgy is the most materials-intensive sector of the national economy. Some 41 percent of the country's pig iron, 35 percent of the steel and 30 percent of the finished rolled metal is produced in the Ukraine. Some 6.2 billion rubles [R] worth of material resources (77.1 percent of the total expenditures) is consumed for their output. In 1990, as compared with 1985, the specific expenditure of skip coke was reduced by 7.6 kg (saving of 341,000 tons), the consumption of iron to smelt pig iron—by 18.5 kg (1.5 million ton saving of iron ore raw material), pig iron to steel—by 3.2 kg (155,000 ton saving) and metal to rolled metal—by 24.7 kg (934,000 ton saving). The utilization of ferraloys and refractory materials was improved. The total expenditures of fuel-energy resources estimated per ton of rolled metal was reduced by 4.9 percent (from R56.9 to R54.1 per ton). The total saving of material resources was over R120 million.

The rates of reducing the materials-intensiveness of the products, however, are insufficient (3.88 percent per year). In 1989 and 1990 the materials-intensiveness increased. There are still no stable trends toward providing for the sector's additional need for material resources through their conservation, which was satisfied in 1988<sup>1</sup>: for iron ore raw material—by 62.1 percent, for metallurgical coke—by 80 percent, pig iron for steel smelting—by 31 percent, and metal for rolled metal—by 26.6 percent. These data also attest to the substantial difference in the effectiveness of introducing resource-conserving measures within the basic limits of metallurgical production and the need to seek additional reserves to conserve material resources.

One of the reserves is to reduce the losses of iron in all the conversions of metallurgical production. The total amount of iron wasted in ferrous metallurgy is 35 million tons. An additional R1.2 billion worth of metal products could be produced from this amount of iron.

The largest part of the iron wasted is in the mining industry—17 million tons (almost 50 percent of the total losses). Of this amount, approximately 13-13.5 million tons is contained in wastes, representing feebly magnetic oxidized ores, which do not lend themselves to enrichment through the methods used to process iron ore raw material.

Considerable iron is still lost at the stage of enriching the iron ore extracted. Here, while the degree of extracting iron from crude ore at YuGOK [Southern Mining and Enriching Combine] in 1990 was 81.76 percent, at NKGOK [Novo Krivorozhye Mining and Enriching Combine] it was 68.49 percent. The basic direction for increasing the output of iron ore concentrate at mine-enriching combines is a further rise in their technical level: replacing obsolete equipment with modern, using high-intensity magnetic separators, expanding the use of ore-crushing technology to two to three stages, automating processes, etc.

DonNIIchermet made a technical economic evaluation of the basic directions in conserving material resources in the sinter production of metallurgical enterprises in the Ukraine, the results of which are systematized in Table 1. The introduction of new wholesale prices, beginning in 1 January 1991 has a substantial influence on estimating the priority of individual directions in resource conservation in 1991-1995. Table 1 gives an estimate of the directions in natural calculations. A comparison of the natural and cost indicators makes it possible to draw a number of conclusions.

Increasing the iron content in sinter will remain, in the future, the most effective direction for conserving material resources in sinter production, despite the fact that the proportion of this direction is being reduced because of fewer possibilities for a further substantial rise in the degree of enriching raw iron ore. The role of raising the technical level of the sintering plant is growing, because of the capital repairs being carried out, with modernization and stage-type renovation, and also with a simultaneous improvement in the technological processes. Particular attention should be paid in 1991-1995 to utilizing ferruginous slurries and bringing their specific consumption at each sintering plant to 60-90 kg per ton of sinter, using the work experience of the Krivorozhstal Metallurgical Combine, where, through efficient technology for preparing the ferruginous slurries for utilization, their specific consumption over a long period is on the average 144 kg per ton of sinter.

The main reserves for reducing expenditures for fuel-energy resources in ferrous metallurgy lie in improving the use of fuel in blast-furnace production, which is its main consumer in the sector. In the ferrous metallurgy fuel balance, up to 40 percent falls to coke for smelting pig iron, the expenditures for which are now R1.5 billion a year, and in the 13th Five-Year Plan will increase by a factor of 1.4.

Table 1.

## Basic Directions for Conserving Material Resources in Sinter Production

List of basic directions	Years	Conservation of material resources (thous. t/thous. rubles)				Proportion of direc- tions with respect to profit (%)
		Iron ore raw mate- rial(blast- furnace)	Lime- stone	Sinter- fuel	Ship coke	
Utilizing ferruginous slurries	1985	292	81	18	—	10.0
	1990	5840	243	630	—	21.3
	1991	402	96	21	—	—
	1995	12301	432	1607	—	—
Raising height of sintered layer	1985	25	—	43	15	4.4
	1990	500	—	1470	976	—
	1991	63	—	104	38	18.4
	1995	1928	—	6968	3948	—
Modernizing equipment and improving technology	1985	49	—	116	38	10.3
	1990	980	—	4030	1820	—
	1991	69	—	64	42	12.5
	1995	211	—	4388	3906	—
Increasing iron content in sinter from 51.4 to 53.2%	1985	1435	1167	30	351	75.4
	1990	28700	3501	2065	16315	—
	1991	604	424	24	104	47.7
	1995	18482	1908	1808	9072	—
Total	1985	1801	1248	235	294	100
	1990	36020	3744	8225	19110	—
	1991	1138	520	213	162	100
	1995	32922	2340	14271	16836	—

Table 2: Basic Directions for Conserving Coke in Smelting Pig Iron at the Metallurgical Enterprises of the Ukraine

List of basic directions	Coke conservation (thous. t)		Profit increase (million rubles)		Proportion of directions (%)	
	1986-1990	1991-1995	1986-1990	1991-1995	1986-1990	1991-1995
Increasing iron content in mixture	905	124	57.9	11.6	63.87	21.45
Using coke substitutes (natural gas, coke gas, pulverized coal)	350	120	22.4	11.2	24.70	20.76
Raising the temperature of the heating	-319*	76	-20.4*	7.1	—	13.15
Replacing scale cars with conveyor mixture-feeds	75	75	4.8	7.0	5.29	12.97
Reducing consumption of crude limestone	62	110	3.9	10.3	4.38	19.03
Installing radical distributors of mixture and cokeless charging devices	25	35	1.6	5.1	1.76	9.52
ASU for dosing and mixing	—	18	—	1.6	—	3.12
Total	1,098	578	70.2	54.3	100	100

\* The coke consumption increased because of the reduction in the blast temperature.

Table 2 systematizes the results of technical-economic estimates of the basic directions for conserving coke in blast-furnace production at the metallurgical enterprises of the Ukraine. As follows from the data presented, a coke conservation trend such as using substitutes for it is being carried out extremely inadequately. At the same time, according to the data of domestic and foreign practice, coke substitutes ensure a substantial reduction in its specific consumption: for natural gas—by 0.6-1.2 kg per 1 m<sup>3</sup> of gas, for coke gas—by 0.5-0.8 kg per 1 m<sup>3</sup> of gas, for mazut—by 0.8-2 kg per 1 kg of mazut, for coal resin—1.1-1.14 kg per kg of resin, for coal—by 0.94-1.19 kg per kg of coal.<sup>2</sup>

The effectiveness of different directions in coal conservation is usually evaluated on the basis of comparing its specific consumption. This type of evaluation, however, should be recognized as provisional. The point is that the effectiveness of using resources should not be evaluated only according to the nature of using one of them, since a reduction in the consumption of some resources requires the additional expenditure of others. For example, from 1979 to 1988, the specific consumption of skip coke for smelting 1 ton of conversion pig iron dropped from 551.2 kg to 512.2 kg, that is, by 7.1 percent. The average sectional fuel-intensiveness for one ton of conversion pig iron, however, dropped during this same period by only 3.1 percent (from 1.047 kg to 1.014 kg of conventional fuel).

An analysis showed that the main reason for this was the increased consumption of natural gas, from 98.7 m<sup>3</sup>/t in 1979 to 109.6 m<sup>3</sup>/t in 1988. The use of natural gas makes it necessary to use oxygen, the consumption of which for pig iron smelting rose from 102.5 m<sup>3</sup>/t to 116.3 m<sup>3</sup>/t. Some 601 kW-hrs of electric power are consumed to

produce 1,000 m<sup>3</sup> of oxygen, and 0.3871 kg of conventional fuel are consumed for 1 kW-hr. In 1988, 5.5 billion m<sup>3</sup> of oxygen were consumed in blast-furnace production, and over 3.3 million kW-hrs of electric power were spent to produce it. The generation of this amount of electric power in turn required about 1.4 million tons of conventional fuel, or 290,000 tons of conventional fuel more (by 20.8 percent) than in 1979.

The problem discussed, of reducing the fuel-intensiveness of pig iron, makes it possible to draw a number of generalizations. The effectiveness of using resources must not be evaluated from the standpoint of just one sector. Under today's conditions of the transition to a market economy, the efficient use of resources can be achieved only on the basis of combining the intrasectional and intersectoral solutions and interests. In large-scale sectors (which includes ferrous metallurgy), which consume a tremendous amount of fuel-energy resources, their cost should be evaluated according to stable state prices, based on the consumer properties. The study and analysis of the reserves for conserving material resources should always be based on a comprehensive approach.

The analysis of the reserves for conserving pig iron in steel-smelting production, the results of which are systematized in Table 3, is made on the basis of this type of approach. The average specific pig iron consumption for the USSR was 625.8 kg/t of steel in 1989, and for the Ukraine—710.5 kg/t, that is, over 4 million additional tons of pig iron a year are consumed in our republic. The basic direction for conserving pig iron is the use of technological methods for its maximum possible replacement with scrap metal. On the average for the USSR, 461.8 kg/t of scrap metal are consumed in smelting steel, and at the steel-smelting shops of the UKSSR metallurgical enterprises—402.8 kg/t of steel.

Table 3: Basic Directions for Conserving Pig Iron in Steel Smelting at the Metallurgical Enterprises of the Ukraine

Basic directions	Pig iron conservation (thous. t)		Profit increase (million rubles)		Proportion of directions (%)			
					for pig iron conservation		for profit	
	1986-90	1991-1995	1986-90	1991-1995	1986-90	1991-1995	1986-90	1991-1995
Oxygen converters	836	840	35.7	57.9	100	100	100	100
including								
use of heat carriers	150	165	5.9	11.3	17.9	19.7	16.6	19.6
small slag technology	170	190	6.8	13.1	20.3	22.6	19.0	22.6
combined blowing	120	180	4.5	12.4	14.4	21.4	12.8	21.3
use of chips	130	170	7.8	11.7	15.6	20.3	21.8	20.2
increasing pig iron smelting temperature, reducing wastes, increasing compactness of scrap, etc.	266	135	10.6	9.3	31.8	16.0	29.8	16.1
Open-hearth furnaces	506	370	18.6	25.5	100	100	100	100
including								
deep blowing of tank with oxygen, using intensive heat conditions	366	190	12.8	10.3	72.3	40.5	68.5	40.5
reducing the smelting of steel made from phosphorus pig iron	140	220	5.8	15.1	27.7	59.5	31.5	59.5

Decreasing the difference in the price for pig iron and for scrap metal would contribute to increasing the proportion of scrap in the steel-smelting mixture, through improving the quality of scrap metal preparation (increasing its volume weight, the proportion of baled scrap, shears cutting, crushing pre-cooled scrap, etc.). Raising the prices for scrap metal under the conditions of the scrap-processing enterprises on a full cost-accounting and self-financing basis will ensure a rise in their technical level and will make it possible to solve the problem of setting up small scrap-processing production facilities (small enterprises) using mobile mechanized complexes to process scrap at the sites where it is formed, particularly in the ramified network of agricultural enterprises.

An important reserve for conserving pig iron in the near future is the development of new technology, using steel chips in oxygen converters, menders and units to refine steel in a ladle developed by DonNikkhomer. The specific consumption of pig iron can be reduced by 10-40 kg/t of steel. The introduction of this technology at just three metallurgical enterprises (Krivorozhstal, Dneprovskiy imeni Dzerzhinskii and Dnepropetrovsk imeni Petrovskii) will reduce the cost of steel by R1.4 million a year.

The effectiveness of using pig iron depends to a decisive extent on the level of production equipment and technology. While as a whole for the UKSSR metallurgical enterprises, the specific consumption of pig iron for smelting was reduced by 3.6 kg in 1984-1990, in the modern oxygen-converter shop (KKTs) of the combine imeni Dzerzhinskii

in the same period—it was reduced by 60.4 kg (the shop was put into operation in 1983). At the same time, the level of specific consumption of pig iron in the KKTs of this combine was substantially lower than in the KKTs of other enterprises. For example, at the combine imeni Dzerzhinskii, in 1990 it was 801.3 kg/t, Krivorozhstal—from 824.1 kg/t (in KKTs-2) to 1,033.2 kg/t (in KKTs-1), at the Yenakieyevsk—805.6 kg/t, the Azovstal—850.4, imeni Illich—806.4, imeni Petrovskii—1,016.6 kg/t. On the average for all the KKTs, it was 851.0 kg/t.

The industrial wastes and losses of metal in the basic conversions of metallurgical enterprises are: when smelting pig iron—6.7 percent, steel—12.1 percent and in rolled metal production—21.8 percent. The largest proportion of metal wastes is therefore formed at the concluding stage of metallurgical conversion, when the cost of metal is highest. A reduction in the consumption of metal in rolled metal production is therefore an extremely important factor, on which an increase in the work efficiency of the metallurgical enterprises through resource conservation depends.

The basic directions in metal conservation are classified in Table 4. Casting steel on continuous blank-casting machines (MNLZ) is one of the most efficient directions in reducing metal wastes. Replacing rolled slabs with cast ones reduces metal consumption by 140-270 kg/t and increases the output by 16-17 percent. In 1990, 4.1 million tons of steel (7.8 percent) were cast on MNLZ. The introduction of MNLZ in the KKTs of the following combines is slated for 1991-1994. Dneprovskiy imeni Dzerzhinskii—2, and Manupolskiy imeni Illich—2.

**Table 4: Basic Directions for Conserving Metal in the Production of Rolled Metal at the Metallurgical Enterprises of the Ukraine**

Basic directions	Metal conservation (thous. t)		Profit increase (million rubles)		Proportion of directions (%)			
					for metal conservation		for profit	
	1986-1990	1991-1995	1986-1990	1991-1995	1986-1990	1991-1995	1986-1990	1991-1995
Casting steel on MNLZ	84	795	3.7	58.1	8.02	60.69	7.60	69.80
Improving the heat-automation of the head of killed steel ingots	83	15	3.7	0.7	7.93	1.15	7.56	0.82
Improving the quality and refining the structural shape of ingots and stabilizing their weight	75	130	3.3	5.8	7.16	9.92	6.84	6.97
Two-stage discard of rolled semi-products, using cogging mill shears	290	46	11.2	1.6	23.88	3.05	22.76	2.16
Waste-free cutting of rolled semi-products and blanks	217	120	11.8	6.6	20.73	9.18	23.90	7.93
More complete utilization of the minus field of tolerances in the production of finished rolled metal	28	80	1.5	4.4	2.67	6.17	3.13	5.29
Improving the conditions for heating metal and the rolling technology	190	60	6.7	2.7	14.33	4.58	13.65	3.25

**Table 4: Basic Directions for Conserving Metal in the Production of Rolled Metal at the Metallurgical Enterprises of the Ukraine (Continued)**

Basic directions	Metal conservation (thous. t)		Profit increase (million rubles)		Proportion of directions (%)			
					for metal conservation		for profit	
	1986-1990	1991-1995	1986-1990	1991-1995	1986-1990	1991-1995	1986-1990	1991-1995
Improving the calculation of the weight of ingots and finished rolled metal, as well as cost-accounting relations between the cogging and steel-smelting shops	160	70	7.2	3.1	15.28	5.34	14.56	3.78
Total	1,047	1,310	49.4	83.2	100	100	100	100

The volume of casting steel on MNLZ is to be brought to 6.8 million tons in 1995, or to 13.9 of all the steel smelted. The additional saving in metal through this will be about 460,000 tons, or R30 million.

Ukrainian ferrous metallurgy is a pioneer in the development of MNLZ. MNLZ began operation for the first time in the world in the 1960's at the Donetsk Metallurgical Plant. The method has been patented in 28 foreign countries. Licenses have been bought by many industrially developed countries. Japan, the United States, France, Italy and Germany are now casting up to 80 percent and more of their smelted steel on MNLZ. The most important future tasks and goals for Ukrainian ferrous metallurgy in drawing up scientific-technical programs for resource conservation are:

Substantial updating of the furnace stock in the by-product coke industry and introduction of new technology to obtain high-quality coke under the conditions of increasing the proportion of noncoking and low-caking coal;

Radical renovation and reequipment of the refractory production facility to provide for metallurgy's need for new types of highly stable refractory products and materials, including synthetic, ensuring a considerable reduction in their specific consumption and longer between-repair periods in the work of thermal units and equipment;

Reequipment of sinter-blast-furnace production through renovating and modernizing the existing shops and replacing obsolete equipment;

A radical improvement in the structure of steel-smelting production through increasing the smelting of steel in oxygen converters and electric steel-smelting ovens in a complex with combined blowing, out-of-furnace processing and casting metal on MNLZ;

Outstripping development of the production of economical types of metal products, expanding their assortment, improving the quality and considerably heightening

their strength properties, reducing the specific consumption of metal for rolled metal through improving production technology, modernizing and reconditioning the existing units and replacing obsolete rolling mills with new ones;

Widescale introduction of advanced industrial processes and highly productive equipment on the basis of complete mechanization and automation and the use of microprocessor equipment and robot equipment in order to save labor, material and power resources;

Introducing equipment and technology new in principle, ensuring a considerable reduction in the materials-intensiveness of the finished product (obtaining metal without a blast-furnace; direct reduction of ores with subsequent remelting of metallized raw material in electric ovens; a continuous steel-smelting process; combining continuous casting and rolling; obtaining articles approximating the finished product in shape, by using continuous casting methods, with subsequent pressure processing; plasma, electron-beam and electric slag smelting; setting up continuous lines to finish rolled metal and apply protective coatings).

The special feature of ferrous metallurgy in the Ukraine in the near and more distant future remains the ensuring of a rise in the production of rolled metal and other types of metal products, without increasing the production of pig iron, coke and iron ore raw material, that is, through conservation and efficient use of all types of material and energy resources.

Of decisive importance in achieving this goal is a fundamental turning away from an expensive economic mechanism to an effective resource-conservation mechanism, which consists of a comprehensive system of mutually coordinated organizational-economic factors and structures: restructuring the management of the economy, concentrating attention on economic methods of management and the future; converting the enterprises to full cost-accounting and self-financing, expanding the boundaries of their economic independence; developing commodity-money relations; creating a unified all-union, regulated commodity market; developing foreign

economic relations; reinforcing the cost-accounting basis of direct, mutually profitable intrasectorial and intersectorial economic relations; drawing up and carrying out republic and sectorial comprehensive scientific-technical target programs to raise the quality and lower the materials-intensiveness of the products; stimulating the acceleration of introducing the achievements of science and technology and efficient use of material resources; developing forms of ownership with a prevalence of collective ownership by the enterprise workers in the ferrous metallurgy of the republic.

**Footnotes**

1. The metallurgy production volume was smaller in 1989-1990 than in 1988.
2. See: K. Yeremeyeva and R. Zhak, "The Blowing-In of Different Reagents in the Hearths of Blast-Furnaces Abroad", Moscow, BYULLETEN TsNIIChM, No 9, 1973, pp 2-17.

**COPYRIGHT:** Izdatelstvo "Radyanska Ukraina", "Ekonomika Sovetskoy Ukrainy", 1991

**Assessment of Wear Resistance of Diamond-Hard Alloy Cutting Tips**

927D0035G Kiev SVERKHTVERDYYE MATERIALY in Russian No 5(74), Sep-Oct 91 pp 34-36

[Article by V.M. Epshteyn, G.S. Nikiforov, N.P. Vinnikov, Superhard Materials Institute at the Ukrainian Academy of Sciences, Kiev]

UDC 621.9.025.7:671.152

[Abstract] The wear resistance of diamond-hard alloy cutting tips (ATP) during the machining of the VK15 hard alloy is measured by determining the size of wear scratch marks formed on their rear surface during the turning of hard alloys. Square and round diamond-hard alloy cutting tips with various diamond layer depths and grain sizes made at the Superhard Materials Institute at the Ukrainian Academy of Sciences and Lvov Diamond Instrument Tool Plant are tested; in addition, BPA and kompaks tips made at the Superhard Materials Institute at the Ukrainian Academy of Sciences and German tips are examined. It is shown that wear resistance of certain diamond-hard alloy cutting tip modifications is close to that of kompaks and that diamond-hard alloy cutting tip wear resistance increases with a decrease in the initial diamond powder grain size. The tests' coefficient of variation does not exceed 0.1 and the experiment error does not exceed 3%. The wear resistance spread does not exceed 25% while the total wear resistance range of all diamond-hard alloy cutting tip modifications reaches 200%. Figures 2; tables 3.

**Investigation of Microimpurity Content of Ultradisperse Diamond**

927D0035F Kiev SVERKHTVERDYYE MATERIALY in Russian No 5(74), Sep-Oct 91 pp 30-34

[Article by T.M. Gubarevich, N.M. Kostyukova, R.R. Satayev, L.V. Fomina, Altay Scientific Production Association, Biysk]

UDC 666.233

[Abstract] The characteristic properties which distinguish ultradisperse diamond (UDA) synthesized by the detonation method from other diamond, i.e., a high defect density, a developed active surface of up to 400 m<sup>2</sup>/g, and excessive enthalpy of formation are discussed and the noncarbon component in ultradisperse diamond impurities is investigated. To this end, a change in the microimpurity content of ultradisperse diamond powders as a result of various types of additional chemical treatment is examined. The unburned residue is analyzed by burning the sample after treatment with the help of a Links X-ray microanalyzer and the concentration of various elements in it is determined from the relative peak intensities of their characteristic emission and total incombustible impurity content as well as the presumed chemical composition of the elements' oxides.

As a result, incombustible impurities are classified on the basis of the qualitative and quantitative changes in their composition after various types of ultradisperse diamond purification. The most efficient methods of additional ultradisperse diamond treatment in order to produce a powder with an elevated purity and stable quality are identified. All impurities present in ultradisperse diamond are tentatively divided in water-soluble ionized, chemically bound, water-insoluble, and interstitial or encapsulated. It is emphasized that the presence of various impurities significantly affects diamond behavior during sintering, flotation, sedimentation, and other processes, so diamond properties may be controlled by manipulating the impurity content. Figures 1; tables 2; references 7.

**Properties of Compacts From Natural Diamond Crystals From Metamorphic Rocks**

927D0035A Kiev SVERKHTVERDYYE MATERIALY in Russian No 5(74), Sep-Oct 91 pp 3-8

[Article by O.A. Voronov, A.A. Kaurov, A.V. Rakhmanina, High-Pressure Physics Institute at the USSR Academy of Sciences, Troitsk, Moscow oblast]

UDC 621.921.27

[Abstract] High-pressure sintering of natural diamond powder for making pure isotropic crystalline diamond from metamorphic rock crystals is examined and an experimental sintering unit is described. Prior to sintering, the initial diamond powder is sorted by fractions and treated in hydrofluoric and perchloric acids; sintering is performed in toroidal chambers at an initial pressure of 8 GPa and at a constant force. The mean diamond density in the reaction zone is 2.1 g/cm<sup>3</sup> and after the pressure application—2.8 g/cm<sup>3</sup>. The reaction zone is heated at a 75%/s rate to a given temperature and exposed to it for a given time. In the experiment, the cell design with a protective housing prevents the pressure-transfer medium ingress either through diffusion or extrusion. An analysis shows that diamond grains coalesce due to the carbon atom diffusion in a pure form and that the process is not complicated or obscured by the effect of any impurities or additions. The density of the nonadamantine allotropic modification of carbon forming during the sintering and its porosity and quantity are measured and the strength, electric resistivity, and thermal conductivity of diamond compacts produced at various temperatures and heating duration are determined. It is shown that the parameters ensuring the maximum thermal conductivity of compacts also ensure the best strength. Thus, the compressive strength of cylindrical compacts is 4.1-4.2 GPa and is maintained when they are heated to 1,200°C in an inert medium, making it possible to use them successfully in many engineering applications. Figures 4, tables 1, references 10.

**Use of Differential Diamond Crushers for Cocoa Bean Grinding**

927D0036J Kiev SVERKHTVERDYYE MATERIALY in Russian No 6(75), Nov-Dec 91 pp 58-60

[Article by E.D. Kizikov, I.P. Kushtalova, L.P. Kogosov, A.S. Petrin, Superhard Materials Institute at the Ukrainian Academy of Sciences, Kiev]

UDC 641.642

[Abstract] Implementation of diamond tools in food processing and the use of diamond grinders in differential mills for producing cocoa powder—the principal component for making chocolate—is discussed and the design and operating principle of differential diamond grinders is described. Various indicators of three samples of powdered cocoa beans produced by such diamond grinders are summarized and compared to existing standards. The study shows that Ti- and Ni-containing diamond-adhesive alloys are the most suitable for metallic matrices. The differential diamond grinders used in the tests have a Kh18N9T stainless steel body and AS50-AS80 high-strength synthetic diamond in the grinding wheels. The test results demonstrate the high reliability and efficiency of differential diamond grinders and a normal service life of 2-4 thousand hours. The new tools make it possible to decrease the ground cocoa bean particle size, decrease the product viscosity, increase the mill yield, simplify its maintenance, and reduce the electric power consumption. Figures 4; tables 1

**Turning of Car Parts Rebuilt by Spraying With Subsequent Coat Fusing**

927D0036J Kiev SVERKHTVERDYYE MATERIALY in Russian No 6(75), Nov-Dec 91 pp 56-57

[Article by V.N. Potseluyko, S.V. Ignatyev, Yu.A. Mukovoz, S.A. Klimenko, I.V. Kovalenko, N.P. Bezenar, Navoi Integrated Mining and Metal Works and Superhard Materials Institute at the Ukrainian Academy of Sciences, Kiev]

UDC 621.793.72

[Abstract] The problem of turning car parts rebuilt by thermal spraying deposition of Ni-Cr-B-Si powders with subsequent fusing due to the hardness of the resulting coat is identified and the results of turning inside and outside surfaces of parts from BelAs-549 quarry dump trucks rebuilt with the help of a PG-AN9 powder (HRC=48-57) containing 2.8-3.5% B, 0.5-1.2% C, 1.5-3.5% Si, 3% Fe, 6-10% Cr, and Ni (the remainder) are summarized. Tests demonstrate that tools from the VK8 hard alloy and 01 and 10 composites are virtually useless for such parts and that cutting tools from kiborit should be used. At a cutting speed of 0.3-0.4 m/s, a feed of 0.10-0.15 mm/rev, and a depth of cut of 0.1 mm, kiborit tools used for turning various dump truck parts last

30-120 min vs. 30-35 min for composite 10 and 10-20 min for composite 01. It is also shown that the PT-10N-01, PS-12NVK-01, PG-SR3, PG-SR4, PG-KhN80S4R4, PN85Yu15, PTYu-5N, PTYu-10N powders and 65G wires produce the best results in turning rebuilt car parts with subsequent fusing. Tables 1; references 2.

**Optimization of Diamond Microturning Conditions of Metal Mirrors**

927D0036H Kiev SVERKHTVERDYYE MATERIALY in Russian No 6(75), Nov-Dec 91 pp 44-46

[Article by G.G. Dobrovolskiy, Yu.A. Dyatlov, V.V. Melnichenko, I.V. Koltsov, Superhard Materials Institute at the Ukrainian Academy of Sciences, Kiev]

UDC 621.941.01

[Abstract] The use of diamond microturning (AMT)—a promising method of making mirrors with a 96% specular reflectance (KZO) and high shape precision for solar power plants—is discussed. It is shown that the machining output may be increased by increasing the cutting speed and feed and that the speed virtually does not affect the machined surface roughness and, consequently, specular reflectance. Feed per turn is the second factor increasing the machining output although it calls for compensating for the increased surface roughness by increasing the cutting tool radius. An analysis of the factors reveals that optimal diamond microturning conditions for aluminum solar power plant reflectors with a 600 mm diameter are a 600 RPM spindle speed, a 0.010 to 0.012 mm/rev feed, and a 0.005-0.01 mm depth of cut. The cutting tool should have the following configuration:  $-3^\circ \leq \gamma \leq 3^\circ$ ;  $\alpha = 8^\circ$ , and  $r_B \approx 2.8$  mm. The optimization procedure makes it possible to select diamond microturning conditions for solar power plant mirrors which ensure the maximum productivity without degrading the quality of the machined surface. Figures 1; references 5: 4 Russian; 1 Western.

**Diamond Powder Deironing in Linear Traveling Magnetic Field**

927D0036G Kiev SVERKHTVERDYYE MATERIALY in Russian No 6(75), Nov-Dec 91 pp 38-40

[Article by V.P. Terekhov, A.P. Shiryayev, Mekhanobr Institute, Leningrad]

UDC 541.124.16:546.25:666.233

[Abstract] The shortcomings of existing methods used to remove ferrous impurities forming during the diamond bort grinding are identified and the use of traveling magnetic field creating the necessary ponderomotive force for this purpose is discussed. A chart of forces and torque affecting a ferromagnetic particle in the traveling magnetic field is presented and a separator designed for removing ferromagnetic impurities from diamond

powder and its components are described. The results of tests to remove ferromagnetic particles from the -400+40 and -40+10  $\mu\text{m}$  fractions of diamond powder demonstrate that in the former case product losses are insignificant while in the latter, losses rise to 18%, necessitating the ferromagnetic fraction separation itself. The resulting diamond powder may be regarded as a ready product since the impurity content is less than the permissible level (1-2%). The separator developed at the Mekhanobr Interbranch Scientific Technical Complex makes it possible to decrease the proportion of diamond powder deironed with the help of toxic acids by 70-80%. Figures 2; tables 1; references 4.

### Metallographic Investigation of Sintered Diamond Compacts: Discussion

927D0036F Kiev SVERKHTVERDYYE MATERIALY in Russian No 6(75), Nov-Dec 91 pp 26-28

[Article by G.M. Kimstach, A.A. Urtayev, T.D. Molodtsova, Rybinsk Aviation Engineering Institute]

UDC 666.233

[Abstract] The assumption that a polymorphous graphite  $\rightarrow$  diamond transformation catalyzed to a certain extent by iron occurs during the static synthesis of crystal diamond in a Fe-C system under a high pressure and lowers the requisite pressure in the diamond's thermodynamic stability regions is checked experimentally. Diamond crystals are produced by traditional static synthesis methods in a toroidal chamber at a 1,500°C temperature and a 60 kbar pressure; fractures of the resulting sinters and the microstructure of the metallic matrix are examined by a TeslaBS-300 scanning electron microscope and a MIM-7 metallographic microscope. The studies show that diamond crystals are formed not in the graphite region where one might expect them but in the metallic matrix, i.e., under the conditions in question they form a phase of their own which is separate from the graphite phase. This makes it possible to confirm predominant localization of diamond crystals in the metallic matrix regions adjacent to graphite while no diamond crystal formation is observed directly in graphite. Thus, no signs of polymorphous transformation are detected in static synthesis. It is speculated that synthesis occurs by the mechanism described in deposition No. 4130 to the Chermetinformatsiya institute on 10 Aug 87 and that further studies of this mechanism may help improve diamond synthesis methods. Figures 2; references 4.

### New Brands of Graphite-Like Boron Nitride: High-Quality Precursor for Synthesizing Superhard Materials

927D0036E Kiev SVERKHTVERDYYE MATERIALY in Russian No 6(75), Nov-Dec 91 pp 20-22

[Article by A.N. Porada, S.N. Pikalov, L.I. Feldgun, M.I. Gasik, Zaporozhye Production Association Abrazivnyy kombinat and All-Union Scientific Research Institute of Abrasives and Grinding]

UDC 546.273.171

[Abstract] The unique combination of graphite-like boron nitride (GNB) properties making it suitable for use in high-temperature processes, producing composite materials, in radio engineering and electronics, and in synthesizing superhard modifications of boron nitride and the high economic and technical indicators of tools made from borazon and elbor, kubonit, and geksanit borazon materials is discussed and production of graphite-like boron nitride in the USSR and abroad using various methods is summarized. The graphite-like boron nitride production output in 1980-1990 and the production output of three GNB brands in 1980-1990 is illustrated. The characteristics of various brands of graphite-like boron nitride made in the USSR and by Union Carbide in the USA and Showa Denko in Japan are compared. It is shown that the broad range of properties of new graphite-like boron nitride brands makes it possible to use them effectively in various synthesis technologies for producing superhard material (STM) powders and polycrystals. Figures 2; tables 1; references 4.

### Physicomechanical Properties of Nickel-Molybdenum-Bonded Titanium Nitride Cermets

927D0036D Kiev SVERKHTVERDYYE MATERIALY in Russian No 6(75), Nov-Dec 91 pp 16-19

[Article by M.A. Kuzenkova, O.N. Kaydash, B.A. Atamanenko, S.A. Artemyuk, Superhard Materials Institute at the Ukrainian Academy of Sciences, Kiev]

UDC 621.762

[Abstract] The elasticity modulus and strength properties of nickel-molybdenum-bonded titanium nitride cermets are examined as a function of structure and production methods. The initial test charge prepared by grinding is then sintered in a vacuum and especially pure nitrogen. The dynamic elasticity modulus is measured by the resonance method with the help of an ultrasonic multimeter at room temperature. Resonant frequencies are measured in 5x5x35 mm samples while the bending strength is measured by the three-point loading method. An analysis helps to identify the optimum production method: annealing in a vacuum and sintering in nitrogen, resulting in a bending strength of 677+/-5 MPa, compressive strength of 1,924+/-54 MPa, and HRA = 80.6+/-0.4. Since the elasticity modulus depends on porosity, it must be taken into account in comparing materials with different compositions. An increase in the metallic binder content increases strength but decreases the elasticity modulus; the alloy strength increases with sintering temperature, isothermal exposure duration, and cooling rate after sintering, peaking at first, then dropping due to the competing processes of decreasing porosity and increasing titanium nitride grain size. Figures 5; tables 1; references 8: 5 Russian; 3 Western.

**Simple Phonon Frequency Distribution Functions for Diamond and BN<sub>sph</sub>**927D0036C Kiev SVERKHTVERDYYE MATERIALY  
in Russian No 6(75), Nov-Dec 91 pp 10-15

[Article by L.A. Shulman, Superhard Materials Institute at the Ukrainian Academy of Sciences, Kiev]

UDC 539.2:546.26-162:546.171.1

[Abstract] The importance of knowing the phonon states density function and phonon frequency distribution for understanding such physical properties of crystals as heat capacity, internal energy, entropy, root mean square atom displacements, etc., is emphasized and a simple phonon frequency distribution function is proposed for diamond and BN<sub>sph</sub> (i.e., the sphalerite modification of boron nitride). The function is plotted on the basis of the fact that monoatomic cubic solids are characterized by two distribution function maxima: one near the upper frequency limit  $v_m$  and one near  $v_m/2$ . As a result, approximate functions are derived for the phonon states density function and RMS lattice atom displacements are calculated within a broad temperature range and compared to those computed analytically in the framework of Debye's approximation. The temperature curve of the characteristic temperature corresponding to the Debye-Waller factor and equivalent Debye frequencies are found and the dependence of heat capacity on temperature is plotted and compared to the one produced with the help of the proposed phonon states density; both values are found to be consistent with each other as well as with experimental data. It is demonstrated that other thermodynamic functions, including the entropy, can also be compared in the framework of these approximations. The proposed two-frequency functions are suitable for calculations and estimates. Figures 5; tables 2; references 24: 14 Russian; 10 Western.

**Carbon Phase Transformations in Diamond Under Laser Irradiation**927D0036B Kiev SVERKHTVERDYYE MATERIALY  
in Russian No 6(75), Nov-Dec 91 pp 6-9

[Article by A.P. Rudenko, A.I. Gorshkov, V.A. Spivak, I.I. Kulakova, V.L. Skvortsova, E.G. Karelina, V.M. Abramov, Moscow State University, Ore Deposit Geology, Petrography, Mineralogy, and Geochemistry Institute at the USSR Academy of Sciences, and Kristal Scientific Production Association]

UDC 549.211:621.375.826:536.42

[Abstract] Phase transformations in solids developing under the effect of laser irradiation at high temperatures (up to several thousand degrees) are addressed and carbon phase transformation occurring in diamonds heated in the air to 3,000K by laser radiation and rapidly cooled afterwards are examined. An analysis shows that

the surface layer exposed to laser radiation in diamond crystals becomes graphitized and graphite formations with varying degrees of crystallinity and structural perfection form in it. Moreover, the formation of polycrystalline diamond and diamond-graphite aggregations is possible. The study is conducted by the selective oxidation method and electron spectroscopy while an LTI-502 solid-state YAG:Nd Q-switched single mode pulsed continuously pumped laser is used for irradiation. Both finely dispersed graphite with an extremely low structural ordering degree (turbostratic) and basal-plane textured graphite (two-layered 2H modification) are found in the graphitization products. It is noted that the recrystallization effect observed in diamond crystals makes them especially valuable for use in abrasive tools. Figures 2; references 5: 3 Russian; 2 Western.

**Effect of Nongraphitized Starting Carbon Material Phase on Synthesis Behavior and Diamond Crystal Quality**927D0036A Kiev SVERKHTVERDYYE MATERIALY  
in Russian No 6(75), Nov-Dec 91 pp 3-6

[Article by B.K. Dymov, Ya.A. Kalashnikov, A.N. Shadiyev, S.N. Selyukov, Scientific Research Institute of Graphite, Moscow, and Poltava Synthetic Diamond and Diamond Tool Plant]

UDC 621.921.34.666.233

[Abstract] The effect of the starting carbon material (UM) on the yield and quality of diamond crystals synthesized from it in general and the effect of the presence of a certain amount of a nongraphitized carbon material in the well-crystallized graphite matrix in particular are investigated. The samples for the study are prepared by the electrode method and examined by the methods of X-ray phase (RFA) and metallographic analyses; the diamonds are synthesized at a 5 GPa pressure and a 1,200°C temperature with a 1 min exposure in an anvil-type high-pressure chamber. Pursuant to GOST 9206-80, two batches of synthetic diamonds—one with 20% and one with close to 2% of nongraphitized phase—prepared from a -800+400  $\mu\text{m}$  carbon material fraction mixed in a 1:1 mass ratio with a -1,250+400  $\mu\text{m}$  nickel-manganese alloy catalyst fraction are tested. Strength tests of both batches with a 160/125 graininess demonstrate that the first has a breaking load of 7.3 N and the second—9.3 N, i.e., 20% higher. Moreover, diamond crystals from the first batch are less perfect but their structural composition is almost identical to those of the second batch. The total yield of the +125  $\mu\text{m}$  diamond crystals is 46% from the first batch and 59% from the second. Thus, the yield increases sharply with a decrease in the nongraphitized phase concentration while strength decreases. Figures 2; references 3: 2 Russian; 1 Western.

**Refractories Made of Molten Materials With a Mullite Composition**

927D0024A Moscow OGNEUPORY in Russian No 7, Jul 91 pp 2-4

[Article by V.A. Ustichenko and N.V. Pitak, Ukraine Scientific Research Institute of Refractories]

UDC 666.762.14.046.512

[Abstract] The regimen used to cool a mullite melt is an important factor in mullite formation. The authors of the study reported herein examined the effect that molten materials made up of mullite crystals of different sizes and in different amounts have on the properties of mullite products. Molten mullite materials were produced by melting a mixture of G-0 silica and quartz sand containing more than 99%  $\text{SiO}_2$  in arc and high-frequency furnaces. The resultant melts were cooled at different rates by producing blocks and ingots of different volumes in ingot molds and molds and by blowing a stream of molten mullite with compressed air and cooling it in water. In the case of induction furnace melting, the mullite mixture was subjected to quick melting in small amounts followed by rapid cooling at the outlet from the melting zone. Four different cooling methods were tested on the melts produced in an arc furnace. In the first case, the melt was poured into cooled chill molds and was left for several days to solidify into blocks weighing about 1 ton. The second technique involved pouring the material (in amounts ranging from 3 to 80 kg) into molds; the molded mullite cooled 5 to 50 times faster than did the large blocks. In the third technique used, the melt was poured into water; the material cooled and solidified in the form of granules. The fourth method, which was designed to achieve even quicker cooling, involved blowing the melt with air to form spheres up to 3 mm in size. Two fractions (consisting respectively of particles 3 to 0.5 mm in size and finer than 0.5 mm) of the materials produced by each of the aforesaid methods were then used to produce specimens that were in turn subjected to comparative tests. The tests performed showed that in all cases, the specimens had a high softening temperature (above 1,750°C) despite their high porosity. This confirmed the feasibility of using mullite products as a construction material subjected to high loads and temperatures. The products that were calcined at 1,750°C and based on nonisometric mullite grains from blocks were found to undergo the least shrinkage and to have the highest strength. Their softening temperature under a load of 0.6 N/mm<sup>2</sup> was higher than that of samples containing powders produced from blocks. Annealing at 1,750°C was found to pack and strengthen the refractories and to complete the mullite formation process. The mullite content in individual specimens reached 97.7% in some cases. Even samples produced from initial charges containing only 33% mullite contained a mass fraction of more than 93.5% mullite after annealing. The tests further established that the regimen used to cool the mullite melt did indeed determine the quality of the finished material

and had a significant effect on the properties of calcined mullite specimens. Products made from large-crystal acicular mullite were found to have a low amount of creep and were recommended for use in heating units operating at high temperatures under heat and mechanical stresses. Figures 4, tables 3; references 4 (Russian).

**Electron Microscopy Studies of the Structure and Phase Composition of the System  $\text{BaO-B}_2\text{O}_3$  in Metallization Coatings**

927D0024E Moscow OGNEUPORY in Russian No 7, Jul 91 pp 20-22

[Article by E.L. Karyakina and L.G. Rabinkov, Ukraine Scientific Research Institute of Refractories]

UDC 621.793.017:539.26

[Abstract] The authors of the study reported herein examined the structure and phase composition of two specimens from the system  $\text{BaO-B}_2\text{O}_3$ . For their studies the authors selected the lowest-melting eutectic compounds (eutectic temperature, 859°C) of the said system. Specifically, specimen 1 had a calculated composition of 22.1%  $\text{BaO}$  and 77.9%  $\text{B}_2\text{O}_3$ , and specimen 2 was calculated to consist of 33.0%  $\text{BaO}$  and 67.0%  $\text{B}_2\text{O}_3$ . As starting materials the authors used barium carbonate and boric acid (graded chemically pure). The two were mixed in the respective proportions and were transformed into glass at 1,500°C by holding them at that temperature for 1 hour. The respective melts were poured off into water and ground in a ball mill by ceramic balls. The two specimens were then heated to the melting point, immediately cooled in air, and subjected to annealing (by heating them to 700°C, holding them for 30 minutes, cooling them to 600°C, holding them for 15 minutes, heating them to 650°C, and holding them for a final 30 minutes). To study the effect of pyroceram-forming catalysts, the authors added  $\text{Cr}_2\text{O}_3$  and  $\text{ZrO}_2$  to specimens 1 and 2 in the amount of 1.5% (by mass). The two specimens were then subjected to studies on an EVM-1000AK electron microscope. The two specimens were found to have very similar finely granular structures containing microsegments with fuzzy granulation (these segments ranged in size from about 0.2 to 3.0  $\mu\text{m}$ ). Their surface was smoother than the base. Specimen 2 had a more distinct and sharper globule pattern. A sheared surface of specimen 1 was found to have a homogeneous structure in the form of spherolites 0.013 to 0.025  $\mu\text{m}$  in diameter. A break of specimen 2 was found to consist of indistinctly bounded particles 0.02 to 0.3  $\mu\text{m}$  in size with spherical elements evident as in specimen 1. Subjecting the two specimens to annealing to form a pyroceram resulted in a system of two or more phases consisting of mat glass and crystals and nucleation centers of various sizes and amounts. Specimens annealed in a hydrogen medium formed different microstructures than did those annealed in air. The process of nucleation center formation in the glass specimens was found to depend on the nature of the catalyst used.

$\text{Cr}_2\text{O}_3$  was found to increase stratification of the material significantly and was thus not recommended. Adding  $\text{ZrO}_2$  in the amount of 15%, on the other hand, did not result in any similar stratification that would preclude its use as a crystallization catalyst. Figures 5; references 8: 4 Russian, 4 Western.

#### **Natural Aluminosilicate Raw Material for Producing Mullite-Silica Fibrous Materials**

927D0024F Moscow OGNEUPORY in Russian No 7, Jul 91 pp 25-27

[Article by I.G. Subochev, N.V. Pitak, I.V. Yeremina, Ukraine Scientific Research Institute of Refractories]

UDC 666.762.1-486

[Abstract] The authors of this article have outlined a process for using natural aluminosilicate raw material as a basis for producing mullite-silica fiber materials. The new process includes the following operations: preparing the starting materials, melting the charge, extruding the aluminosilicate melt in a stream with a constant cross section and flow rate, dispersing (atomizing) the molten stream into individual fibers by means of an energy carrier (steam or compressed air), cutting the resultant fiber mat into the required dimensions, rolling it into rolls, and packing the finished product. The process used to transform natural aluminosilicate materials into mullite-silica fibers is essentially the same as that used with mixtures of silica and quartz sand. The fibrous material produced from the natural aluminosilicate is gray. From all other standpoints it fully conforms to the requirements specified for a material made of a mixture of silica and quartz sand. More than 200 tons of the new mullite-silica fibrous material and products based on it have already been produced in test batches, and the material has been deemed suitable for use as thermal insulation operating at temperatures up to 1,100°C. The new process of producing mullite-silica glass fiber materials has been introduced at the Ogneupory [refractories] Production Association in Bogdanovich. Adoption of the practice of using a natural aluminosilicate raw material will enable enterprises producing refractories to reduce their production costs and thus increase their profits under a cost accounting system. Tables 2; references 11: 10 Russian, 1 Western.

#### **Research on the Technology of Castable Refractory Thermal Insulation Products**

927D0024B Moscow OGNEUPORY in Russian No 7, Jul 91 pp 4-7

[Article by Ya.Z. Shapiro and L.G. Litvin, Ukraine Scientific Research Institute of Refractories]

UDC 666.762.1-127.2

[Abstract] The authors of the study reported herein worked to develop a new process of producing castable

refractory thermal insulation materials. The new process is particularly attractive in that it is based on using readily available materials as a filler and may be implemented on a production line consisting of standard pressing equipment. In accordance with the new process, castable refractory thermal insulation products are produced by the method of semidry pressing. Types ShGR-3, ShGR-4, and ShGR-5 chamotte (fireclay) in fractions finer than 15 mm were used along with broken pieces of products made of type ShL-1.3 fireclay (with an apparent density above 2.0 and 1.3 g/cm<sup>3</sup>) and wastes of types MKRL-0.8 and ShL-0.4 lightweight refractories. High-alumina cement products by the pilot plant of the Ukraine Scientific Research Institute of Refractory Materials and the plant in Klyuchevsk and alumina cement from the plant in Pashiya were used as binders. Samples were pressed under pressures of 3 and 5 N/mm<sup>2</sup> and left to set up under moist conditions or in air for 3 and 7 days, respectively, followed by drying in the first case and no drying in the second case. Tests performed on the specimens indicated that the specimens produced from compounds with an 18 to 20% moisture content had the maximum strength. The apparent density of the specimens decreased as the pressure was reduced from 5 to 3 N/mm<sup>2</sup>. The specimens produced from broken pieces of fireclay containing 20% perlite and pressed under a pressure of 3 N/mm<sup>2</sup> were found to have the best thermal insulation properties. After further refining the composition of the charge to be used in the new process, the authors succeeded in using the semidry pressing technique to produce thermal insulation material with the following indicators: apparent density, 0.9 to 1.1 g/cm<sup>3</sup>; compression strength, 2.6 to 3.9 N/mm<sup>2</sup>; linear shrinkage, 1.2 to 2.0%; heat conduction at an average temperature of 350 +/- 25°C, 0.22 to 0.34; heat conduction at an average temperature of 600 +/- 50°C, 0.26 to 0.39 W/(m x K); mass fraction of  $\text{Al}_2\text{O}_3$ , 38.09%; mass fraction of  $\text{SiO}_2$ , 56.78%; mass fraction of  $\text{TiO}_2$ , 0.51%; mass fraction of  $\text{Fe}_2\text{O}_3$  (total), 0.75%; mass fraction of  $\text{CaO}$ , 68.4%; and mass fraction of  $\text{MgO}$ , 0.26%. Figures 5, tables 3; references 3 (Russian).

#### **Lime Binder-Based Dinas Products for Lining Coke Furnaces**

927D0024G Moscow OGNEUPORY in Russian No 7, Jul 91 pp 36-38

[Article by V.L. Bulakh and R.F. Rud, Ukraine Scientific Research Institute of Refractories]

UDC 666.762.2:66.043.1:662.741.041

[Abstract] The current domestic practice in lining coke ovens is to use Dinas (silica brick) products containing a mineralizing additive consisting of 2.2 to 2.7%  $\text{CaO}$  and 0.8 to 1.0%  $\text{Fe}_2\text{O}_3$ . These mineralizing additives cause several problems when used in materials lining coke ovens. One problem is that because iron oxides are catalysts of the reduction of silica at the high temperatures found in coke oven flues, they lead to corrosion of

the lining surface. In an effort to circumvent this problem, the authors of the study reported herein examined the prospects of using Dinas based on a lime binder as a lining material for coke ovens. During the study, the iron oxide additives that are normally used as mineralizers were replaced by lime milk. The lime milk was added to crystalline quartzite with a mass fraction of  $\text{SiO}_2$  between 97.5 and 98.4%. Commercial-grade lignosulfonate was used as an adhesive. The compounds were prepared in a centrifugal mixer. The products were formed on a friction press and were then dried and annealed in accordance with the generally accepted regimens established for coke products. The calcined products had a density of  $2.33 \text{ g/cm}^3$ , an open porosity of 15.3 to 15.9%, a compression strength of  $50 \text{ N/mm}^2$ , an additional growth of 0.1% at  $1,450^\circ\text{C}$ , and a temperature of deformation initiation under a load of  $0.2 \text{ N/mm}^2$  of  $1,650$  to  $1,660^\circ\text{C}$ . The test products were characterized by better physicoceramic properties than their conventional counterparts, and their heat conduction was 10 to 18% higher. Samples of the new material were tested as flue linings in two pilot semiproduction coke ovens. A test lining 90 mm thick was used in the first coke oven for 186 days. A test lining 105 mm thick was used in the second coke oven for 2 years. Both test linings were taken out of service for reasons that were not related to their performance. Tests performed on the lines after their test service periods indicated that they underwent a 1.5 to 2.0% increase in open porosity and some zonal changes in phase composition. In general, however, the basic properties of the two linings either improved somewhat or remained practically unchanged after their trial service period. Thus, the tests conducted on the new lime binder-based Dinas products to assess their effectiveness in lining experimental coke ovens have confirmed their serviceability and promise as new materials for use in lining the flue areas of coke ovens. Tables 5; references 7: 4 Russian, 3 Western.

### A Study of the Effectiveness of Refining Melts by Filtration

927D0024D Moscow OGNEUPORY in Russian No 7, Jul 91 pp 10-13

[Article by V.N. Kozhurkov, E.B. Yarikhin, A.M. Panfilov (Ural Polytechnic Institute imeni S.M. Kirov), N.M. Permikina, V.I. Kozhevnikova, (VostIO [not further identified]), and S.V. Galperina (Ural Ferrous Metallurgy Scientific Research Institute)]

UDC 666.762.1:669.054.2

[Abstract] The authors of the study reported herein examined the effectiveness of using filtration to refine an iron melt containing about 3% boron and about 5% silicon. That particular melt composition was selected because it is close to the composition of commercial alloys capable of amorphization at sufficient hardening speeds. The residual content of nonmetallic inclusions was also studied as a function of their nature and the type of filters used. The studies performed demonstrated that filtering Fe-Si-B

melts through a poured filter consisting of 2- to 3-mm corundum granules results in a fourfold reduction in the level of contamination due to  $\text{B}_2\text{O}_3\text{-SiO}_2$  inclusions when a filtering layer 2 cm high is used. The refined metal is virtually free of inclusions greater than  $5 \mu\text{m}$  in size. Using a combined filter consisting of granules and a corundum foam filter resulted in a threefold reduction in the content of solid-phase magnesium oxide inclusions; however, such filters proved to have a low efficiency from the standpoint of removing large inclusions. Figures 2, tables 2; references 4 (Russian).

### New Types of Calcium-Containing Mineralizers To Produce Dinas Products

927D0024C Moscow OGNEUPORY in Russian No 7, Jul 91 pp 7-10

[Article by I.V. Khonchik, V.I. Drozd, B.G. Alapin, and E.L. Karyakina, Ukraine Scientific Research Institute of Refractories, and M.I. Ryshchenko, Kharkov Polytechnic Institute imeni V.I. Lenin]

UDC 666.762.2:666.368

[Abstract] Calcium-containing additives in the production of Dinas (silica brick) refractories facilitate mineralization of the Dinas and accelerate the transformation of quartz during annealing without significantly changing the products of the calcined products. Calcium hydroxide (lime milk) is currently the most widely used calcium-containing additive for this purpose. In an effort to avoid the problems that arise when lime milk is used (including hazardous labor conditions), the authors of the study reported herein examined the feasibility of using new types of calcium-containing mineralizers to produce Dinas products. Specifically, they examined the prospects of using various calcium-containing industrial wastes. Physico-chemical tests were performed on three types of calcium-containing materials: lime siftings smaller than 10 mm in size from the Komsomol Ore Administration, granulated blast furnace slag from the Donetsk Metallurgy Combine, and phosphogypsum wastes from the production of orthophosphoric acid at the Khimprom Production Association in Sumy. The said materials were subjected to derivative thermogravimetric analysis, x-ray and infrared spectroscopy studies, electron microscopy studies, and petrographic analysis. The tests performed confirmed that all three of the materials have mineral compositions that make them suitable for use as calcium-containing mineralizing additives in the production of Dinas products. Moreover, they do not contain any impurities that would have an adverse effect on the properties of the Dinas products produced. Sample products containing the said additives were produced under laboratory conditions. The products were in complete conformity with Branch Standard [OST] 14-41-78, and their compression strength and additional growth indicators actually surpassed those specified in the standard. Figures 5, tables 2; references 2 (Russian).

**New Powder Friction Materials in Braking Devices**

927D0048G Minsk *TRENIYE I IZNOS* in Russian  
Vol 12 No 4, Jul-Aug 91 pp 710-713

[Article by A.D. Ignatovskiy, I.Z. Tomsinskiy, Leningrad Mechanical Institute]

UDC 621.825

[Abstract] The sharp increase in the absorbed power characterizing the operation of today's friction brakes and transmissions necessitating the use of new materials is discussed and the recommendations for using new composite sintered materials produced at the Material Science Problems Institute at the Ukrainian Academy of Sciences for improving the operation of various friction devices, e.g., safety clutches and transmissions, couplers, and braking gears, are outlined. The materials are examined in a braking mode in an experimental unit developed at the Leningrad Mechanical Institute. Compositions of copper- and iron-based sintered powder materials are investigated and compared for reference to the MK-5, one of the most popular copper-based friction materials used in heavily and medium-loaded mechanisms. Tests are carried out with a forced delivery of a mixture of 40% MT-16P oil and 60% AU spindle oil as well as without oil. The experiments demonstrate that the use of the new composite materials prepared by the powder metallurgy methods in braking devices expands their capabilities and makes them more efficient and durable. Figures 1; tables 2; references 2.

**Mechanism of Additional Iron Powder Reduction in Falling Layer**

927D0033A Kiev *POROSHKOVAYA METALLURGIYA* in Russian No 9(345), Sep 91 pp 1-5

[Article by V.A. Maslov, Yu.A. Aleksandrov, Mariupol Metallurgy Institute]

UDC 669.046.46

[Abstract] Powder treatment before compaction and sintering and its role in the cermet production cycle are discussed and the principle of reduction annealing of an iron powder in the suspended state which makes it possible to complete the reduction process and decarburize the powder, remove cold working without making the particles stick or form a crust at temperatures of up to 1,200°C in several seconds. The mechanism of additional oxide reduction on the surface of iron powder particles obtained by the thermal carbon reduction method at the Sulinskiy Integrated Iron and Steel Works is studied and the special lab unit developed for this purpose which makes it possible comprehensively to examine the particle motion dynamics, the powder heating and cooling process, surface oxide reduction kinematics, and the powder decarburization kinematics is considered. The experimental procedure is described.

The specific additional reduction rate of oxide films on iron particles in the falling layer is  $0.078 \text{ g(O)/m}^2 \text{ s}$  and the reduction activation is 54.16 kJ/mole for the  $-160+100 \mu\text{m}$  monodisperse fraction. The finishing reduction rate in the falling layer reaches 1.2-3.1% [O]/s. The experimental results and a comparison to known data show that the surface oxide reduction process in the falling layer in the 800-1,000°C range falls within the kinetic reaction range and is limited by the interaction of hydrogen with iron's surface oxides. Figures 3; references 10.

**Effect of Powder Dispersion on Brass' Hot Compaction Temperature**

927D0033B Kiev *POROSHKOVAYA METALLURGIYA* in Russian No 9(345), Sep 91 pp 5-9

[Article by V.S. Kruzhakov, T.G. Garbovitskaya, Kharkov University]

UDC 621.762

[Abstract] The difficulty of producing brass from a brass powder of a mixture of copper and zinc alloying compositions by conventional methods due to the specific features of zinc behavior resulting in the development of a nonuniform surface layer and porosity and poor mechanical properties is discussed and it is shown that this problem may be overcome by using the methods of hot compaction and hot die forging of porous blanks. An attempt is made to determine whether it is possible to decrease the temperature of hot extrusion of brass from a mixture of copper and zinc alloying composition powders. A virtually pore-free powder brass with a 10  $\mu\text{m}$  mean grain size may be produced by compaction at a 120-150 MPa pressure at a 650-700°C temperature in 3-5 min. Diffusion annealing of the alloy during the hot compaction process is limited by zinc diffusion in copper and  $\alpha$ -brass. The hot compaction temperature may be reduced to 500°C by using a very fine dispersed copper powder or ground alloying composition powder with a thin copper layer on the particles without decreasing the brass quality. The use of powders coated with a more refractory component ensures its unidimensional homogeneity and shortens the two-component alloy time. The authors are grateful to B.M. Kipnis for helping with disintegration powder treatment. Figures 4; references 5.

**Methods of Estimating Ductility During Plastic Working of Powder Metals. II. Fracture Criteria Allowing for Stressed State**

927D0033C Kiev *POROSHKOVAYA METALLURGIYA* in Russian No 9(345), Sep 91 pp 10-14

[Article by A.A. Notych, Ye.V. Zvonarev, Zaporozhye Mechanical Engineering Institute and Belarus Republican Scientific Production Association of Powder Metallurgy]

UDC 621.762

[Abstract] Studies of powder metal ductility during plastic working on the basis of fracture criteria of powder metals using the cumulative strain concepts developed by various researchers are summarized. Criteria which directly take strain into account and criteria based on physical models of the powder material are examined. An analysis of the surveyed sources shows that the ductility of porous metals is largely affected by the initial porosity, pore dimensions and shape, and the state of interparticle contacts; yet the stressed state index is still dominant. The inclusion of structural parameters in the porous body ductility theory makes it possible to predict the failure moment although the procedure of determining the coefficients which take into account structural parameters has not been developed. The state of research in the field of ductility of porous bodies demonstrates that today there is no adequately reliable criterion of porous metal fracture during plastic working which would take into account all factors affecting ductility and be convenient for practical applications. Figures 2; references 20: 18 Russian, 2 Western.

**Shock Waves During Dynamic Compaction of Powders and Porous Bodies. II. Shock Wave Propagation in Porous Materials With Reinforcing Frame**

927D0033D Kiev POROSHKOVAYA  
*METALLURGIYA* in Russian No 9(345),  
Sep 91 pp 19-23

[Article by L.A. Maksimenko, A.L. Maksimenko, G.G. Serdyuk, M.B. Shtern, Material Science Problems Institute at the Ukrainian Academy of Sciences]

UDC 621.762

[Abstract] The principal feature of dynamic powder compaction in rigid dies—the development of shock waves and the related piecewise-constant axial velocity and density component distribution which differ dynamic compaction most significantly from quasistatic compaction—and the relationships between stress and strain and pressure and density are discussed. The effect of strain hardening of the powder and porous body frame and the straining method on the development and character of shock wave propagation are investigated. To this end, the possibility of shock wave generation in a porous material with a reinforcing frame during its compression in a rigid cylindrical die is considered. To estimate the punch rate ensuring the development of shock waves, the longitudinal displacement equation of porous medium particles in the case of compaction in a die is considered and it is demonstrated that during the compaction of such a material in a rigid cylindrical die, the punch rate at which the shock wave forms decreases with the initial billet porosity assuming that the punch is a perfectly rigid body. The particle density and velocity during dynamic compaction of the hardenable material are

calculated and compared to analytical data for powders with perfectly ductile frames. Figures 4; references 4.

**Joint Effect of Various Flow Mechanisms in Porous Polycrystalline Body During Hot Compaction. III. Series Connection Model**

927D0033E Kiev POROSHKOVAYA  
*METALLURGIYA* in Russian No 9(345),  
Sep 91 pp 19-23

[Article by M.S. Kovalchenko, Material Science Problems Institute at the Ukrainian Academy of Sciences]

UDC 621.762

[Abstract] The incompatibility of certain mechanisms in their parallel connection model described in previous issues is mentioned and the model of a series connection of various flow mechanisms is examined in order to analyze the possibility of the simultaneous effect of two flow mechanisms in porous polycrystalline bodies during hot compaction. A covalent polycrystalline material is considered. The resulting relationships make it possible to use experimental data to estimate the kinetic parameters of two flow mechanisms in a series connection model. An expression is derived for calculating the lower bound of Laplacian pressure with the help of the ratio of straining rates under different external pressures with an identical relative density on the basis of experimental data on the sintering kinetics under pressure. References 2.

**Extrusion Patterns of Bimetal Powder Materials. I. Taut Strained State During Extrusion of Dissimilar Materials**

927D0033F Kiev POROSHKOVAYA  
*METALLURGIYA* in Russian No 9(345),  
Sep 91 pp 23-28

[Article by N.V. Manukyan, S.G. Agbalyan, G.A. Tumanyan, G.Kh. Karapetyan, N.L. Akopov, R.G. Samvelyan, Yerevan Polytechnic Institute]

UDC 621.762:621.771.8

[Abstract] Synthesis of heterogeneous powder materials by extrusion, and in particular bimetallic materials whose straining patterns are not known in sufficient detail, is discussed. The extrusion process in such materials is examined primarily by investigating the taut strained state of the cladding of monometallic materials and determining ideal values of the bimetal material billet's taut strained state components by analyzing the permissible ratio of properties. For convenience in investigation, the porous body straining during extrusion is tentatively divided into two stages: 1) compaction or upsetting and flow and 2) the flow of a cylindrical bimetallic powder (a rod-bushing design) through a conical die. To this end, extrusion of a cylindrical powdered body is considered in a spherical system of coordinates.

An analysis shows that bimetallic material rod dimensions must be specified on the basis of an optimal combination of geometric billet parameters, die angle, and plastic properties of the components at the extrusion temperature which ensure minimal shearing strain on the contact surface of the heterogeneous materials. A formula making it possible to determine the optimum bimetallic material rod radius on the basis of the geometric parameters of the billet and tools and ductile properties of the components is derived. Figures 2; references 7.

**Metal Coating of Diamond Powders With Adhesion-Active Metals. I. Refractory Metal Deposition From Gaseous Phase**

927D0033G Kiev POROSHKOVAYA METALLURGIYA in Russian No 9(345). Sep 91 pp 33-37

[Article by A.P. Oganyan, Yerevan Polytechnic Institute]

UDC 621.762.34:621.922.02

[Abstract] The processes of coating diamond powders with metals, and in particular titanium and chromium, and the outlook for commercial applications of metal-coated diamond particles for tool-making are discussed. Experimental diamond particle coating with titanium and chromium by the thermal diffusion saturation method in a rotary cylinder whereby a charge prepared by mechanical mixing of metal powders, AS15 diamond, and  $\text{NH}_4\text{Cl}$  ammonium chloride was treated in an atmosphere of argon in an electric furnace is described. A mathematical model of the research experiment is developed and its adequacy is checked using the variance analysis by Yates's method. The check reveals that the model is suitable. The metal coating parameter optimization range is expanded by the mathematical experiment design methods. As a result, the dependence of the metal-coated diamond breaking strength on the process temperature and duration and ammonium chloride concentration in the charge is established. The curves are similar, demonstrating that as the principal factors increase, the breaking load increases too. The following parameters are recommended for coating AS15 315/250 diamond with titanium and chromium:  $T^{\text{Ti}} = 700^\circ\text{C}$ ;  $T^{\text{Cr}} = 800^\circ\text{C}$ ;  $t = 1$  h; and  $N$  of close to 2.5%; the remaining parameters are the same as for iron coat application: a container rotational speed of 40 RPM, a container volume utilization factor of 25-30%, a diamond fraction in the burden by volume of 20-25%, and a 40  $\mu\text{m}$  metal powder fraction. The proposed methods make it possible substantially to increase the strength of both defective and perfect diamonds and thus improve their serviceability. Figures 2; tables 6; references 3.

**Resistivity of Iron Disilicide-Molybdenum Trioxide-Glass Composites**

927D0033H Kiev POROSHKOVAYA METALLURGIYA in Russian No 9(345). Sep 91 pp 43-47

[Article by S.I. Vecherskiy, F.A. Sidorenko, Urals Polytechnic Institute]

UDC 669.018.9:669.15'782:537.311.3

[Abstract] Metal-glass composite systems used in thick-film technologies of resistive electronic elements and the physical-chemical interaction among the components leading to changes in the crystalline phase composition which fills the gaps between metallic particles and greatly affects the electric resistance of the system as a whole are discussed. Certain features of the molybdenum trioxide interaction with the components of a heterophase system consisting of iron disilicide and barium borate glass are investigated and the character of its effect on the electric resistance of the composite system is examined. The component makeup used in the study is described; the resistance of the samples is measured by the standard four-contact method. To decrease the temperature gradient along the samples, they are placed in a thermostat. A phase analysis points to an intense interaction among the components. The results show that as a result of the reactions, molybdenum trioxide is reduced by iron disilicide to lower oxides on the one hand and on the other, it reacts with glass forming barium molybdate. The specific shape of the concentration and temperature curves of the samples' resistivity is determined by the degree of reaction among the components and the iron disilicide and transition metal oxide concentrations. The spread of resistivity values is attributed to the statistical irregularities of component distributions in the samples. Figures 2; references 8: 6 Russian, 2 Western.

**Powder Magnetic Abrasive Tool Forming. III. Annular Turning Magnetic Abrasive Tool Forming**

927D0033I Kiev POROSHKOVAYA METALLURGIYA in Russian No 9(345). Sep 91 pp 47-52

[Article by M.D. Krymskiy, Material Science Problems Institute at the Ukrainian Academy of Sciences]

UDC 621.762:621.921-492.2

[Abstract] Various designs of turning magnetic abrasive tools (MAT) are analyzed and it is shown that certain application problems can be effectively solved by an annular magnetic abrasive tool formed by a magnetic field from a ferromagnetic abrasive powder (FAP) between opposite-positioned synchronously spinning annular poles. The capabilities of an annular magnetic abrasive tool are examined using a device assembled on a vertical drilling machine 2118A. A commutator unit is used to supply direct current to the coils. An analysis of the results shows that the normal cutting force in such a

magnetic abrasive tool used for machining rods (wire) and planar sheet edges largely depends on the powder magnetization and depends little on the field structure rotation speed. The ferromagnetic powder magnetization affects the normal cutting force and determines the synchronism of its rotation with the poles. The effect of the powder grain size, winding space factor, and magnetic induction on the magnetic abrasive tool properties is investigated. In particular, in machining a rod with a 3 mm diameter by an R6M5 abrasive material, the normal cutting force reaches 40 N while the mean ferromagnetic abrasive powder pressure reaches 170 N/cm<sup>2</sup>. Figures 5; references 11.

**Hafnium Interaction With Ruthenium and Iridium**  
927D0033J Kiev POROSHKOVAYA METALLURGIYA  
in Russian No 9(345), Sep 91 pp 56-62

[Article by V.N. Yeremenko, L.S. Kriklya, V.G. Khoruzhaya, T.D. Shtepa, Material Science Problems Institute at the Ukrainian Academy of Sciences]

UDC 669.297.5'236.232

[Abstract] Hafnium's interaction with ruthenium and iridium examined in various sources is summarized and Hf-Ru and Hf-Ir systems are investigated in greater detail because studies of the Hf-Ru-Ir ternary system phase equilibria produced results which contradict the known Hf-Ru system constitution diagram. Hf-Ir alloys were prepared and examined as reference compositions in order to clarify the phase homogeneity regions and the coordinates of the nonvariant equilibria points. All alloys were prepared in an electric arc furnace with a nonconsumable electrode on a water-cooled copper hearth in a gettered argon atmosphere. Hafnium iodide and sintered 99.9% pure ruthenium powder and 99.7% pure iridium wire remelted in the arc furnace beforehand were used as source materials. The study was carried out by the methods of microstructural (MSA), X-ray phase (RFA), and differential thermal (DTA) analyses while the melting point was measured by the Pirani-Alterthum method. Data show that a single HfRu compound-based intermediate phase forms in the Hf-Ru system. The coordinates of the nonvariant equilibria points are 1,610°C and 20% at. Ru, 1,790°C and 78% at. Ru, 1,310°C and 8% at. (Ru). Intermediate Hf<sub>2</sub>Ir, Hf<sub>3</sub>Ir<sub>3</sub>, HfIr, and HfIr<sub>2</sub> phases are discovered in the Hf-Ir system and their homogeneity regions are established. Moreover, the HfIr-based phase undergoes a polymorphous transformation and its high-temperature modification has a CdCl<sub>2</sub>-type crystal lattice which is successively transformed into tetragonal and monoclinic (pseudorhombic) with a decrease in temperature. Figures 3; tables 1; references 11; 3 Russian; 8 Western.

**Conductivity and Thermoelectric Coefficient of Hot-Compaction Aluminum Boride and Carbaboride Samples**

927D0033K Kiev POROSHKOVAYA METALLURGIYA in Russian No 9(345), Sep 91 pp 62-65

[Article by A.I. Kharlamov, L.M. Murzin, S.V. Loychenko, T.I. Duda, Material Science Problems Institute at the Ukrainian Academy of Sciences]

UDC 621.762.4:661.65:661.862:537.311.312.6

[Abstract] High-boron aluminum compounds—structural analogues of boron with a unique combination of chemical and physical properties—and especially polycrystalline aluminum dodecaborides are investigated. In order to measure electric conductivity and thermoelectric coefficient, samples were produced by the hot compaction method from disperse aluminum dodecaboride and carbaboride powders as well as AlB<sub>12</sub>-B<sub>4</sub>C composites with various carbon concentrations. Conductivity was measured by the potentiometric method by Shch-302 and V7-21 digital electronic voltmeters. The temperature curves were plotted in a helium medium within a 297-1,100K range using alumel wire probes. Data show that the dependence of conductivity and thermoelectric coefficient on temperature of hot-compaction polycrystalline samples are both qualitatively and quantitatively consistent with similar characteristics of single crystals. The proposed method makes it possible to manufacture samples of any size and fills a gap in the knowledge of the temperature dependence of the thermoelectric coefficient of  $\beta$ -AlB<sub>12</sub>. Figures 4; tables 1; references 7; 3 Russian, 4 Western.

**Structural Modification of Sintered Composite Tube Cathodes in High-Current Gaseous Discharge**

927D0033L Kiev POROSHKOVAYA METALLURGIYA in Russian No 9(345), Sep 91 pp 66-68

[Article by V.I. Baranova, S.N. Novikov, Moscow Electronic Engineering Institute]

UDC 621.385.735.2

[Abstract] The use of heterogeneous composite materials produced by the methods of powder metallurgy for making gaseous discharge tube cathodes is necessitated by the scarcity and cost of tungsten. Structural changes in composite cathodes in a high-current gaseous discharge are investigated and the factors affecting their high strength, i.e., a refractory metal matrix (made of tungsten or molybdenum) carrying the thermal load and a reinforcing phase which facilitates the dislocation structure development, are examined. Washer-shaped cathodes are made by powder metallurgy methods and tested in commercial tubes filled with krypton to a 2 MPa

pressure in a rapid on-off mode (a 15-20 s working cycle and a total of 500, 3,000, and 7,000 cycles) at a current density of  $10^3$ - $10^4$  A/cm<sup>2</sup>. The examination is carried out with the help of a JSM-35CF scanning electron microscope with a Link-860-500 X-ray microscopic analysis system. The study reveals thermal cathode aging in a high-current gaseous discharge which is characterized by a metallic phase crystal growth, molybdenum grain elongation in the discharge direction, and a decrease in the amount of activator in the cathode's subsurface layer. The above changes sharply decrease the normal life of high-pressure tubes. Figures 3; references 3.

#### Comparison of Requirements for Vehicle Cardan Shaft Tubes and Ways to Improve Their Quality

927D0051G Dnepropetrovsk  
METALLURGICHESKAYA I GORNORUDNAYA  
PROMYSHLENNOST in Russian No 4/162).  
Oct-Dec 91 pp 44-45

[Article by G.I. Gulyayev, K.I. Shkabatur, V.I. Mizera, A.I. Derevyanko, T.P. Rodionova. Pipe and Tube Industry Research Institute]

UDC 006.44.001.36:[621.774.21:621.791.7]:621.825.6

[Abstract] The requirements imposed on mechanical properties of foreign and domestic tubes pursuant to GOST 5005-82 are compared to those of Japan's JASOC 301-77 because Japan is a leader in making tubes for the automotive industry. The principal steel specifications used in both countries for making automotive tubes are summarized. The good properties of foreign tubes are attributed to the use of coils of hot-rolled strip with an elevated carbon content and new-generation electric tube welding machines equipped with modern quality control attachments and finishing machines. The use of rimmed steel for skin-rolling results is recommended for producing a strip with twisting not exceeding 5 mm per 10 m of length. Process specifications for producing the strip for automotive tubes are outlined and it is suggested that GOST 5005-82 be revised so as to expand the assortment and dimensions of tubes. Tables 1; references 7: 4 Russian, 3 Western.

#### Electrically Welded Thin-Walled Tubes for Automotive Industry

927D0051H Dnepropetrovsk  
METALLURGICHESKAYA I GORNORUDNAYA  
PROMYSHLENNOST in Russian No 4/162).  
Oct-Dec 91 pp 45-46

[Article by V.I. Mizera, K.I. Shkabatur, Yu.D. Volper, A.I. Derevyanko, T.P. Rodionova. Pipe and Tube Industry Research Institute]

UDC 621.774.21:621.791.7]:621.825.6

[Abstract] Experiments demonstrating that steel 08GSYuT may be used in place of steel 08kp for making tubes of the same diameter while reducing the wall thickness by 20% without sacrificing performance are reported. Bench tests of thinner-walled tubes performed at the Volga Automotive Works (VAZ) reveal that they can be used as blanks for making automotive parts immediately after welding or following heat treatment in place of the cold-drawn tubes used before. The results of measurements and tensile, flare, flattening, and flanging tests demonstrate that 25x1.2 mm tubes from 08GSYuT steel meet the requirements of standards and specifications and that commercial production of tubes from the new brand of rolled steel for other purposes may be accelerated as a result of these tests. I.P. Mozharenko, Yu.N. Truskov, Ye.N. Logvinenko, S.D. Kupriy, and A.D. Vetylanskaya participated in the study.

#### Temperature and Mechanical Conditions of Hot Die Forging of Titanium Powder Blanks

927D0052A Kiev POROSHKOVAYA  
METALLURGIYA in Russian No 11(347).  
Nov 91 pp 1-5

[Article by V.A. Pavlov, M.I. Nosenko, L.A. Karlov. Zaporozhye Mechanical Engineering Institute]

UDC 621.762.4

[Abstract] Hot die forging of powder blanks which makes it possible to produce almost pore-free items whose strength and ductility are equal to those of rolled stock is addressed and the depth and character of metal penetration by gases (the gas-saturated layer) as a function of temperature, time, and heating medium (i.e., air or argon), and relative blank density are examined in order to ascertain the patterns of powdered titanium oxidation. To this end, the microhardness of the surface and deep sample layers is measured under various loads. The hot strain force is measured in a 800-1,000°C range and the effect of hot straining on compaction is evaluated on the basis of the shearing strain intensity. An analysis reveals the optimum temperature and straining degree and pressure ensuring the maximum part density for closed die forging and for forging with outlet elements: a 900-950°C temperature range and a 700-800 MPa effective pressure range for closed die forging. Hot die forging is expedient if the relative blank density is  $\geq 80\%$ , the resulting product's relative density reaches 98-98.5%. It is shown that a virtually pore-free metal (99.8-100%) may be produced at lower pressures of 560-650 MPa using dies with outlet elements. Figures 5. references 3

**Role of Elastic Stresses During Sintering of Nonisomeric Crystal Particles**

927D0052B Kiev POROSHKOVAYA  
METALLURGIYA in Russian No 11(347),  
Nov 91 pp 6-10

[Article by Yu.I. Boyko, Yu.L. Galchintakaya, Yu.I. Klinchuk, S.L. Molodtsov, I.T. Chizhikova, Kharkov University]

UDC 621.762

[Abstract] Sintering of nonisomeric iron particles obtained by special cryogenic machining from spheroidized powders with a 40  $\mu\text{m}$  mean particle size which are ground in a specially designed ball mill at a liquid nitrogen temperature (77K) is investigated. The particle dimensions and geometrical configuration are examined by a scanning electron microscope. After milling, the particles are sintered at a 1-10 MPa pressure and compacted into cylinders with an 8 mm diameter and 3 mm height. The sintering process is monitored by means of dilatometer measurements. The samples are then annealed within a 500-800°C range in pure dry hydrogen and the changes in the sample dimensions are examined during the isothermal annealing. A powder activity manifested by a considerable increase in the compact sintering rate in a direction perpendicular to the particle orientation plane is observed; this phenomenon is attributed to the considerable store of elastic energy of the straining origin whose relaxation determines the specific features of the sintering process. The principal mechanism responsible for the substance transport during the sintering process is the movement of dislocations which eventually reach the particle surface. The radial dilation of compacted powder sample produced by cryomechanical treatment occurs by the mechanism of diffusion-viscous particle sliding relative to each other under the effect of capillary stresses. Figures 5; references 7.

**Structure Formation Processes in Powder Copper-Chromium-Graphite Materials**

927D0052C Kiev POROSHKOVAYA  
METALLURGIYA in Russian No 11(347),  
Nov 91 pp 18-21

[Article by V.A. Dymchenko, Ye.A. Kurilova, Gorlovka Branch of the Donetsk Polytechnic Institute]

UDC 669.018.9

[Abstract] Certain constituent interaction processes occurring during the sintering of a copper-chromium-graphite powder system—the principal material of sliding contacts—are investigated. Experimental

samples are manufactured from PMS-2u copper (GOST 4960-75) and GK-1 graphite (GOST 4404-78) powder and ground metallic chromium Kh99 (GOST 5905-79) screened through a 0.2 mm mesh sieve and sintered twice. The structure is examined after the first and second sintering using an optical microscope and a Kamebaks X-ray structural microanalyzer. The sample mass variation as a function of carbon content and sintering duration and the effect of the carbon concentration on the volume variation during sintering are plotted. The phase ratios and distribution character as a function of the protective medium and charge composition are examined. The final system has a structure of a mechanical mixture of copper and chromium which is distinguished from the initial charge by a higher chromium inclusion dispersion degree. It is speculated that the processes occurring in the system are thermodynamically stimulated by its tendency toward decreasing the number of phases appearing at the initial sintering period, i.e., chromium oxides and carbides. Figures 5; references 1.

**Diamond Powder Metallizing by Adhesion-Active Metals. II. Structural Analysis of Metallized Diamond Powders**

927D0052D Kiev POROSHKOVAYA  
METALLURGIYA in Russian No 11(347),  
Nov 91 pp 11-13

[Article by A.P. Oganyan, Yerevan Polytechnic Institute]

UDC 621.762.34:621.922.02

[Abstract] Surface phenomena on the diamond grain's interface with the coal and binder are discussed and carbide and metal layers formed by coating AS40 diamond with transition metals, particularly chromium and titanium, using the gas transport reaction method are investigated in CuK $\alpha$  radiation by a DRON-2 X-ray diffractometer. The phase composition of synthetic diamond powders AS40 315/250 coated with titanium at 700-750°C for 1 h and natural diamond powder AZ 630/650 at 800-850°C for 1 h are measured and compared to data obtained by other researchers. Mutual diffusion of the coat and binder metals is established and its relationship to the chemical composition of the alloy is determined. The durability of the metallized diamond powder is measured using the specific diamond consumption as a benchmark. An analysis shows that metal coating by the titanium-copper alloy decreases the specific consumption of diamond by 1.7 times. Figures 1; tables 2; references 4.

**Mold Design for Electric Discharge Sintering of Diamond Tool From Cu-Sn-Based Powder Composites**

927D0052E Kiev POROSHKOVAYA  
METALLURGIYA in Russian No 11(347),  
Nov 91 pp 78-82

[Article by A.V. Svechkov, A.A. Baydenko, V.P. Popov,  
M.Sh. Goldberg, Material Science Problems Institute at  
the Ukrainian Academy of Sciences]

UDC 621.762.07

[Abstract] The design of molds for making powder composite tools by the electric discharge sintering (EDS) method characterized by a combination of treatment and mechanical action is considered and several

designs of molds for electric discharge sintering of rectangular and cylindrical ring diamond tools from a powder composition containing 80% Cu and 20% Sn by mass are presented. Diamond powder with a particle size varying from 20 to 350  $\mu\text{m}$  is used as the abrasive component. The specific requirements imposed on the punch for both types of molds are described and preference is given to a mold design with a sliding needle punch which also serves as a heating electrode. As a result of electric discharge sintering method refinement, the punch electrode design is improved; the final electrode is made as a liner whose inside diameter is 2-3 mm smaller than the needle diameter; this makes it possible to decrease the punch mass and increase its resistivity and thus equalize the temperature field uniformity in the sintered product and improve its quality. Figures 2; references 19.

### Controlling Continuous Rolling Mill Rate Condition

927D0054C Moscow *IZVESTIYA VYSSHIKH UCHEBNYKH ZAVEDENIY: CHERNAYA METALLURGIYA* in Russian No 6, Jun 91 pp 31-32

[Article by A.S. Fedosiyenko, Chelyabinsk Polytechnic Institute]

UDC 621.771.25:011.56

[Abstract] The rolling process in a single-strand small-section tension mill is considered and it is shown that the rolling rate conditions in a such a continuous mill are generally controlled by maintaining the specified strip tension between the stands, loop tension between the trains, and the rolling rate itself. A model of the train of stands is formulated as an instantaneous controlled entity and the control action on this entity is examined. The problem of synthesizing the unknown control actions is formulated. Rolling rate control of a loop rolling mill is considered as a particular case of the continuous rolling mill. It is demonstrated that an automatic device for controlling the mill's rolling rate conditions executing the aforementioned control actions satisfies the necessary non-interaction criteria. Thus, the procedure for determining the selective control actions on the stand-to-stand tension and train-to-train strip loops of the continuous single-strand rolling mill employing *a priori* data on its properties is effective.

### Strip Thickness Measuring System of Narrow-Strip Hot Rolling Mill

927D0054D Moscow *IZVESTIYA VYSSHIKH UCHEBNYKH ZAVEDENIY: CHERNAYA METALLURGIYA* in Russian No 6, Jun 91 pp 33-35

[Article by B.I. Kuznetsov, V.I. Kovalev, Ukrainian Correspondence Polytechnic Institute]

UDC 621.771.23:62-52

[Abstract] A data-measurement system whose development was prompted by the adoption of state ready rolled stock quality approval standards in 1987 is described. The system developed at the Ukrainian Correspondence Polytechnic Institute makes it possible to monitor the product quality during the rolling process. System operation is illustrated using the example of the thickness variation oscillogram of a 5x348 mm strip of steel 18YuA and the correlations of the longitudinal thickness variation of various rolled strips made at the Novosibirsk Metal Works as well as the spectral density of longitudinal strip thickness variation obtained by estimating the correlation functions. The economic impact from using the data-measurement system in a

semicontinuous five-stand hot rolling mill 810 is 150,000 rubles a year just from eliminating manual measurements. The computer-aided system makes it possible to obtain reliable data on the product quality, making it possible to decrease the amount of rejects, retool the mill for a given standard size, and conduct rolling in the negative tolerance zone. The resulting correlation functions and spectral thickness variation magnitude densities may be used to synthesize optimal geometrical rolled stock parameter control systems on the basis of Kolmogorov's and Wiener's concepts and Kalman-Bucy filters. Figures 4; references 7

### Crack Resistance of Steel 20Kh13 Following Electron-Beam Machining and Plasma Jet Spraying

927D0054E Moscow *IZVESTIYA VYSSHIKH UCHEBNYKH ZAVEDENIY: CHERNAYA METALLURGIYA* in Russian No 6, Jun 91 pp 46-49

[Article by V.I. Petrov, V.A. Kuznetsov, V.N. Detsak, N.A. Stolyarova, N.A. Chernyshev, Siberian Metallurgical Institute]

UDC 669.018.25:621.9.048

[Abstract] Surface hardening by means of highly focused energy sources, i.e., electron and laser beams, and worn-out surface rebuilding by means of a combined method involving jet spraying with subsequent electron and laser beam fusing are analyzed. The effect of the structure and composition of the coats fused by the electron beam on the propagation of incipient cracks in them is investigated. For illustration, Ni-Ti coats with intermetallic hardening and Fe-Cr-Mn-V-C-B-Si with carbon boride hardening, plasma-jet sprayed on the base from steel 20Kh13 with subsequent electron-beam machining as well as a layer obtained by electron-beam fusing of steel 20Kh13 are examined. Propagation of cracks in cast steel 20Kh13 after standard heat treatment is used as the frame of reference. Powders with a 60-100  $\mu\text{m}$  size are used to form a 0.45-0.50 mm surface layer. The samples are examined by a Neophot-21 optical microscope and Camscan electron scanning microscope with an X-ray spectral microanalysis attachment. The microhardness distribution in the fusion zone depth and the dependence of the crack propagation rate on the notch sensitivity index span are plotted. The study shows that steel 20Kh13 or plasma-jet sprayed surface modification by an electron beam considerably increases the surface hardness in the machining zone and reflects the coats' structure and phase and chemical composition in the fusion zone. The method may be recommended for developing protective coats on parts operating under cyclical loading. It is shown that Fe-Cr-Mn-V-C-B-Si coats are preferable. Figures 6; tables 1; references 3.

### Investigation of Cooling Rate's Effect on Structural Parameters of Steel 38KhN3MFA

927D0054F Moscow *IZVESTIYA VYSSHIKH UCHEBNYKH ZAVEDENIY: CHERNAYA METALLURGIYA* in Russian No 6, Jun 91 pp 50-51

[Article by Yu.F. Ivanov, E.V. Kozlov, Tomsk Civil Engineering Institute]

UDC 669.112.227.34-192:620.187.3

[Abstract] Since the structure of the heat affected area of welded steel is virtually always austenitic above certain temperatures and the secondary structure of this zone is affected predominantly by the heat cycle shape or the cooling rate, the phase composition, morphology, and defect structure of steel 38KhN3MFA quenched at a 1.050°C temperature in two hours at rates varying within a 1-300°C/s range are examined by the methods of electron microscopy of thin foils. The sample cooling rate is controlled by changing its thickness. The effect of the cooling rate during quenching on the volume fraction of high-temperature lamellar martensite and stacks with a nonuniform layer structure, the dependence of the mean transverse dimensions of various types of martensite formations on the cooling rate, and the effect of the cooling rate on the scalar and excess dislocation density, volume fraction, and longitudinal and transverse dimensions of cementite particles located in martensite crystals are plotted. Electron microscopy analyses of the steel 38KhN3MFA structure as a function of cooling rate make it possible to identify the cooling rate range (1-20°C/s) within which significant structural changes are observed simultaneously at the martensite phase morphology, individual martensite crystal size, and dislocation structure and cementite phase parameter levels and establish the functional relationship between the above structural parameters of steel and its cooling rate. These data are used for nondestructive structural material testing. Figures 3; references 12: 10 Russian; 2 Western.

### Investigation of Brand D Steel Ingot Piercing Process

927D0055J Moscow *IZVESTIYA VYSSHIKH UCHEBNYKH ZAVEDENIY: CHERNAYA METALLURGIYA* in Russian No 7, Jul 91 pp 55-57

[Article by V.Ya. Osadchiy, I.N. Leontyeva, V.K. Shumilin, A.V. Safyanov, A.S. Golodyan, Moscow Instrument-Making Institute and Chelyabinsk Tube Rolling Mill]

UDC 621.774.35

[Abstract] The difficulties of piercing ingots from brand D steel at the Chelyabinsk Tube Rolling Mill (ChTPZ) and the resulting defects necessitated a comprehensive study whose results are processed by the mathematical statistics method so as to determine the effect of the carbon content in brand D steel, ingot heating time, final ingot piercing temperature, and ingot height on the formation of "triangle" defects. A batch of 700 ingots pierced into 570x90 mm blanks (containing 10-11% defective ingots) is examined. An analysis shows a nonlinear correlation between the heating duration and the number of triangles described by a regression equation and a nonlinear correlation between the ingot height and the number of triangles described by a regression equation. A linear relationship between the final piercing temperature and the number of triangles described by a direct regression equation is established. The effect of the carbon content on the appearance of the triangle is also examined. The results make it possible to recommend optimal ingot dimension ratios and final drifting temperature as well as the furnace temperature conditions. Figures 5; tables 1; references 2.

### Diamond Drawing Die Strength Analysis

927D0055J Moscow *IZVESTIYA VYSSHIKH UCHEBNYKH ZAVEDENIY: CHERNAYA METALLURGIYA* in Russian No 7, Jul 91 pp 59-62

[Article by V.N. Kissyuk, V.N. Lvov, G.P. Maltseva, Ye.V. Lvova, All-Union Correspondence Polytechnic Institute]

UDC 621.778.1.07

[Abstract] The problem of increasing the durability of drawing dies made from natural and synthetic diamond—an indispensable tool for making thin and ultrathin wires—by decreasing their cracking under the effect of considerable tensile stresses is addressed and an attempt is made to develop a computation procedure for evaluating the stressed state of the diamond blank which would facilitate the drawing dies' operational durability. Extensive experimental studies were conducted beforehand so as to examine diamond fastening methods in the die. Stress distributions in the diamond crystal with newly developed fastening techniques are plotted experimentally under the effect of external pressure and crimping in a nonreinforced diamond blank and a prestressed one. Numerical strength analysis data are compared to the results obtained by Lame for different types of tool holders. The proposed strength analysis procedure is analytically quite simple and consistent with existent methods of crimping the diamond crystal in the holder beforehand. Figures 3; tables 2; references 2.

**Dislocation Density Behavior in Steel Under Electrically Stimulated Drawing**

927D0055K Moscow *IZVESTIYA VYSSHIKH UCHEBNYKH ZAVEDENIY: CHERNAYA METALLURGIYA* in Russian No 7, Jul 91 pp 70-72

[Article by T.V. Yerilova, V.Ye. Gromov, Yu.V. Baranov, L.B. Zuyev, Siberian Metallurgy Institute and Strength Physics and Materials Science Institute at the Siberian Branch of the USSR Academy of Sciences, Tomsk]

UDC 669.017:548:621.778:621.3.014.3

[Abstract] A promising method of intensifying the cold drawing process by using an external current pulse action is discussed and the results of the dislocation density behavior study in steel 08G2S obtained by various methods are presented and compared. Low-alloy welding filler wire is selected in the experiments since a rising demand for this wire necessitates a search for ways

of intensifying its production methods. In particular, 8.5 and 5.5 mm wire made without special annealing pursuant to GOST 2246-70 is examined under five straining conditions. Two wire batches produced by these drawing methods are investigated and an annealed sample made from the starting wire is used as a standard. The dislocation density is examined in one batch while the fine structure parameter are analyzed in the other one on a computer (EVM). The dependence of the coherent scattering, microstrain, and dislocation density on the percent reduction is established for various rates of convectional and electrically stimulated drawing. An analysis of these data shows that the dislocation density increases gradually with an increase in percent reduction both for conventional and electrically stimulated drawing regardless of the drawing rate. Yet according to the results of X-ray diffraction analysis, the dislocation density for electrically stimulated drawing is always lower than that of conventionally drawn wire given the same percent reduction. Tables 5; references 8: 7 Russian, 1 Western.

**Ecology of Massive Explosions in Quarries**

927D0051A Dnepropetrovsk  
**METALLURGICHESKAYA I GORNORUDNAYA PROMYSHLENNOST** in Russian No 4(162),  
 Oct-Dec 91 pp 5-7

[Article by E.I. Yefremov, V.D. Petrenko, Ukrainian Academy of Sciences]

UDC 622.233.012.3:622.235.023.22]:628.511

[Abstract] The issue of keeping down the dust and gases resulting from explosions in the mining industry, especially strip mining where millions of cubic meters of the dust and gas mixture are ejected 1.5 km high into the atmosphere, the dust concentration in the plume reaches 2 g/m<sup>3</sup>, and the dust plume volume from a single explosion may reach 0.6-5.7 million cubic meters, is addressed. The principal factors upsetting the ecological balance during massive explosions in a colliery are established by analyzing and scientifically classifying available data. The dust-like particles in the drilling mud are evaluated quantitatively and the fraction composition of other borehole drilling products primarily responsible for the dust-formation is examined. The fraction analysis shows that the drilling mud contains, on the average, 18% of the 0-250 µm fraction while its lowest concentration is found in ocherous shale (15.12%) and the highest in the silicate magnetite quartzite (22.27%). Several dust and gas mixture suppression methods are examined and tested in commercial operation. It is shown that one of the most efficient dust and gas mixture suppression methods is liquid-based tamping. Other methods include drilling mud removal, utilization, or binding as well as using special explosive charges and explosion methods. References 4.

**Ways of Increasing Exploitation Efficiency of Deep Levels at Ingulets Mining and Ore Dressing Combine**

927D0051C Dnepropetrovsk  
**METALLURGICHESKAYA I GORNORUDNAYA PROMYSHLENNOST** in Russian No 4(162),  
 Oct-Dec 91 pp 53-55

[Article by A.V. Krivosheyev, Ingulets Mining and Ore Dressing Combine]

UDC 622.341.1:[622.012.3:622.221.3]:[622.647:65.011.46]

[Abstract] New trends in strip mining being implemented in Ukraine and abroad are discussed and designs which make it possible to reduce the volume of motor vehicle usage for hauling by employing a method of gravity transfer of rock excavated at higher colliery levels toward a fixed crushing and transfer station are

described. The ore from lower levels is transported to the fixed crushing and transfer stations by conveyor lifts. Extensive implementation of conveyor ore transfer methods is identified as one of the principal trends in increasing the mining efficiency, reducing harmful discharges into the air, and saving motor fuel. M.S. Chetverik and V.P. Shportko assisted in developing the gravity ore transport system.

**Electric Fuze Network Switching System to Expand Short-Delay Blasting Capabilities**

927D0051D Dnepropetrovsk  
**METALLURGICHESKAYA I GORNORUDNAYA PROMYSHLENNOST** in Russian No 4(162),  
 Oct-Dec 91 pp 57-59

[Article by V.R. Dyadyushko, V.A. Zayarnyuk, Yu.N. Kireyev, S.A. Kovrigin, A.G. Lukashenko, Dnepropetrovsk Mining Institute and Sokolovsko-Sarbayskiy Ore Dressing Association]

UDC 622.235.432.352.001.76:621.316.1.014.2

[Abstract] The need for a large set of different blast delay intervals with high electric detonator operation accuracy when working in two-to-three subdrifts is identified and an electric fuze wiring network configuration for successively initiating two groups of charges, in which electric detonators with an identical set of delay times are used, is described. The special switching network (SRS) consists of two groups of electric detonators (ED), a controlling electric detonator, adjustable series resistors, and a shunt resistor. Electric fuze network (EVS) specification which meet unified safety rules (YePB) and ensure the necessary blasting conditions are cited. The proposed switching network makes it possible to increase the number of delay steps in successive blast priming systems. The system has been tested in commercial operation and has received USSR State Engineering Inspection permit for use at industry enterprises engaged in underground blasting with electric ignition systems. Figures 1.

**Fertile Mixture Application: New Soil Reclamation Method**

927D0051B Dnepropetrovsk  
**METALLURGICHESKAYA I GORNORUDNAYA PROMYSHLENNOST** in Russian No 4(162),  
 Oct-Dec 91 pp 7

[Article by V.M. Rakhmanin, Yu.M. Gukaylo, V.I. Shinkarenko, L.A. Mazhbits, All-Union Scientific Research and Design Institute of Marine Machinery]

UDC 622.271:[622.882:631.452].001.76

[Abstract] Ecological changes occurring in Ukraine in general and in the Dnepr river basin in particular due to strip mining and the destruction of a large area of rich

soil are discussed and a new method of placing a fertile mixture consisting of soil, grass seed, and enhancing additions on top of the land to be reclaimed is described. This man-made soil reclamation method may partially alleviate the negative impact of strip mining. The new

method makes it possible to use the reclaimed land for planting and grazing as well as gardening. The method is characterized in that outlays of chernozem topsoil are reduced and there is no need to plow the soil and plant grass.

**Effect of Powder Material Structure Factor on Strength and Ductility of WC-Co Detonation Gun Coatings**

927D0052G Kiev *POROSHKOVAYA METALLURGIYA* in Russian No 11(347), Nov 91 pp 24-30

[Article by V.K. Fedorenko, R.K. Ivashchenko, V.Kh. Kadyrov, A.M. Khayrtdinov, V.V. Segeyev, Material Science Problems Institute at the Ukrainian Academy of Sciences]

UDC 621.793:669.018.45

[Abstract] Protection of structural members from wear under cracking and fretting corrosion conditions with the help of wear resistant hard-alloy coats made from WC-Co powders is addressed and an attempt is made to establish the relationship between physical-chemical properties and process parameters of the source powder materials, temperature kinetics parameters of the deposition process, structural phase state, and physical-mechanical properties of the resulting coats in order to optimize their application technology. As a result, the dependence of the coat and base strength, ductility, hardness, and adhesion on the composition, structure, and process parameters of the powders and the design features of the detonation equipment, the deposition process temperature kinetics, and the coat thickness is established and an efficient "medium" combination of the coat strength, ductility, and adhesion properties which realizes the system potential to the utmost with the least sacrifice of individual properties is found. The study reveals that compacted powders are superior to mechanical mixtures and alloys with respect to their properties. Detonation gun coatings produced at the medium deposition conditions have a bending strength of 1.5-1.65 GPa and an adhesion strength of 90-130 MPa. Figures 4; tables 2; references 5: 3 Russian; 2 Western.

**Permanent Isotropic Magnets From Ferromagnetic Powders With Organic Composite Coating**

927D0052F Kiev *POROSHKOVAYA METALLURGIYA* in Russian No 11(347), Nov 91 pp 21-23

[Article by V.V. Nepomnyashchiy, Material Science Problems Institute at the Ukrainian Academy of Sciences]

UDC 621.752.4;538.221:669.5.17.255

[Abstract] The molding of permanent powder magnets (PPM) is examined and their magnetic and physical and mechanical properties as a function of binder content are investigated. Iron and iron-cobalt alloy powders with a 0.8-1.0  $\mu\text{m}$  particle size for the study are produced in a two-layer plating bath and subjected to reduction

annealing; 5-25% (by mass) of PEP-177 (TU ChP 141-75) thermosetting epoxy powder is added as a binder. The samples are compacted at a 1 GPa pressure. The dependence of the magnetic properties on the compaction pressure and the dependence of the physical properties on the binder content are measured in magnets made from iron and an iron-cobalt alloy in a 82:18 ratio. An analysis shows that the use of powder thermosetting resins makes it possible to increase the compression strength of permanent powder magnets from 1.5 to 5.3 MPa and that isotropic powder magnets with the optimum density and magnetic properties are molded at a compaction pressure of 0.8-1 GPa. It is recommended that commercial quantities of magnets be produced by compaction with subsequent binder polymerization. Figures 1; tables 2; references 5.

**Probabilistic Method of Monitoring Performance Margin of Aircraft Gas-Turbine Engine Parts on Basis of Maximum-Temperature Criterion**

927D0013A Kiev *PROBLEMY PROCHNOSTI* in Russian No 10, Oct 91 pp 54-58

[Article by A.N. Vetrov, A.G. Kucher, and N.A. Sniegirev, Kiev Institute of Civil Aeronautics Engineers]

UDC 539.4:620.1

[Abstract] For performance control of aircraft gas-turbine engines and their design optimization, a method of predicting the possibility of failure of engine parts due to sudden excessive rises of the gas temperature at the turbine inlet is proposed which considers the random nature of such temperature rises and which uses the maximum permissible operating temperature for a part degradable by overheating as the criterion of still available performance margins. The method is based on a probabilistic mathematical model for flight data evaluation, namely for comparing the maximum temperatures of any engine part directly or indirectly recorded during each flight with the not to be exceeded temperature limit for the material of that part. The algorithm of this method yields estimates of the probability  $P(N_{R_{\max}}(N_{R0} < T_{\lim})$  of failure-free performance of the given engine part during  $N_R$  engine operating cycles in scheduled subsequent flights. The distribution of maximum temperatures recorded in each of  $N_c$  control flights is describable by type-III statistics of extreme values, where the highest hardly ever reached maximum temperature  $T_{M0}$  of a part in operation is constant and assumed to be 1600°C but the two parameters  $\psi(N_c)$  and  $\beta(N_c)$  are functions of the number of control flights. This distribution is, for practical purposes, transformed into a linear relation and the two parameters  $\psi, \beta$  are evaluated by the method of least squares, after statistical data sampling by the Monte Carlo method. The temperature limit  $T_{\lim}$  is assumed to be 70-150°C above the maximum operating temperature and its distribution over this range to be one of the Weibull kind. On the basis of all these premises is obtained an expression for the

reliability function  $P(N_R)$  in the form of a finite integral with respect to a referred excess temperature  $T$  from  $T = 0$  to  $T = \infty$ . The integral is evaluated by numerical methods for various ranges of the key temperatures and various values of the distribution parameters. Further calculations yield the remaining gamma-percentage life of engine parts  $P(N_{R_\gamma}) = \gamma$  ( $\gamma$ - specified probability of failure-free operation based retention of nominal high-temperature load capacity). Figures 5; tables 2; references 2.

#### Automatic Stand for Testing Structural Materials in Compound State of Stress

927D0013B Kiev PROBLEMY PROCHNOSTI  
in Russian No 10, Oct 91 pp 70-74

[Article by F.F. Giginyak, O.K. Shkodzinskiy, R.K. Fedorov, M.V. Storchak, and V.V. Bashta, Institute of Strength Problems, Ukrainian Academy of Sciences, Kiev]

UDC 623.169.1

[Abstract] An automatic stand SNT-8U has been developed and built for testing thin-walled tubes made of structural materials under compound static and cyclic loads over a wide temperature range. This test stand consists of an axial-and-pressure loading device with cylinder and piston sets of various sizes (diameters), an axial-and-torsional loading device, "TIS Delta-16" force and strain gages with recording instruments a heating- and cooling system with temperature regulation, a pressure generator, a low-pressure

stage with a low-pressure manometer and a limit valve, a hydraulic pressure amplifier with a high-pressure manometer, and an axial load reversing device. The stand is designed to ensure stabilization of three control parameters (pressure, axial load, deformation) while it operates automatically in any of the following five modes: 1) one-shot load application with either load or deformation control; 2) one-shot application of a load with loading rate or deformation rate control up to creep or relaxation level with stabilization of stress or strain respectively; 3) application of soft or stiff cyclically varying but not alternating loads with sinusoidal, triangular, or saw-tooth waveform by a G6-15 special-purpose oscillator; 4) and 5) trapezoidal application of cyclic load by this oscillator with an attachment for regulation of the cycle period over the 1-1000 s range or through an integrator for regulation of the load duration up to 2 h respectively. The stand can also be operated manually, with the drive mechanism running at a constant speed, mainly for setup and preliminary adjustments. The stand is designed for testing with axial loads up to 0.1 MN, torsional loads up to 300 N.m, and pressures up to 150 MPa, at temperatures from -150°C to 400°C, and for cyclic loading at frequencies from 0.001 Hz to 1 Hz. The ratio of axial load to pressure could be varied by changing the size of cylinder and piston in the loading device, friction being minimized by use of teflon herringbone seals so that this ratio then remains practically constant during a proportional loading operation. As the working medium in the high-pressure stage, AMG-10 fluid was selected for operation at high temperatures and isopentane for operation at low temperatures, "Industrial grade-20" oil being used in the low-pressure stage. Figures 6; tables 1; references 11.

**END OF**

**FICHE**

**DATE FILMED**

5, May 1992